Schriftenreihe IWAR

231

TECHNISCHE UNIVERSITÄT DARMSTADT

IWAR

Marian Brenda

Hybrid Sludge Modeling in Water Treatment Processes

Herausgeber:
Verein zur Förderung des Instituts IWAR der TU Darmstadt e.V.

Hybrid Sludge Modeling in Water Treatment Processes

Vom Fachbereich Bau- und Umweltingenieurwissenschaften
der Technischen Universität Darmstadt
zur Erlangung des akadem. Grades eines
Doktor-Ingenieurs (Dr.-Ing.) genehmigte Dissertation

von

Dipl.-Ing. Marian Brenda
aus Landshut

Darmstadt, Juni 2015
D17

Brenda, Marian

Hybrid Sludge Modeling in Water Treatment Processes / Hrsg.: Verein zur Förderung des Instituts IWAR der TU Darmstadt e.V.
Darmstadt: Eigenverlag, 2015
(Schriftenreihe IWAR 231)

ISSN 0721-5282
ISBN 978-3-940897-30-5

Referent: Prof. Dipl.-Ing. Dr. nat. techn. Wilhelm Urban
Korreferent: Prof. Dr.-Ing. habil. Yongqi Wang

Tag der schriftlichen Einreichung: 13.03.2015
Tag der mündlichen Prüfung: 12.05.2015

Herstellung: Lasertype GmbH, Holzhofallee 19
64295 Darmstadt

Vertrieb: Institut IWAR
TU Darmstadt
Franziska-Braun-Straße 7
64287 Darmstadt
Telefon: 06151 / 16 3648
Telefax: 06151 / 16 3739

About the author:

Marian Brenda was born on 1982 in Landshut (Bavaria). He studied civil engineering at the Technische Universität Darmstadt with specialization on hydraulic engineering. As a student, he became acquainted with the CFD Software FLUENT and the diploma thesis is about sludge modeling in river estuaries. After finishing his studies in 2007, he worked for one year at the KfW development bank within the frame of the UN international year of sanitation. In 2008, he begun to work as a researcher at the Technische Universität Darmstadt, Institut IWAR, department Water Supply and Groundwater Protection. Within the cuvewaters.net project, he installed and operated four small scale desalination plants in rural areas of Namibia. After accomplishing several CFD-Analysis of the drinking water treatment plant in Langenau, the Fritz und Margot Faudi-Stiftung accepted a proposal to develop the hybrid sludge model. Marian Brenda is a member of the DWA (German Association for Water, Wastewater and Waste) and contributed with his CFD skills to the technical guideline DWA-M 544 since 2012.

About the content:

Using Computational Fluid Dynamics (CFD) in design, and optimization of water treatment plants delivers valuable insights into flow conditions and related processes. The hybrid sludge model can be used to simulate processes, where sludge occurs (activated sludge process, flocculation, decarbonization).

The hybrid sludge model is a user defined scalar for the commercial CFD code ANSYS FLUENT. Depending on the sludge concentration, it calculates the density, the settling velocity and the viscosity as well as the diffusion for the single-phase fluid, which is a mixture of sludge and water. The hybrid sludge model provides significant improvements for the measurement and modeling of the viscosity of sludge. Within the thesis, measurement methods and modeling concepts are provided, which need a minimum of measurement and calculation efforts, which is a contribution that CFD-Analysis will be used more often in designing and optimizing water treatment plants.

ISBN 978-3-940897-30-5

If any of you lacks wisdom
you should ask God
who gives generously to all without finding fault,
and it will be given to you.
(The Bible, James 1:5)

Preface

After I had completed the measurements for this thesis, there was a time during which I had difficulties in understanding the results. Since no one had tried to measure viscosity with a process-viscometer before, I had nothing to refer to. It is my personal belief that God gave me the right ideas at that time to carry on and, finally, complete this thesis with good results and new insights. Therefore I want to give the glory to the Creator of all things and I am thankful that He gave me some insights in a very special field of His marvelous creation.

And of course there were people who helped and supported me during my thesis work. First of all, I want to mention my mentor, Dr. Alexander Sonnenburg. His expertise with computational fluid dynamics (CFD), project acquisition and management contributed a great deal to this thesis, from the very beginning to the end. He was, incidentally, the person who encouraged me to become a researcher and to develop my CFD skills and the hybrid sludge model, which is presented here. I really enjoyed working together with him.

Special thanks are due to Professor Wilhelm Urban. He gave me the confidence and freedom to accomplish things the way I preferred. This was not true only for this thesis but also for the CuveWaters project in Namibia. In the beginning, this was hard for me, since, as a young professional, I was looking for guidance and orientation. Now, I can say that it was the best thing that could have happened to me and I am grateful for this chance to develop my personality in an atmosphere of trust and freedom. I know that times such as those when I worked in the Namibian bush, then with high-end CFD Software, gave lectures, travelled around the world with students, or visited conferences will never come back; but I am thankful for these experiences. Professor Yongqi Wang helped me to obtain a deeper understanding of the formulae that form the core of every CFD software. Even after years of working with CFD, I still learned about some inter-dependencies and connections that I had never seen before.

Lothar Gehm not only provided the viscometer; his great expertise in measuring viscosity helped tremendously in the conception of the process-viscometer. He and Fabian Gensmantel from proRheo GmbH invested great efforts into developing the process-viscometer for this special field of application.

The measurements would not have been possible without treatment plants that allowed me to make them. Thanks to Armin Metzler and Franz Menrath (waste water treatment plant Eberstadt), Willi Sommerkorn (waste water treatment plant Griesheim), and Rudi Winzenbacher (drinking water treatment plant Langenau).

Three students helped me with my thesis project. Jessica Beck spent hours with me on waste water treatment plants, measuring the settling velocity of sludge.

Christopher Bickert and Christoph Knecht conducted a number of simulations for me.

I want to thank my colleagues for that wonderful time at the IWAR institute. Lunchtimes were always a great pleasure and working together in projects was wonderful. Ana Cangahuala spent 5.5 years in the same office with me; thanks for the great time. I remember the times with Alexander Jokisch and Martin Zimmermann in Namibia. Renate Schäfer helped me very much with the administration of my projects and we spent hours together, sorting things out, as well as with Vera Soedradjat. Herbert Schmitt, Markus Heiligenthal, and Christian Georg always figured out a solution when something with the process-viscometer or in the testing plant did not go as intended. Their valuable input also helped me to design the plants. Thanks to Anita Curt, Sylvia Borsch, and Oliver Beer, who performed all the measurements of sludge concentration.

Finally, I want to acknowledge the Fritz und Margot Faudi-Stiftung for funding this project.

Abstract

Sludge occurs in many waste water and drinking water treatment processes. The numeric modeling of sludge is therefore crucial for developing and optimizing water treatment processes. Numeric single-phase sludge models mainly include settling and viscoplastic behavior. Even though many investigators emphasize the importance of modeling the rheology of sludge for good simulation results, it is difficult to measure, because of settling and the viscoplastic behavior. In this thesis, a new method is developed that combines rheological measurements with a process-viscometer and numeric simulations, in order to produce flow curves that most probably display the real viscoplastic behavior of sludge below a concentration of 10 g/l. The settling velocity is determined with a hybrid approach combining standard measurements and numeric simulations of the measurements. This is called the hybrid sludge model, which finally demonstrates its power by simulating a complex lamella clarifier. The results of the simulation fit the measurements and observations of the testing plant well. This demonstrates that the hybrid sludge model contributes to the development of a numerical model that requires a minimum of measurements and computational effort, in order to simulate water treatment plants. Finally, sludge properties (settling and viscoplastic behavior) from different waste water treatment plants and drinking water treatment plants are compared, with remarkable results. This thesis provides efficient tools for including numeric modeling in the design and optimization processes of water treatment plants.

Keywords: sludge, water treatment, Computational Fluid Dynamics (CFD), viscosity of sludge, rheology, shear thinning, settling, compression

Contents

List of Tables

List of Figures

Abbreviations

CAD	Computational Aided Design
CFD	Computational Fluid Dynamics
DCB	Divalent Cation Bridging theory (flocculation)
DLVO	Derjaguin, Landau, Verwey and Overbeek theory
DNS	Direct Numerical Simulation
DWTP	Drinking Water Treatment Plant
EFD	Experimental Fluid Dynamics
EPS	Extra-cellular Polymers
FEM	Finite Elemente Methode
FDM	Finite Differenzen Methode
FVM	Finite Volumen Methode
FSI	Fluid Structure Interaction
LES	Large Eddy Simulation
MRF	Moving Reference Frame Model
PDE	Partial Differential Equation
RAM	Random Access Memory
RANS	Reynolds Averaged Navier Stokes
udf	User Defined Function
uds	User Defined Scalar
SV	Sludge volume [ml/l]
SVI	Sludge volume index [ml/g]
WWTP	Waste Water Treatment Plant

Symbols

a, b	Parameters settling (Vesilind)
A	Area $[m^2]$
B_4^*	Parameter of correction function (Härtel and Pöpel)
c	Sludge concentration (suspended solids SS) [g/l]
c_0, h_0	Parameters of correction function (Härtel and Pöpel)
C_η, $C_{\epsilon 1}$, $C_{\epsilon 2}$	Empirical parameters for the $k-\epsilon$ model
d	Particle diameter [m]
D	Diffusion coefficient $[m^2/s]$
E	Elastic modulus [Pa]
E_r	Roughness parameter (9.793)
F	Force [N]
Fr	Froude-Number [-]
g	Gravity $[m/s^2]$
G	Generation of turbulent kinetic energy $[kg/(ms^3)]$
G_b	Generation of turbulent kinetic energy including stratified flow $[kg/(ms^3)]$
h_o	Height of overflow [m]
j_D, k_D	Parameters rheology (Dick and Ewing)
k	Turbulent kinetic energy $[m^2/s^2]$
k_v	Constant of viscometer $[m^{-3}]$
K	Parameter rheological model (Ostwald-de Waele, Herschel and Bulkley)
K_{SVI}	Parameter of correction function (Härtel and Pöpel)
l	Length [m]
L	Length of the bob [m]
n	Parameter rheological model (Ostwald-de Waele, Herschel and Bulkley)
M	Moment [Nm]
M_η	Moment due to pressure [Nm]
M_p	Moment due to viscosity [Nm]
p	Pressure [Pa]
Pr_t	Turbulent Prandtl-Number (0.85)
r	Radius coordinate [m]
r_h, r_p	Parameters settling (Takács)
R_i	Radius of inner cylinder (bob) [m]
R_a	Radius of outer cylinder (cup) [m]
Re	Reynolds-Number [-]
S	Source term

SV	Sludge volume [ml/l]
SVI	Sludge volume index [ml/g]
t	Time [s]
T	Temperature [°C]
u	Flow velocity in x-direction [m/s]
u_i, u_j	Velocity with index notation [m/s]
$\overline{u}$	Time averaged velocity [m/s]
u'	Fluctuating velocity [m/s]
u^*	Shear stress velocity [m/s]
v	Flow velocity in y-direction [m/s]
v_s	Settling velocity [m/s]
v_0	Parameter settling (Takács)
w	Flow velocity in z-direction [m/s]
x	Coordinate [m]
x_i, x_j	Coordinate with index notation [m]
y	Coordinate [m]
y^+	Nondimensional wall distance [-]
y_W	Distance from wall to cell center [m]
z	Coordinate [m]

γ	Deformation [-]
$\dot{\gamma}$	Shear rate [1/s]
$\dot{\gamma}^*$	Parameter (Windhab)
Γ	Turbulent Schmidt number [-]
δ	Ratio of inner and outer radius $\delta = R_a/R_i$ [-]
δ_{ij}	Kronecker-Delta $\delta_{ij} = \begin{cases} 1 & \text{for } i = j \\ 0 & \text{for } i \neq j \end{cases}$
ϵ	Turbulent dissipation rate $[m^2/s^3]$
η	Molecular dynamic viscosity [Pas]
η_t	Turbulent dynamic viscosity [Pas]
η_0	Low shear rate viscosity (Worrall and Tuliani) [Pas]
η_∞	High shear rate viscosity (Windhab, Worrall and Tuliani, Casson) [Pas]
κ	Von Kármán constant (0.41)
ν	Molecular kinetic viscosity $[m^2/s]$
ν_t	Turbulent kinetic viscosity $[m^2/s]$
ρ	Density $[kg/m^3]$
ρ_s	Density of dry sludge $[kg/m^3]$

ρ_w	Density of water $[kg/m^3]$
σ_k, σ_ϵ	Empirical parameters for the $k-\epsilon$ model
τ	Shear stress [Pa]
τ_y	Yield stress [Pa]
τ_B	Yield stress in the Bingham model [Pa]
ω	Angular velocity [rad/s]
Ω	Angular velocity of the bob [rad/s]
Ω_{HP}	Correction factor (Härtel and Pöpel)

1 Introduction

Many design standards for water treatment plants, including waste water treatment plants (WWTPs) and drinking water treatment plants (DWTPs), are based on assumptions and model conceptions that existed before computational fluid dynamics (CFD) came into existence. One example is the plug flow concept, which is the basis for the design of aeration tanks in WWTPs (DWA-A 131). Although the automotive industry, among many others, makes intensive use of CFD analysis in the design phase of new products, CFD is rarely used to design a water treatment process. Usually, CFD is introduced when the plant is built and does not function as intended. The flow within a treatment plant is crucial for whether the process is working or not. The separation of sludge in a secondary clarifier, for example, is usually achieved by sedimentation. For sludge to settle, it is necessary to have evenly distributed, low flow velocities. However, it is not easy to achieve such flows, but CFD can help to understand flows within treatment plants and to find better solutions, which reduce volumes and costs.

The basic flow equations have been known for a long time, but an analytic solution was possible only for some special cases, for instance, hydrostatics. Thus, it was common to use hydraulic models (here referred as Experimental Fluid Dynamics - EFD) to analyze flows. When computers appeared, it became possible to solve the basic flow equations numerically (CFD). Both approaches have their advantages and disadvantages; this is why it is wise to make use of both, which is called hybrid modeling.

The overall goal of this thesis is to describe the behavior of sludge in drinking water and waste water treatment plants numerically with adequate accuracy and a minimum of computational and measurement effort. The hybrid sludge model should contribute to enabling CFD to become integrated into the design process of water treatment plants - not as a substitute, but as a supplement to existing design standards. The draft version of the edited DWA-A 131 (2015) mentions already CFD in order to optimize distribution structures, flows within aeration tanks and secondary clarifiers, but admits that simulation has been used predominantly for academic purposes in the last decades.

For water treatment processes, there are two important properties of sludge: settling (see Chapter 2.3) and viscosity (or rheology in a broader sense, see Chapter 2.4). The settling behavior and velocity is crucial for designing secondary clarifiers. Therefore, Stobbe 1964, Vesilind 1968, Merkel 1971, and many others investigate the settling behavior of sludge. The relevance of the viscosity of sludge for water treatment processes is often described in literature, but the viscosity of sludge is analyzed for a variety of reasons. The pioneers of rheological investigations on sludge - Dick and Ewing 1967 - hoped that the “study of the rheological pro-

perties of activated sludge also may result in operational control techniques based on rheological measurements“ (p 543). However this did not eventuate; however, viscosity influences the treatment process in many ways, as other authors have reported. Klinksieg 2010 emphasizes the influence of viscosity on the settling behavior. Günder 1999 and Cornel and Krause 2005 investigate the influence of the sludge viscosity on the oxygenation in aeration tanks. The necessity for scrapers in the secondary clarifiers, due to the viscoplastic behavior of sludge, is described by Lakehal et al. 1999. They also state that the height of the sludge in secondary clarifiers depends highly on the viscosity. Slatter 1997 mentions the importance of knowledge about rheological properties for the design of pumps. The design of agitators requires knowledge about the viscoplastic behavior (Knoch 1997). Optimizing the layout of pumps and pipes for WWTPs is also the objective of Proff and Lohmann 1997a. Abu-Orf and Dentel 1997, Moshage 2004, and others emphasize the relevance of sludge rheology for the dewatering of sludge and for polymer dosing. Viscosity also plays a major role in more recent process techniques, such as membrane reactors, especially in the cleaning process of the membranes, as described by Ratkovich et al. 2012.

1.1 Central Questions

Because sludge plays a major role in many water treatment processes, it is necessary to model sludge numerically, in order to model water treatment processes. For a variety of reasons, it is not easy to define the sludge properties in such a way that they can be modeled accurately. The hybrid sludge model, which is presented in this thesis, contributes to increasing the accuracy of numerical sludge models. The focus here is on the viscosity of sludge, an important parameter for numerical simulation and the settling velocity. Finally, the properties of different sludges are compared.

The central questions in this thesis are:

- What is the physical viscosity of sludge?
- Is the hybrid sludge modeling concept suitable for modeling water treatment processes, and what are its advantages, compared to conventional modeling concepts?
- How different are the properties (viscosity and settling velocity) of different sludges?
- Which factors have the greatest influence on the properties of sludge?
- How can CFD support the design and optimization of water treatment plants?

1.2 Scope of the Thesis

Within the scope of this thesis, the following sludges were analyzed:

- Activated sludge from the WWTP in Eberstadt
- Digested sludge from the WWTP in Eberstadt
- Thickened digested sludge from the WWTP in Eberstadt
- Activated sludge from the WWTP in Griesheim
- Digested sludge from the WWTP in Griesheim
- Thickened digested sludge from the WWTP in Griesheim
- Flocculation sludge from the DWTP in Langenau (compact-flocculation)
- Flocculation sludge from the DWTP plant in Langenau (Accelator)
- Lime sludge from the DWTP in Langenau

These sludges are representative for the sludges produced by waste and drinking water treatment plants in Germany. Whereas activated and digested sludge occur in virtually all WWTPs and are investigated by numerous authors, the situation is somewhat different in DWTPs. Lime sludge and flocculation sludge form a major part of sludges occurring in DWTPs, but other sludges also occur (see Chapter 2.1).

1.3 Field of Application and Limitations

Based on the scope of this thesis, the broad field of application of the hybrid sludge model in water treatment processes is obvious. However, the sludge model is not restricted to water treatment processes. The sludge model is also used in simulations of river estuaries to model fluid mud (Brenda 2007). Virtually every suspension in which flocculation and coagulation processes take place can be modeled with the hybrid sludge model, because these flocculation and coagulation processes produce a settling velocity, which depends on concentration. The sludge matrix causes viscoplastic behavior. This settling and rheological behavior is modeled with the hybrid sludge model.

There are also limitations on where the sludge model can be used. As long as the suspension is stable and flocculation or coagulation processes do not take place, the sludge model cannot be used. For these kinds of suspensions, the modeling of water with species transport is usually sufficient (e.g. modeling a waste water plume in a river). Another example is the mixture of water and coarse sediments. Coarse

sediments do not coagulate and therefore settling does not depend on concentration but on the grain size, which is more or less constant. Furthermore, the structure formed by sediments is a solid one and not viscoplastic. Here, the usage of multi-phase approaches is recommended, for example, with a level-set method (Kraft, Wang and Oberlack 2011), or a simple variation of the sludge model with constant settling velocity for several grain size groups, in combination with morphodynamic models (Wurpts 2006). Untreated waste water can also not be modeled with the sludge model, because coarse contents have a major impact on the flow behavior. However, the sludge model might be a part of a waste water model, at least to some extent. It is also important to understand that the sludge model is a single-phase approach. The sludge flocs cannot have a velocity relative to the bulk fluid, even though, due to stratified flow effects, highly concentrated sludge can move independently of the clear water. Nevertheless, in a given cell of the mesh, there is only one velocity vector for the fluid. In addition, the sludge model does not model single flocs, but sludge as a continuum. In some processes, it might be necessary to model single flocs or the relative velocities with a multi-phase approach.

2 Literature Review

2.1 Basics of Flocculation Processes

Even though the numerical modeling is more or less the same for all sludge types (only the parameters differ), it is important to understand the nature of these sludges and the flocculation process itself. The water treatment processes described in this thesis usually try to remove suspended solids from the water. The suspensions (waste water or raw water from rivers or lakes) consist of water and undesirable organic (bacteria, algae, carbon compounds in general) and inorganic (clay, nitrate, and others) contents. These suspensions are stable, because the electrostatic repulsive forces overwhelm the Van-der-Waals attraction forces (Roth 1991). This means that the undesirable contents do not settle in technical time scales (DVGW W-217). In order to remove these contents, special treatment processes are necessary.

The majority of WWTP use activated sludge processes. Following pre-treatment, the waste water is oxygenated in an aeration tank. The oxygen, together with the carbon compounds, promotes the growth and multiplication of microorganisms. The microorganisms also produce extracellular polymers (EPS), which has been identified as one reason why the microorganisms agglomerate and form flocs (Eriksson and Alm 1991). There are three theories that describe the flocculation process: the alginate theory, the Derjaguin, Landau, Verwey and Overbeek (DLVO) theory and the divalent cation bridging (DCB) theory. Sobeck and Higgins 2002 state that "the sedimentation process quickly became recognized as the weak link in the activated sludge treatment scheme when larger scale, continuous flow systems were brought on line" (p. 527) at the beginning of the activated sludge process history (which began 1914, with Ardern and Lockett). Many research efforts were undertaken and still are undertaken to understand the flocculation process and optimize the settling process, to which this thesis also contributes. According to Sobeck and Higgins 2002, the DCB theory fits best for activated sludge. "According to the DCB theory, divalent cations bridge negatively charged functional groups within the EPS and this bridging helps to aggregate and stabilize the matrix of biopolymer and microbes and therefore promote bioflocculation" (p. 529); cations such as calcium and magnesium support the flocculation process (Sobeck and Higgins 2002). The flocs can then be separated from the liquid phase by sedimentation, which is performed in a secondary clarifier. The EPS account for a significant part of the dry mass content of sludge. Froulund et al. 1996 found that 85-90% of the organic content of activated sludge is EPS.

During the digestion process, two phenomena influence the sludge properties: biogas production and the reduction of the length of polymers. Due to the production of biogas, flocs start to float, while others settle down. The reduction of the size

of macromolecules reduces the viscosity of digested sludge (see Monteiro 1997). Finally, the organic fraction (glowing loss) is reduced, due to digestion.

Another kind of flocculation process is typically applied in DWTPs when the raw water source is surface water (rivers, lakes, reservoirs, seas). Following pretreatment, flocculants are added to destabilize the suspension. Most of the undesirable contents are colloids and have a negative surface charge. In order to overcome these repulsive forces, flocculants with positive charges are added (usually the cations Fe^{3+} or Al^{3+}). They reduce the negative repulsive charges, so that the Van-der-Waals forces become dominant and microflocs occur. To accelerate the flocculation process, polymers are added, to create larger flocs. The sludge consists of these additives and the colloids and not of microorganisms and extracellular polymers, as does activated sludge. This explains why the parameters for settling velocity and viscosity differ. These flocs can be separated from the liquid phase by sedimentation (in sedimentation tanks, lamella clarifiers, to name a few options). The same process occurs naturally in estuaries. When water from the river mixes with salt water from the sea, flocculation starts and fluid mud appears. The cations here are Na^{+} and, in smaller amounts, Mg^{2+} and Ca^{2+}.

Decarbonization is a purely chemical process in which no microorganisms are involved. The pH value is increased by adding calcium hydroxide ($Ca(OH)_2$) or sodium hydroxide ($NaOH$). This leads to a precipitation of calcium carbonate ($CaCO_3$). The properties of lime sludge are determined by calcium carbonate crystals. The process can be accelerated by adding fine sand or return sludge, in which the precipitated calcium carbonate can adhere to the crystals, so that they grow faster (DVGW W-235).

Flocculation sludge and lime sludge represent a major part of sludges occurring in DWTPs in Germany. According to Lipp and Dammann 2013, with data from 2012, 27% of sludges from drinking water sludges in Germany are lime sludges, 4% flocculation sludges, 43% iron sludges from deferrization, and 26% other kinds. Wichmann and Akkiparambath 2001 reported, for 1998, 41% lime sludges, 13% flocculation sludges, 15% iron sludges from deferrization, and 33% other kinds. Schneider 1995 reported, for Germany in 1992, 55% lime sludges, 34% flocculation sludges, 10% iron sludges from deferrization, and 11% other kinds (see also Wichmann and Riehl 1997). From these figures one can see a slight decrease in the share of lime sludges and a marked decrease in the share of flocculation sludges over the past 20 years. On the other hand, the share of iron sludge from deferrization increased. However, as Wichmann and Riehl 1997 state: “There are only few data on mechanical properties of waterwork sludges published.“ (p. 44)

2.2 Numerical Sludge Modeling

There are, in general, two approaches to model sludge numerically: multi-phase and single-phase.

Multi-phase approaches, like the Eulerian, solve the basic flow equations (Navier Stokes and mass conservation) for every phase (water and sludge, whereby sludge is often treated as a set of several phases, which requires significant computational effort). The coupling of both phases is realized as an exchange of momentum at the interface. Sludge flocs are regarded as spheres; therefore, settling processes are modeled in principle with the Stokes equation (Equation 1). The most sensitive parameter is the diameter of the sphere but, for sludge flocs, it is relatively difficult to measure their size and changes in size. The size of a sludge floc depends on the probability of collision and breakup. Depending on the applied model, the probability of collision is a function of concentration, differential settling (particles of various sizes have different settling velocities), turbulence, and Brownian motion. The probability of breakup is a function of shearing and collision.

Krishnappan 1990 divides the flocs into different discrete size classes. The concentration (not the diameter) of flocs in the various size classes changes only as a function of differential settling.

Greenspan and Ungarish 1982 use a continuous size distribution that depends on fluid velocity, concentration, particle velocity, and size.

Friedlander 1977 calculates the probability of collision from turbulence, differential settling, and Brownian motion. The breakup is modeled as a function of shearing and collision.

Winterwerp 1999 has developed a model in which only turbulence and concentration were considered for calculation of the probability of collision. Breakup is only a function of shearing.

Weilbeer 2004 chooses discrete size classes and considers Brownian motion, turbulence, and differential settling for modeling the growth of flocs and shearing for breakup.

A useful survey of the various methods used to model sludge with the multi-phase approach can be found in Göthel 2002. He modeled 2-D settling tests with FLUENT, using the model of Winterwerp 1999.

Single-phase approaches calculate the basic flow equations only for the bulk fluid and solve a transport equation for the concentration of sludge. Computational efforts are lower in comparison to multi-phase approaches. Settling, density and viscosity are usually functions of the sludge concentration.

Krebs et al. 2000 simulates secondary clarifiers with the single-phase approach. Settling, density, and viscosity are described as a function of the sludge concentration. **De Clercq** 2003 expands the model to describe shear thinning (viscosity as a function of shear rate).

Armbruster 2004 simulates secondary clarifiers with a 2-D code, called FAST-2D, using the single-phase approach. Settling for low concentrations (increasing settling velocity), hindered settling for medium concentrations (decreasing settling velocity) and compression for high concentrations are described as a function of sludge concentration. Viscosity is only a function of concentration.

Schumacher 2006 implements a function for the settling velocity in which the settling velocity for low concentrations increases, due to the growth of the flocs. For higher concentrations, the settling velocity decreases, due to hindered settling. Viscosity depends on the concentration and the shear rate. He uses the "biviscosity" approach and states that the viscosity has a major influence on the flow in a secondary clarifier.

2.3 Settling Velocity of Sludge

The settling velocity of particles in a fluid generally depends on the difference in density between the fluid and the particles, the viscosity of the fluid and the size and shape of the particles. For spherically shaped particles, **Stokes** formulated following equation:

$$v_s = \frac{g}{18\nu} \frac{\rho_w - \rho_s}{\rho_w} d^2 \tag{1}$$

To adapt this equation to sludge flocs is not easy. The size of a floc, d, varies. Initially, there are micro flocs, which settle slowly. Due to flocculation processes, the flocs grow and the settling velocity increases. The floc size can also decrease due to high shear rates. This can be modeled in multi-phase approaches (see Chapter 2.2). Within the single-phase approach, which is used in this thesis, another approach is needed to describe the settling velocity. Instead of single particles, the sludge concentration is considered.

To measure the settling velocity that is correlated with a certain sludge concentration, a standard method can be conducted, according to DIN 38414. A 1 l graduated cylinder with a diameter of 6 cm is filled with sludge. The height of the sludge interface is recorded over 30 minutes. The height after 30 minutes is defined as sludge volume SV, the dimension is ml/l.

In the standard method, several phases of settling can be defined, according to Coe and Clevenger 1916 (see Figure 1). First, a brief phase of flocculation occurs.

The sludge becalms after the cylinder is filled, flocs develop (E), and a sludge interface appears (F). Thereafter, hindered settling takes place, where the settling of the flocs is hindered by the upwelling water that is displaced by the flocs underneath (G). In this phase, the settling velocity reaches its maximum. Then there is a transient phase (H), after which the compression phase starts (J). During the compression phase, the flocs form a matrix and the water is pressed out very slowly.

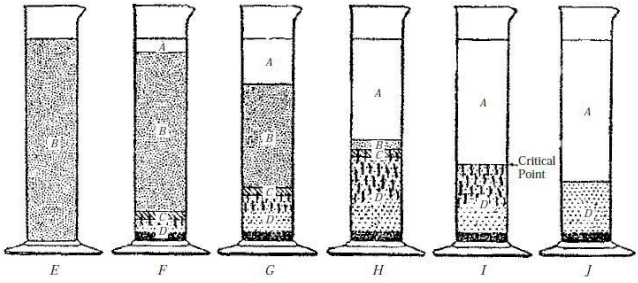

Figure 1: Settling of a flocculent suspension as illustrated by Coe and Clevenger 1916 (found in Concha and Bürger 2002): (A) clear water zone, (B) zone in which the suspension is in its initial concentration (hindered settling takes place), (C) transition zone, (D) compression zone

The phases of settling can be seen in the settling curve (Figure 2), according to Pflanz 1966. After the test, the suspended solids concentration c (dry mass content) of the remixed sample is determined.

The sludge volume index SVI (dimension ml/g) is defined as

$$SVI = \frac{SV}{c} \tag{2}$$

There are two major constraints regarding this standard method. If the sludge volume is below 100 ml/l, the sludge is too dilute and only a diffusive sludge interface can be observed in the first minutes and, usually, there is no graduation below 100 ml/l. If the sludge volume is over 250 ml/l, the wall effects are too dominant. The standard method suggests concentrating or diluting the sludge until the sludge volume is within the range of 100 to 250 ml/l.

A useful review of various approaches for determining the settling velocity of sludge is given by Keudel 2002. In this Chapter, only some selected approaches

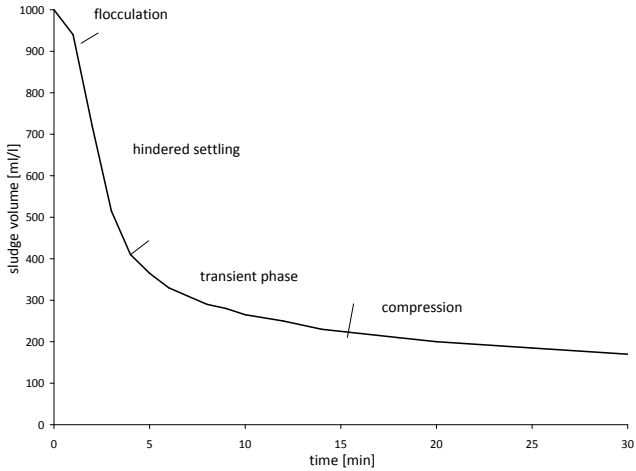

Figure 2: A typical settling curve and the different phases of settling (see Pflanz 1966 and Ekama et al. 1997)

are presented, because they help to understand the kind of measurements that are necessary to determine the parameters of the numerical model that is used in the single-phase approach.

Stobbe 1964 investigates how the geometry of graduated cylinders influences the measurement of sludge volume, settling velocity, and sludge volume index. According to his investigations, a diameter of at least 30 cm is required to avoid a significant influence of wall effects. Using a 1 l cylinder with a diameter of 6 cm is possible, if the sludge volume is below 200 ml/l. Up to this value, a linear relation between the suspended solids concentration and the sludge volume index can be observed. Above 200 ml/l, the relation is non-linear. He also finds a strong correlation between the suspended solids concentration and the settling velocity (see Figure 3).

Merkel 1971 conducts batch settling tests using the standard method with a 1 l cylinder. He states that, during the hindered settling phase, the size of the flocs, the concentration, and the settling velocity remain constant. The concentration near the sludge level is equal to the initial concentration. Therefore, he concludes that

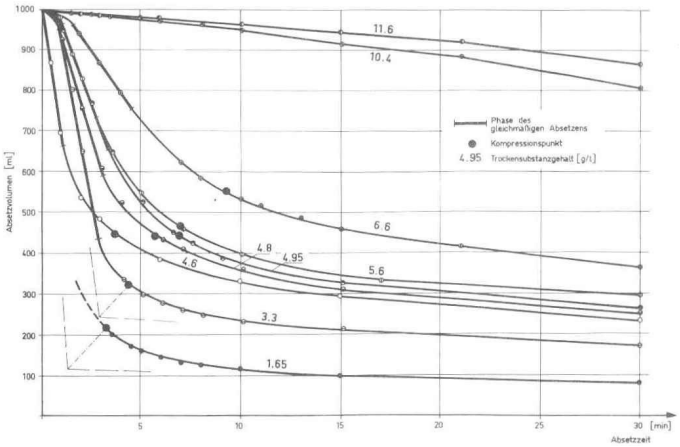

Figure 3: Sludge level over time for different sludge concentrations (Stobbe 1964)

the settling velocity during the hindered settling phase is the settling velocity for the initial concentration. He mentions that, for sludge volumes below 100 ml/l, a sludge level cannot be observed. For sludge volumes above 200 ml/l, he confirms Stobbe's observation: wall effects play a significant role when using cylinders with a diameter of 6 cm. However, he states that wall effects have a similar influence on the settling velocity and the sludge volume. He finds that there is a non-linear correlation between the sludge volume index and the sludge volume. He uses this correlation to calculate sludge volumes, which are not influenced by wall effects. Thus, he can correlate settling velocity and sludge volumes, even for sludge volumes above 200 ml/l (see Figure 4).

At a sludge volume of 480 ml/l, Merkel identifies a break point. After this point compression occurs. Consequently, the derived equation consists of two parts (the dimension of v_s is m/h in this formula):

$$SV = \begin{cases} 1000 - 600\, v_s^{0,21} & \text{for } SV \leq 480\ ml/l \\ 1000 - 840\, v_s^{0,71} & \text{for } SV > 480\ ml/l \end{cases} \tag{3}$$

The DIN 38141 sums up the work of above mentioned authors.

Dick and Vesilind 1969 have undertaken important investigations of the sludge volume index. They find that the sludge volume index is not correlated with

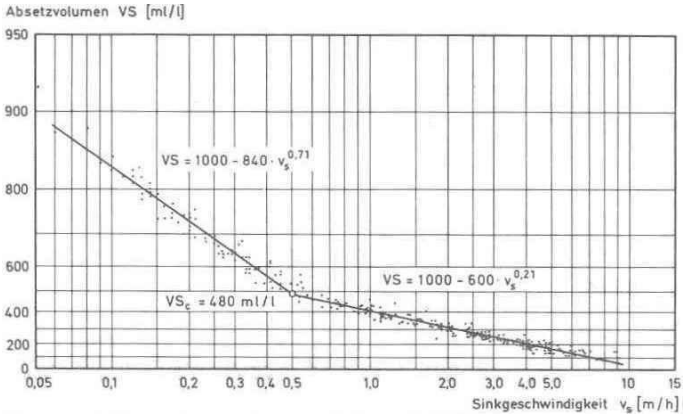

Figure 4: Sludge volume VS (equal to SV) over settling velocity (v_s) according to Merkel (1971)

suspended solids concentration, rheological characteristics such as yield strength or plastic viscosity, cylinder diameter, or initial filling depth. Thus, they conclude that the sludge volume index is valuable when monitoring the operation of a plant, but cannot be used to design plants or compare sludges from different plants. Instead, they suggest measuring the initial settling velocity of the sludge interface for several concentrations. The correlation has the form of an exponential function:

$$v_s = ae^{bc} \tag{4}$$

The parameters a and b have to be obtained from measurements. From a literature review, Billmeier 1978 finds that the values of a=6.56 and b=2.3x(-0.1652) are valid for most communal activated sludges (found in Keudel 2002). Vesilind 1968 refers to it as the “Direct Method“ to design thickeners from a series of batch settling tests.

Wahlberg and Keinath 1980 perform 185 settling tests with sludge from 21 WWTPs. In contrast to many invetigators, they stir the samples during measurements with 1 rpm and state that the scattering of the results is lower than for unstirred measurements. They use the approach of Vesilind 1968 but correlated the parameters a and b to the sludge volume index SVI. They find following relationship, which

fits reasonably to all samples (note: a and, therefore, also v_s have the dimension [m/h] here):

$$a = 15.3 - 0.0615(SVI) \tag{5}$$

$$b = -0.426 + 0.00384(SVI) - 0.0000543(SVI)^2 \tag{6}$$

Härtel and Pöpel 1992 also fit the parameters a and b to the sludge volume index SVI. Using a literature review, they formulate the following relationship (again, the dimension for a and v_s is [m/h]):

$$a = 17.4e^{-0.0113(SVI)} + 3.931 \tag{7}$$

$$b = 0.9834e^{-0.00581(SVI)} - 1.043 \tag{8}$$

This agrees relatively well with measurements by Stobbe 1964. However, the limitation is that this approach is only valid for hindered settling. For the transition phase or the compression phase, this approach does not fit well. They therefore introduced a complex correction function Ω, which also includes the break point, according to Merkel 1971 as well as other parameters that are not described in detail here.

$$\Omega = f(z, SVI, c_0, h_0, B_4^*, K_{SVI}) \tag{9}$$

The results fit reasonable well to measurements by Billmeier 1978 and allow dynamic modeling of secondary clarifiers.

Zhang et al. 2006 confirm the existence of a break point, which distinguishes between hindered settling and compression, similar to Merkel 1971. Thus, they extend Vesilind's approach by introducing a break point and two sets of parameters (again the dimension of v_s is [m/h]).

$$v_s = \begin{cases} 6.79e^{-0.345c} & \text{for } c \leq 5.846\ g/l \\ 64.2e^{-0.667c} & \text{for } c > 5.846\ g/l \end{cases} \tag{10}$$

With this set of parameters, they simulated a single settling test and achieved good agreement.

Takács et al. 1991 state that the settling theory of discrete particles in a clarifier is premature, since little effort has been made to determine the particle size distribution in a secondary clarifier. Secondly "as the concentration of solids increases, the mass of solids tends to settle as a unit. The settling velocity of the sludge blanket has been found to be a nonlinear function of the solids concentration." (p. 1264). Consequently, one should focus on the settling of the sludge blanket (or interface) rather than on particle settling. They refer to the model of Vesilind 1968 with the limitation that it is valid only for hindered settling conditions. For low suspended solids concentrations, this approach would overpredict settling velocities. Thus, they extended Vesilind's approach to make it also valid for low concentrations:

$$v_s = v_0 e^{-r_h c} - v_0 e^{-r_p c} \tag{11}$$

The maximum settling velocity is usually reached at a concentration of 1-2 g/l. The parameters v_0 and r_h can be obtained as described in Vesilind's "Direct Method". Nevertheless, "finally r_p is best assessed using a non-linear optimization search technique, such as the one considered in this study [SIMUSOLV]." (Takács et al. 1991 p. 1268). As mentioned earlier, the settling velocity for low sludge volumes below 100 ml/l or low concentrations is not easy to measure, because only a diffusive sludge interface, which settles rapidly, appears.

Finally, they include the settling velocity in a 1-D approach called the "Layered Settler Model". This model divides the settler (clarifier) into 10 layers of equal height by calculating the solids balance in each layer. They use this solids flux concept to simulate the solids profile in a clarification process.

Armbruster 2004 uses this approach for his simulations but adds a "compression-model" for high concentrations ($c > 6\ g/l$), similar to the break point of Merkel 1971 or Zhang et al. 2006; see Figure 5.

Schumacher 2006 uses the approach from Takács et al. 1991 for his simulations without a break point or modeling compression.

2.4 Basics of Rheology

Rheology describes the flow behavior of fluids but also the deformation of solids under the impact of forces. The deformation can be distinguished into plastic deformation (irreversible) and elastic deformation (reversible).

Almost all matter behaves elastically and plastically, depending on the applied forces. Solids behave more elastically, whereas fluids usually behave plastically. For numerical simulations, codes either for calculating deformation of solids (structural mechanics) or flows (CFD) are distinguished. The discretization is quite similar but the basic equations differ. The coupling of structural mechanics and fluid dynamics

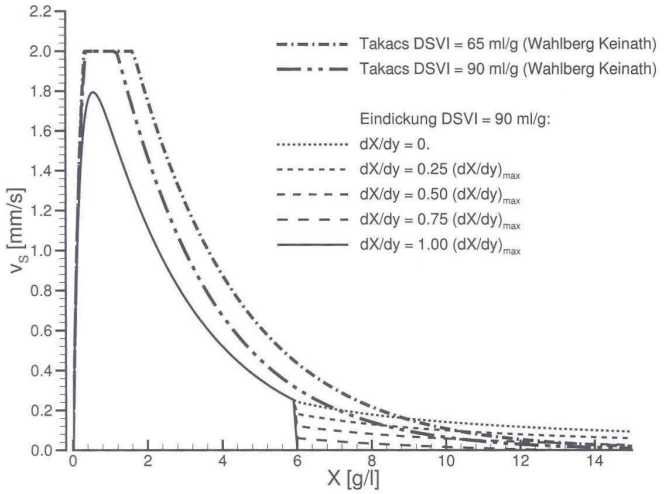

Figure 5: The Takács model modified with compression zone according to Armbruster 2004

is called fluid-structure interaction (FSI). The coupling can be performed in one way (the forces resulting from a flow deform a solid structure) or in two ways (the forces resulting from a flow deform a solid structure, which again changes the flow). In general, however, it is not possible to calculate elastic behavior with CFD codes (explanation follows in Chapter 2.5). This can be problematic for viscoplastic fluids, like sludge, where a distinct yield stress exists.

To link the plastic deformation of fluids with the applied forces, the following consideration is useful: two parallel plates with fluid in between are moved against each other (see Figure 6).

Due to the viscosity of the fluid, a certain force F is required to move the plate with the area A (Couette flow). Thus, one obtains the shear stress τ:

$$\tau = \frac{F}{A} \tag{12}$$

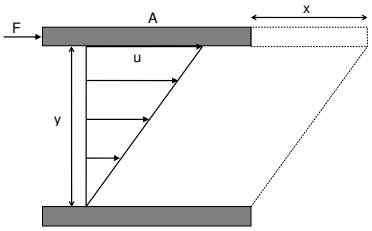

Figure 6: Couette flow

For the rheological considerations here, only the magnitudes of the vectors are relevant. The deformation γ is defined as the quotient of the displacement x and the distance between the two plates y:

$$\gamma = \frac{x}{y} \tag{13}$$

For elastic deformation, according to Hooke's law, the elastic modulus (or Young's modulus) E is defined as:

$$E = \frac{\tau}{\gamma} \tag{14}$$

For plastic deformation, the shear rate $\dot{\gamma}$ is introduced as a quotient of the relative velocity u and the distance between the plates y:

$$\dot{\gamma} = \frac{u}{y} \tag{15}$$

Equation 15 is only valid for linear velocity profiles, as they occur in laminar stratified flows (Couette flow). In general, there are nonlinear velocity profiles and 3 dimensional flows, so that the shear rate $\dot{\gamma}$ is generally defined as the square root of the second invariant of the shear rate tensor:

$$\dot{\gamma} = \sqrt{\overline{D}} \tag{16}$$

$$\begin{aligned}\overline{D} =& 2\left(\frac{du}{dx}\right)^2 + 2\left(\frac{dv}{dy}\right)^2 + 2\left(\frac{dw}{dz}\right)^2 \\ &+ \left(\frac{du}{dy} + \frac{dv}{dx}\right)^2 + \left(\frac{du}{dz} + \frac{dw}{dx}\right)^2 + \left(\frac{dv}{dz} + \frac{dw}{dy}\right)^2\end{aligned} \tag{17}$$

And the shear stress τ is generally defined as the magnitude of the vector

$$\tau = |\vec{\tau}| = \sqrt{\tau_x^2 + \tau_y^2 + \tau_z^2} \tag{18}$$

Finally, the molecular dynamic viscosity η for Newtonian fluids is defined as

$$\eta = \frac{\tau}{\dot{\gamma}} \tag{19}$$

For non-Newtonian fluids, the molecular dynamic viscosity η is not a single value but depends on the shear rate. It can be defined as the derivation of the flow curve, where τ is a function of $\dot{\gamma}$:

$$\eta = \frac{d\tau(\dot{\gamma})}{d\dot{\gamma}} \tag{20}$$

The molecular dynamic viscosity η is referred to as viscosity in this thesis. For clarification, the different types of viscosity are listed below:

- Molecular dynamic viscosity $\eta = \frac{\tau}{\dot{\gamma}}$ [Pas]
- Molecular kinetic viscosity $\nu = \frac{\eta}{\rho}$ $[m^2/s]$
- Turbulent dynamic viscosity η_t [Pas] (see Chapter 3.3.5)
- Turbulent kinetic viscosity $\nu_t = \frac{\eta_t}{\rho}$ $[m^2/s]$ (see Chapter 3.3.5)

Various types of viscometers exist to conduct rheological investigations. Capillary tubes or falling spheres are suitable for Newtonian fluids (Moshage 2004). A disadvantage is that the flow behavior cannot be described accurately (Dick and Ewing 1967). Therefore, a widespread measuring device is the rotational viscometer. A bob rotates in a cup (Searle-type) or a cup rotates around the bob (Couette-type). Most devices measure the moment (or torque) for a given rotational speed (Controlled Rate), but it is also possible to measure the rotational speed for a given

moment (Controlled Stress). With respect to some constraints, the flow in the annulus between the bob and the cup is similar to the Couette flow (see Figure 7). The annulus is defined as the three-dimensional fluid body between the cup and the bob of a viscometer.

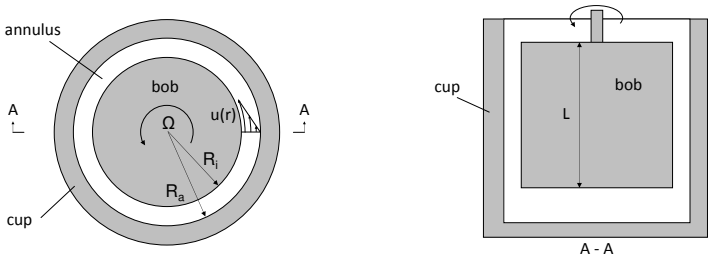

(a) (b)

Figure 7: Flow and geometry of a rotational viscometer (Searle type)

Because the viscosity is not measured directly, it has to be derived from the measured moment and rotational speed. The derivation of the basic equation (Margules equation) for Newtonian fluids, laminar flow, and rotational viscometers is presented briefly here, according to **van Wazer et al.** 1963.

The shear rate $\dot{\gamma}$ is

$$\dot{\gamma} = \frac{r d\omega}{dr} \tag{21}$$

with the angular velocity ω and the radius r. The shear stress τ is

$$\tau = \frac{M}{Ar} = \frac{M}{2\pi r L r} \tag{22}$$

with the moment M, the length of the bob L and the curved surface area A of the bob. The viscosity η is (for Newtonian fluids)

$$\eta = \frac{\tau}{\dot{\gamma}} = \frac{M}{2\pi r^2 L}\frac{dr}{r d\omega} \Leftrightarrow \frac{M}{\eta 2\pi L}\frac{dr}{r^3} = d\omega \tag{23}$$

With integration, one obtains the Margules equation

$$\frac{M}{\eta 2\pi L}\int_{R_i}^{R_a}\frac{dr}{r^3}=\int_0^{\Omega}d\omega \tag{24}$$

$$\frac{M}{\eta 2\pi L}\left(-\frac{1}{2R_a^2}+\frac{1}{2R_i^2}\right)=\Omega \tag{25}$$

Instead of the inner and outer radius R, the ratio δ is often used

$$\delta=\frac{R_a}{R_i} \tag{26}$$

which leads to

$$\frac{M}{\eta 4\pi L}\frac{\delta^2-1}{R_i^2\delta^2}=\Omega \Leftrightarrow \eta=\frac{M}{\Omega}\frac{1}{4\pi L R_i^2}\frac{\delta^2-1}{\delta^2}=k_\nu\frac{M}{\Omega} \tag{27}$$

This is also the basis of the DIN 53019 standard. End effects have not yet been considered. Therefore, a factor c_L is introduced in the DIN 53019 standard (Equation 84 in Chapter 4.2.3), which is 1.0 for ideal (infinite) coaxial cylinders with no end effects and 1.1 for the standard geometry (see also Chapter 4.2.3).

The factor c_L does not only depend on the geometry but also on the fluid, if it is non-Newtonian. The flow in the annulus becomes different (see Figure 8 and compare b with c and d). Therefore, the shear rate is different for non-Newtonian fluids. This becomes apparent for low rotational speeds. But how are the different shear rates accounted for in measurements with standard viscometers? The DIN 53019 standard therefore states that the c_L factor is not constant for non-Newtonian fluids.

2.5 Viscosity of Sludge

The molecular viscosity is a material property, unlike the turbulent viscosity. The turbulent viscosity in turbulent flows is some orders of magnitude greater than the molecular viscosity. The situation changes, however, in settling zones. The flow velocities are low, in order to separate the sludge from the clear water. At the same time, the sludge concentration increases and therefore the molecular viscosity can become dominant. A good survey of the rheological characteristics of sludge from WWTPs can be found in Proff and Lohmann 1997b.

First of all, the molecular viscosity depends on the type of fluid. For water, it is a function of pressure p and temperature T. For sludge, the viscosity is a function

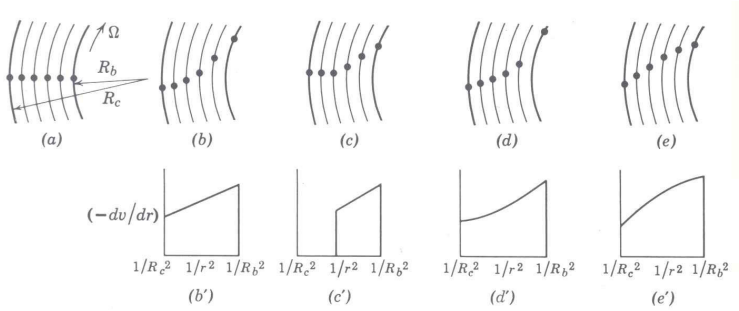

Figure 8: Flow streamlines in the gap of a concentric cylinder viscometer. (a) At rest, (b) Newtonian flow, (c) plastic flow, (d) viscoplastic flow, (e) dilatant flow. Van Wazer et al. 1963

of concentration c, shear rate $\dot{\gamma}$, time t, pressure p, temperature T and other, as yet unknown, factors.

$$\eta = f(c, \dot{\gamma}, t, p, T, \dots) \tag{28}$$

The basic rheological models, which describe the link between the shear stress and the shear rate, as displayed in Figure 9, will now be discussed.

Newtonian fluids are characterized by a proportional relationship between the shear rate and the shear stress: the higher the shear rate, the higher the required shear stress (or force). This relationship can be visualized in a flow curve (see Figure 9 top left) and by the following mathematical expression:

$$\tau = \eta\dot{\gamma} \tag{29}$$

The viscosity is the slope (the derivation) of the flow curve and, as one can see, it is constant for Newtonian fluids. Since water and most gases are Newtonian fluids, this model has a broad field of application.

Bokil and Bewtra 1972 found that the viscosity of activated sludge increases with the concentration and assumed Newtonian behavior for low shear rates. For concentrations above 0.7 g/l, they formulated

$$\eta = 0.00327 \times 10^{0.132c} \tag{30}$$

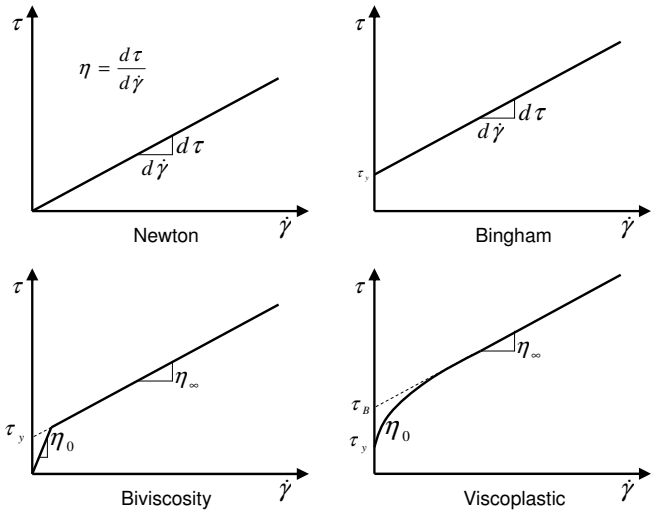

Figure 9: Overview rheological models

Armbruster 2004 uses this approach for his 2-D simulation of secondary clarifiers and compares it with the Bingham model, according to Dahl et al. 1994 and Lakehal et al. 1999. He states that the implementation of a rheological model that depends on concentration provides better results than using the viscosity of water alone, when the results are compared with measurements from a treatment plant. Furthermore, there is a strong relationship between the applied settling function and the rheological model. The Bingham model provides more realistic results than the Newtonian models.

Hanel 1982 measures the viscosity of sludge with a capillary tube viscometer. He states that, for low sludge concentrations, the viscosity is only slightly higher than for water and therefore Newtonian. Low sludge concentration also refers to the concentration of activated sludge in aeration tanks. For higher sludge concentrations, there is viscoplastic behavior, but he does not define how to distinguish between lower and higher concentrations.

However, many fluids cannot be described as Newtonian fluids. **Bingham** thus introduces a yield stress τ_y. This means that only when a certain shear stress is applied, which is higher than the yield stress, does the fluid begin to flow. Otherwise, the "fluid" behaves like an elastic solid. A vivid example is jelly. The flow curve is visualized in Figure 9, top right. The formula is:

$$\tau = \tau_y + \eta\dot{\gamma} \tag{31}$$

At the first glance, it seems that the viscosity of Bingham fluids is the same as for Newtonian fluids. But this is true only for shear stresses above the yield stress. Up to that point, the fluid does not flow at all and the viscosity moves towards infinity. Because numerical models use the viscosity to calculate the Navier-Stokes equation, one can see the difficulties in modeling ideal Bingham fluids. What is usually done (also in ANSYS FLUENT) is to approximate the Bingham model with a **"biviscosity"** model, which means setting a very high but finite viscosity η_0 for low shear rates and the Bingham viscosity η_∞ for higher shear rates (see Figure 9, bottom left, as well as Tanner and Milthorpe 1983, Siew et al. 1992, and Schumacher 2006).

Dick and Ewing 1967 have investigated the rheology of activated sludge fundamentally. They use a rotational viscometer, because

- it can be operated continuously, so that time-dependent effects can be measured (thixotropy),
- multi-phase fluids with particles can be considered by adapting the size of the measuring gap (the distance between the outer wall of the bob and the cup),
- it is applicable for plastic materials like sludge, because the shear rate is variable.

To avoid Taylor vortices at higher shear rates, they modify the rotational viscometer to a Coutte-type and roughen the cylinders to avoid slippage. They also describe the problem of settling during the measurements and thixotropic effects. Thixotropic effects refer to how much shear has been applied to the sample before the measurement starts. Starting the measurements with a viscometer with low shear rates up to a certain level and then decreasing the shear rate again results in a hysteresis in the flow curve. For details on how to model thixotropic behavior numerically, see Toorman 1997 and Brenda 2007. Larger solids were removed by a mesh screen. They predicted a Bingham behavior for the flocculent structure, and correlated the yield stress with the sludge concentration.

$$\tau_y = j_D e^{k_D c} \tag{32}$$

The constants j_D and k_D are specific for the investigated sludge but no values are given for the sludges from the 3 different WWTPs that have been investigated. That η_∞ might also depend on the sludge concentration is not considered.

Dahl et al. 1994 do not directly measure the viscosity of activated sludge, but assume Bingham behavior and calibrate the parameters by 2-D simulations and measurements of a test settling tank. From their curves, Lakehal et al. 1999 approximated the following relationship

$$\tau = \tau_y + \eta_\infty \dot{\gamma} \tag{33}$$

$$\tau_y = 0.00011 e^{0.98c} \tag{34}$$

$$\eta_\infty = \eta + 0.0002473 c^2 \tag{35}$$

The range of sludge concentration is between 0 and 20 g/l. For higher sludge concentrations, the yield stress τ_y becomes unrealistically high. For their 2-D simulation of secondary clarifiers, Lakehal et al. 1999 uses this approach and a slightly modified "biviscosity" model. They state that the removal system in secondary clarifiers is necessary to overcome the yield stress, so that the sludge can flow toward the central withdrawal. The implemented rheological model also influences the height of the sludge blanket.

Schumacher 2006 uses a rotary viscometer to measure the flow curve of activated sludge from a WWTP. He applies the "biviscosity" approach and correlates the parameters with the sludge concentration. From his figures, the following relationships can be derived, with good agreement ($R^2 > 0.99$)

$$\tau = MIN\left(\eta_0\dot{\gamma}, \tau_y + \eta_k\dot{\gamma}\right) \tag{36}$$

$$\eta_0 = 0.0038c^2 - 0.0041c + 0.001 \tag{37}$$

$$\eta_k = 0.00008c^2 + 0.0001c + 0.001 \tag{38}$$

$$\tau_y = 0.0002c^3 - 0.00002c^2 + 0.0049c \tag{39}$$

For a sludge concentration of 0 g/l, the viscosity is equal to the one of water (0.001 Pas). The range he measures is between 0.1 and 12.6 g/l and only for low shear rates up to 10 s^{-1}. He implements this rheological model, together with a model that describes settling, to conduct 2-D simulations of a secondary clarifier. He also states that there is no reliable correlation between sludge parameters and rheological properties; therefore, rheological measurements are necessary for each plant in which simulations are conducted (he simulates 3 different secondary clarifiers). He finds that, in the numerical simulations, the sludge level appears in a zone where very low shear rates occur (between 0 and 1 s^{-1}) and therefore this zone is very important for rheological models. On the other hand, the accuracy of most viscometers at such low shear rates is relatively low.

As measuring instruments have become more accurate, many non-Newtonian fluids show a behavior, at low shear rates, that is called **viscoplastic** (or shear thinning). This means a nonlinear shear rate - shear stress relationship and a decreasing viscosity with increasing shear rates. A flow curve for this phenomenon is shown in Figure 9, bottom right.

It is obvious that the yield stress τ_y is much lower than in the Bingham model τ_B. Barnes and Walters 1985 conclude therefore, that there is no yield stress and the viscosity is always finite. This assumption has some advantages for numerical models, but neglects the following effect: when a mixture of water and sand is modeled as a fluid (single-phase or multi-phase) and one pours sand into a glass of water, a conical heap with a specific angle of repose will appear. With a finite viscosity, this conical heap will deliquesce after some time, due to the shear stresses resulting from pressure and gravity forces. In reality, however, the conical heap will not deliquesce. From this consideration one can conclude that there are fluids in which a yield stress exists.

Various mathematical functions are used to describe this nonlinear relationship; these are listed below:

Ostwald-de Waele

$$\tau = K\dot{\gamma}^n \tag{40}$$

Herschel and Bulkley

$$\tau = \tau_y + K\,\dot{\gamma}^n \tag{41}$$

Windhab

$$\tau = \tau_y + (\tau_B - \tau_y)\left[1 - e^{\frac{-\dot{\gamma}}{\dot{\gamma}^*}}\right] + \eta_\infty \dot{\gamma} \tag{42}$$

Casson

$$\sqrt{\tau} = \sqrt{\tau_y} + \sqrt{\eta_\infty \dot{\gamma}} \tag{43}$$

$$\tau = \tau_y + \frac{(\eta_0 - \eta_\infty)\dot{\gamma}}{1 + \frac{(\eta_0 - \eta_\infty)\dot{\gamma}}{\tau_B - \tau_y}} + \eta_\infty \dot{\gamma} \tag{44}$$

Slatter 1997 uses a rotary viscometer to measure the flow curve of digested sludge. He uses the Herschel-Bulkley approach and correlated the parameters with the sludge concentration.

$$\tau_y = 13400 \frac{c^3}{0.425 - c} \tag{45}$$

$$K = 0.001 \left(1 - \frac{c}{0.425}\right)^{-35.3} \tag{46}$$

$$n = -15.6c^2 - 4.59c + 1 \tag{47}$$

The sludge mass fraction c in these formulae has, exceptionally, the dimension [g/g]. There are only three samples, with different sludge concentrations, from which he derives the above formulae: 31.7, 46.4. and 66.2 g/l (interestingly, here Slatter uses [g/l] and not [g/g], as in his formulae).

Günder 1999 also uses a rotary viscometer to measure the flow curve of activated sludge. He also applies the Herschel-Bulkley approach and provides a table and flow curves from which the following formulae for the parameters can be derived ($R^2 > 0.98$)

$$\tau_y = 0.0098c^2 - 0.1034c \tag{48}$$

$$K = 0.001c^{0.1487c} \tag{49}$$

$$n = -0.0002c^2 - 0.0007c + 1 \tag{50}$$

The sludge concentration c has the dimension [g/l], as usual, and the range is between 8 and 50 g/l. Based on his measurements, he declares that plastic non-Newtonian behavior starts at a concentration between 3 and 5 g/l.

Rosenberger et al. 2002 investigate activated sludge from 9 Membrane Bioreactors. They use a rotary viscometer and compare the measurements with the Herschel-Bulkley and the Ostwald-de Waele approaches. They argue that the accuracy of measurements for low shear rates is low and the correlation between the yield stress and the sludge concentration is also poor. Therefore they neglect the yield stress and decide to use the Ostwald-de Waele approach with following parameters

$$K = 0.00041e^{2c} \tag{51}$$

$$n = 1 - 0.23c^{0.37} \tag{52}$$

The range of sludge concentration is between 10 and 50 g/l. Even though they investigate sludge from 9 different plants, the parameters for all the sludges were almost identical. They conclude that the sludge concentration is the most important factor for determining the rheological behavior, and not the mode of operation or the type of waste water that is treated.

Moshage 2004 investigates digested sludge from 32 WWTPs and excess sludge from 11 plants with a rotary viscometer. He finds that the rheological properties vary significantly from plant to plant. Even for the same sludge concentration (5%) and the same shear rate (500 s^{-1}), the viscosity differs by a factor of 28. Therefore, he tests the influence of other parameters on rheological properties, namely: temperature, EPS, glowing loss, particle size, pH value and the use of polymers for sludge conditioning.

The temperature has an influence on the rheological properties of sludge but less distinctive than on water. The EPS have an influence on rheological properties but not strong enough to explain the variation mentioned above. For the glowing loss, he observed no significant influence; the same was true for the particle size. The pH value has an influence but he concluded that this occurs due to the breakdown of polymers such as sugar to monomers. The dosage of polymers for sludge conditioning also influences the rheological properties but it is difficult to quantify. He concludes, therefore, that the sludge concentration, temperature and pH value influence the rheological properties but this does not fully explain the differences. Each sludge has to be measured separately to obtain the rheological properties.

To describe the flow curve of sludge, he uses a hybrid model (Ostwald-de Waele for low shear rates and Bingham for high shear rates) and the Windhab approach,

the latter of which is briefly presented here, as well as the correlation with the sludge concentration for one of the plants he has investigated.

$$\tau_y = 0.0146c^{3.5} \tag{53}$$

$$\tau_B = 0.0402c^{3.3} \tag{54}$$

$$\eta_\infty = 0.0019e^{0.44c} \tag{55}$$

$$\dot{\gamma}^* = -1.6c^2 + 17.3c - 13.5 \tag{56}$$

The sludge mass fraction c has, exceptionally, the dimension [%] in these formulae. The range of sludge concentration he measures is between 2 and 10%. The parameter $\dot{\gamma}^*$ had the worst correlation coefficient of $R^2 = 0.71$ and it must be mentioned that, for concentrations below 2%, negative values can occur, which makes it difficult to use these formulae for numerical simulation.

2.6 Discussion about the Viscosity of Sludge

Various models exist to describe rheological properties of sludge that depend on the concentration. Some focus on low sludge concentrations, somewhere between 0 and 20 g/l (Bokil and Bewtra 1972, Dahl et al. 1994 and Schumacher 2006), to model secondary clarifiers. Others focus on more highly concentrated (digested) sludge in the range of 10 to 100 g/l (Slatter 1997, Günder 1999, Rosenberger et al. 2002 and Moshage 2004). Except for Bokil and Bewtra 1997, all investigators report plastic behavior, even though some deny the existence of a yield stress. The flow curves of all models are shown in Figure 10 for 10 g/l and for 40 g/l.

This comparison demonstrates that the Newtonian approach (Bokil and Bewtra 1972) is applicable only for very low shear rates and low sludge concentrations. At 40 g/l, it is already out of range. Also Dahl et al. 1994 is out of range. The Bingham or "biviscosity" approach (Dahl et al. 1994 and Schumacher 2006) is also limited to low shear rates and low sludge concentrations, but delivers good results for simulations of secondary clarifiers.

Except for Dahl et al. 1994, all investigators use rotary viscometers to measure the flow curve. All investigators state a strong relationship between viscosity and sludge concentration and shear rate. The influence of temperature, pressure or time (thixotropy) appears to be relatively small (Moshage 2004, Rosenberger et al. 2002 and Lotito et al. 1997). Monteiro 1997 performs rheological investigations on how

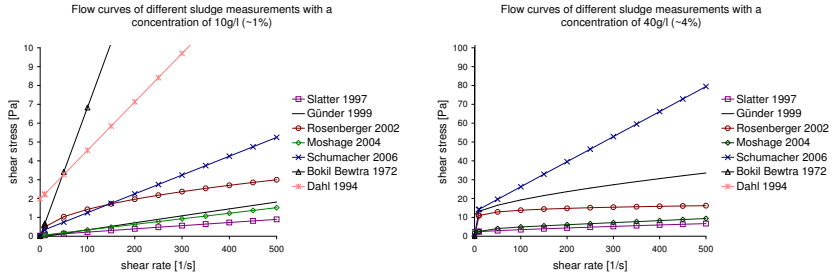

(a) 10 g/l (b) 40 g/l

Figure 10: Comparison of different rheological models for sludge for 2 sludge concentrations

different process stages (namely digestion) influence the viscosity of sludge and states: "The time evolution of the rheological parameters clearly shows that the digestion process has a very strong influence on the rheological behaviour of the sludges" (p. 65). He explains this with two hypotheses:

- "These solids may be considered as macromolecules dissolved in water; the anaerobic digestion changes the rheology of the liquid phase.
- These solids may be considered links between the bacteria and the bigger solid particles, which are gradually removed changing the solid structure of the sludge." (p. 66)

Consideration of the process of anaerobic digestion makes it clear that the organic matter in the activated sludge is gradually transformed into inert matter. This means that the ability of the bacteria to form flocs and to build up certain structures diminishes and the viscosity changes.

Not only the treatment process, but also the measurement method influences the viscosity of sludge. Because a standard method to measure the viscosity of sludge does not exist, there are significant differences in the applied methods. Some investigators use devices with a broad measuring gap (>1 mm), others a narrow gap (<1 mm). Some paid attention to thixotropic effects; others did not. Rosenberger et al. 2002 state that the thixotropic effects are small. The temperature also differs: digested sludge is usually warmer than activated sludge. Most investigators mention that the sludge was filtered prior to measuring. None of the investigators considers the fact that the flow in the annulus for non-Newtonian fluids differs from Newtonian fluids, resulting in different c_L factors (Figure 8). In numerical terms:

the measured viscosity of sludge with a concentration of 10 g/l and a shear rate of 10 s^{-1} varies from 2 to 68 mPas.

Measuring the viscosity of sludge in the range of concentration between 0 and 10 g/l is difficult, due to settling, shear thinning, and thixotropic effects, as many investigators have mentioned (Dick and Ewing 1967, Dentel 1997, Lotito et al. 1997, Schumacher 2006 and others). One strategy to bypass the problem of settling (see Figure 11) is to measure sludge with a concentration higher than 10 g/l, where the settling velocity is low, so that during the time of measurement no separation takes place, and then to extrapolate the rheological model for lower concentrations. When the concentration is too high - for example dewatered sludge - measurements with a viscometer are not feasible at all. Fehlau and Specht 2001 developed a kneading machine in order to characterize the rheology of dewatered sludge.

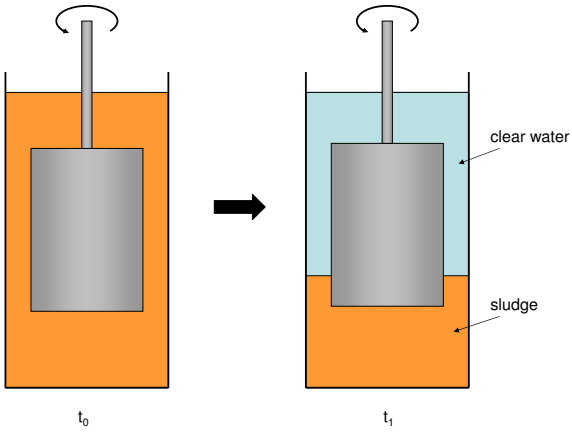

Figure 11: Difficulties while measuring the viscosity of low concentrated sludge with a standard viscometer because of settling

Finally, it can be stated that the comparison of rheological measurements is very limited, because a variety of methods was applied. Lotito et al. 1997 therefore claims that one could define a standard set-up for measuring the viscosity of sludge. This would help to make measurements comparable. But the fact that there is still no standard set-up demonstrates the crucial point: when the results differ so much,

depending on which method is applied, what informative value do the results have? Poitou et al. 1997 use different standard tests from solid mechanics to investigate sludge (triaxial test, squeezing test, and viscometer). “But because of the lack of any real justified three-dimensional mathematical modeling of the materials’ behaviour, particular attention must be paid if one wants to extrapolate these normalised results to make predictions under other loading conditions“ (p. 25). In other words, what is the real physical viscosity of sludge? To quote Dentel 1997: “In summary, the complexities we encounter when dealing with wastewater sludges not only create difficulties due to the creation of more complex rheological models [...]; even worse, they impair the ability to even perform rheological measurements that are fundamentally justified rather than operationally defined“ (p. 5). This question is fundamental, since the numerical sludge model demands a “fundamentally justified“ physical viscosity.

3 Applied Methods

The question whether one should use EFD or CFD for flow investigations is wrong. Good practice is to use both tools in combination. Usually, CFD helps to reduce the number of variations of hydraulic models, but every numerical model should be validated with hydraulic models or prototypes. EFD delivers also numerous parameters that are included in numerical models and it helps to extend numerical models or re-calibrate existing models for a new field of application.

In this thesis, numerical and hydraulic models are used to create a hybrid sludge model that is able to describe the behavior of sludge in water treatment processes with a minimum of computational and measurement effort. The hydraulic models used within this thesis are the settling test and the process-viscometer. The question is, which numerical approach to modeling should be used: the single-phase or the multi-phase approach? The advantages and disadvantages of both approaches are summarized in Table 1. In order to save computational time and effort (as defined in the overall goal of the thesis), the choice is the single-phase approach. The difficulties involved in measuring the viscosity of sludge are tackled in this thesis with a new method that uses a process-viscometer and hybrid sludge modeling.

What is hybrid sludge modeling and how does it differ from conventional sludge modeling? Krebs et al. 2000, Armbruster 2004, and Schumacher 2006 perform measurements in order to obtain parameters for the numerical model (e.g. settling velocity or viscosity). These parameters are incorporated into the numerical model and then plants are simulated and validated with measurements at real plants or prototypes. This is referred as conventional sludge modeling.

In this thesis, a novel, iterative hybrid method (hybrid sludge modeling) is developed: parameters are delivered by measurements, but the measurements themselves are simulated with CFD, in order to interpret the measurements and to calibrate and adjust the parameters of the hybrid sludge model. This iterative process results in a higher quality of the parameter set and a higher reliability of the sludge modeling. For the viscosity, it is assumed that the agreement between measurement and simulation indicates the “fundamentally justified“ physical viscosity. Finally, a testing plant (here a lamella clarifier) is simulated with the validated parameters. The results of the simulation are compared with measurements from the real plant, which emphasizes the high reliability of the hybrid sludge model. The hybrid sludge modeling approach, compared to conventional sludge modeling approaches, is visualized in Figure 12.

The numerical single-phase sludge model, as part of the hybrid sludge modeling approach, consists basically of the following elements:

- Diffusion as a function of turbulent viscosity (Equation 64)

	Modeling sludge	
	Multi-phase	Single-phase
Advantages	• Relative velocities between the two phases can be modeled	• Low computational efforts • Few input parameters and submodels necessary
Disadvantages	• High computational efforts • Lot of input parameters and submodels necessary • Sensitive to particle size, which is difficult to define	• No relative velocities between the two phases can be modeled, but hyperconcentrated sludge phase can become nearly independent from bulk flow (stratified flow) • Difficult to measure the viscosity of sludge

Table 1: Comparison of multi-phase and single-phase approaches

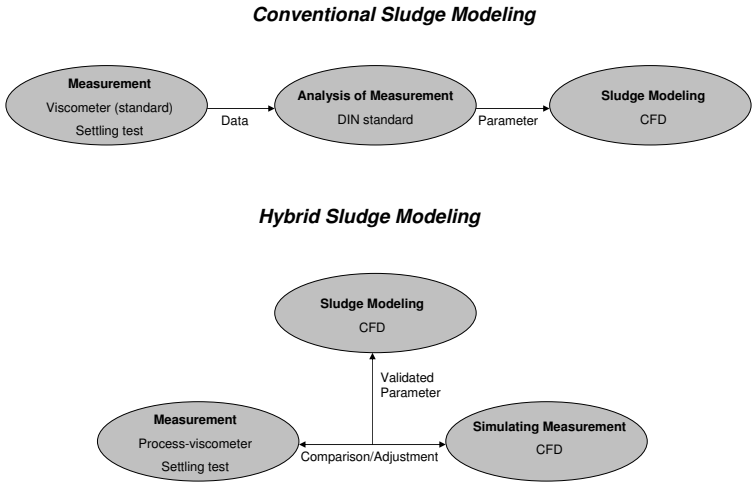

Figure 12: Conventional sludge modeling versus hybrid sludge modeling

- Density as a function of concentration (Equation 66)
- Settling velocity as a function of concentration according to Takács et al. 1991 (Equation 80)
- Viscosity as a function of concentration and shear rate according to the rheological model of Worrall and Tuliani 1964 (Equation 100)

The coupling of the **diffusion** coefficients with the turbulent viscosity is already described in the ANSYS FLUENT user's guide and will be explained in more detail in Chapter 3.3.3.

How to determine the **density** of a mixture of water and dry matter is described by Zanke 1982 and other authors and will be explained in more detail in Chapter 3.3.4. Within this thesis, concentration means the dry matter of sludge with the dimension [g/l] according to DIN 38409. For low concentrations, a filtered sample is dried at $105°C$ (DIN 38409 Part 2); for high concentrations the sample is not filtered beforehand (DIN 38409 Part 1).

Because there are several methods for determining the **settling velocity**, it should be discussed briefly. The numerical model provides the sludge concentration; therefore, a method is needed in which the settling velocity is calculated from the sludge concentration. Dick and Vesilind 1969 provide such a method. The problem is that the maximum settling velocity occurs at a concentration of 0 g/l. This would mean that there is no residual turbidity in the clear water, after settling. Because this is not true, a method is preferred in which the settling velocity decreases for low concentrations. Takács et al. 1991 deliver such a method. The remaining question is whether a break point should be included, as done by Merkel 1971, Armbruster 2004, and Zhang et al. 2006. This will be discussed in Chapter 4.1.2.

The choice of the **rheological model** should also be discussed briefly. As explained in Chapter 2.5, sludge is a non-Newtonian fluid. Since the Bingham model, in its original form, is not applicable in CFD codes, only the viscoplastic models remain. They are continuously differentiable without break points (as in the "biviscosity" approach) and represent a broad range of shear rates and sludge concentrations. For numerical simulation, it is important to correlate the rheological parameters with the sludge concentration in such a way that unrealistic values for the viscosity cannot occur (negative or extremely high values or division by zero). Most investigators apply either the Herschel and Bulkley or the Ostwald-de Waele approach. The author prefers the rheological model of Worrall and Tuliani 1964 for several reasons:

- The parameters of the model can be intuitively understood and are not as abstract as in the other rheological models (see Figure 9 in Chapter 2.5). This is quite important for the curve fitting.

- The yield stress can be set to zero.

- This approach is able to describe Newtonian behavior exactly if $\eta_0 = \eta_\infty$.

Knoch and Malcherek 2011 use this model for simulating fluid mud, but it has not been used for sludge in water treatment processes as often as the Herschel and Bulkley or Ostwald-de Waele approaches.

The sludge model is included into the commercial software ANSYS FLUENT 14.5 via user defined functions (udf).

Because the hybrid sludge model combines hydraulic models (EFD) and numerical models (CFD), the theory and basic equations of these models are presented in the following Chapters, focusing on the aspects that are relevant for the hybrid sludge model.

3.1 Experimental Fluid Dynamics (EFD)

Modeling sludge with hydraulic models is a complex task. Achieving dynamic similarity for sediments is already difficult and considerable efforts have been undertaken and are still undertaken to generate new knowledge about erosion and sedimentation processes, appearance and movement of dunes, etc. (see ATV-DVWK 2003). Modeling sludge is similarly complex and there is a potential hygienic risk associated with the usage of activated sludge. Therefore, Köster and Tacke 2006 attempt to find an artificial substance, which has a dynamic behavior similar to that of activated sludge but is hygienically harmless, and they find Polysulfon.

A hydraulic model is usually smaller, on the length scale, than the prototype. However, when downscaling of the geometry (considering the geometric similarity), one has to ensure that that the time-dependent effects are similar (kinetic similarity) and the dynamic properties (forces) of the flow in the hydraulic model are similar to the flow properties in the prototype (dynamic similarity). This leads to the model laws. For tasks within the field of water and waste water treatment, there are two important model laws: Reynolds model law and Froude model law (see Kobus et al. 1984).

The Reynolds model law is important for flows, where viscosity plays a major role. The Reynolds number in the hydraulic model Re_m must be equal to the Reynolds number of the prototype Re_p:

$$Re_m = \frac{u_m l_m}{\nu_m} = \frac{u_p l_p}{\nu_p} = Re_p \tag{57}$$

Because, in most hydraulic models, water is also used ($\nu_m = \nu_p$) in order to obtain the Reynolds number similarity, the flow velocity scale is inversely proportional to the length scale:

$$\frac{u_p}{u_m} = \frac{l_m}{l_p} \tag{58}$$

For example, if the length scale is 1:10, the flow velocity in the hydraulic model must be ten times higher than the flow velocity in the prototype.

The Froude model law is important for flows in which gravity plays a major role (flows with free surfaces, waves, etc.). Here the Froude number in the hydraulic model Fr_m must be equal to the Froude number of the prototype Fr_p:

$$Fr_m = \frac{u_m}{\sqrt{g_m l_m}} = \frac{u_p}{\sqrt{g_p l_p}} = Fr_p \tag{59}$$

Since all hydraulic models are built on earth ($g_m = g_p$), in order to obtain the Froude number similarity, the flow velocity scale is proportional to the square root of the length scale:

$$\frac{u_m}{u_p} = \frac{\sqrt{l_m}}{\sqrt{l_p}} \tag{60}$$

For example, if the length scale is 1:10, the flow velocity in the hydraulic model must be $\sqrt{1:10} = 0,32$ times of the flow velocity in the prototype.

From this example, one can see that dynamic and kinematic similarity can be obtained only in 1:1 models, which have been adopted within this thesis. In most practical cases, turbulent flows are investigated, which are turbulent rough. In this case, the Reynolds number similarity can be neglected, but a similarity concerning the behavior of sludge is not yet given.

Since Hubert Engel started using model experiments for investigating river flows in Dresden at end of the 19^{th} century, extensive experience and know-how has been collected (Kobus et al. 1984). The advantages are:

- High degree of transparency
- Good validity
- Good transferability of results (when model laws are considered)

On the other hand there are also some disadvantages:

- Construction and measurements of model experiments are expensive
- Limitations due to model laws and size of the laboratory (minimum depth of flow in the hydraulic model should be 3 cm); therefore, the vertical length scale of hydraulic models is often different from the horizontal length scale, so that similarity (especially for the wall shear stress) is not given
- Number of measured quantities is limited

3.2 Computational Fluid Dynamics (CFD)

Numerical models usually have a length scale of 1:1, so that model laws are irrelevant. Because the basic flow equations cannot be solved analytically they are solved numerically. Therefore, the geometry is divided into control volumes, which is called the mesh (or grid). The mesh consists of cells, faces, and nodes (see Figure 13). The generation of the mesh is called discretization. There are several methods for calculating the basic flow equations for these small elements.

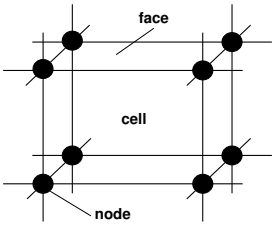

Figure 13: Mesh topology

Finite Difference Method (FDM)

The basic flow equations are partial differential equations (PDE) for infinitesimally small elements. Due to the discretization, there are now finite small elements for which difference quotients can be calculated. This method yields good results for structured meshes.

Finite Element Method (FEM)

Instead of calculating the difference between two nodes, an approximation function is derived, which is incorporated into the basic flow equations. With the Galerkin method, this is transformed into an integral expression. The residuals appearing from the inclusion of the approximation functions are minimized. The advantage of this method is that unstructured meshes can be used, because the approximation functions are independent of the element size. Tetrahedral meshes are most commonly used. A disadvantage is the greater demand for random access memory (RAM), compared to the other two methods.

Finite Volume Method (FVM)

The software applied in this thesis - ANSYS FLUENT 14.5 - is based on the finite volume method. Here, cells are not regarded as nodes, as in the other two methods. All quantities, such as velocity, pressure, concentration, etc., are calculated for one cell and are constant within this cell. Using the Green-Gauß theorem, volume integrals in a PDE are converted to surface integrals; thus, the order of PDEs is reduced by one. With this, one obtains a system of nonlinear equations, which are converted to algebraic equations and then solved. The surface integrals are regarded as fluxes into and out of a cell. Thus, this method is conservative, which is one advantage; in addition, it offers the possibility of using unstructured meshes and low RAM demand (see Oertel et al. 1999 for more details).

Discretization (referred to as pre-processing) for fluid dynamics is challenging. The requirements for the mesh quality are much higher than for structural mechanics calculations. Depending on flow velocities, as well as on the existence of small gaps or curvatures, the cell number might increase dramatically. Therefore, some experience is required to produce good meshes, whereby a good mesh is always a trade-off between an accurate (mesh-independent) solution and the computational effort for calculating the solution.

As a result of the massive development of computers and software in the last decades, it is now possible to solve simple flow problems on a personal computer. The recent trend towards parallel computing makes it possible to calculate flows for larger time and length scales. In general, using numerical models yields the following advantages:

- Boundary conditions can be controlled easily
- In hydraulic models, there is only a limited number of quantities that are measured. In numerical models, the quantities are available for the entire domain.

- In general, numerical models are less expensive than hydraulic models.
- Parameter studies can be conducted to a large extent
- Parameters can be controlled easily, which is not possible with hydraulic models (e.g. switch of the gravity or change in the viscosity of a fluid)

On the other hand, there are also some disadvantages:

- Divergence of the solution may occur
- Inaccuracies due to discretization or empirical models used (e.g. turbulence models)
- Computational effort for complex or large models can be very high (supercomputers might be required)
- Transferability of results should be analyzed critically

Work Flow of Computational Fluid Dynamics

The general work flow of CFD Analysis is presented here briefly (see Figure 14). It begins with the pre-processing, which includes several steps. The first one is the drawing of the geometry or, more precisely, the geometry of the fluid body. Usually, existing CAD drawings of plants or a device have to be transferred into a fluid body. Defining the borders of the fluid body, in particular, often requires some experience. Subsequently, the fluid body must be discretized. The process of mesh generation is automatized, but it usually presupposes considerable engineering experience in order to create a mesh with a small number of cells (which directly influences the computational efforts in the calculation) and reasonable quality (i.e. the skewness of the cells should not be too high). Then, the boundary conditions have to be defined, as well as making the decision whether the simulation is transient or steady. Additional models have to be selected (the turbulence model, the sludge model, or others). Depending on the included models, the parameters have to be set. Because the density and the viscosity appear in the Navier-Stokes equation, they represent the minimum of parameters that have to be defined. However, more parameters might be necessary if further models are included. Last but not least, the solver settings have to be set. These settings define how the discretized partial differential equations are translated into a linear algebraic equation system (the matrix) and how the coupling between the variables (pressure-density, k and ϵ, etc.) is realized. Before the calculation can start, one has to define the number of iterations for steady simulations and the number of time steps and the time step size for transient simulations. The time step size is a particularly sensitive parameter; if it is too

large, the accuracy of the simulation is low or the results may even be implausible. Then, the work of the engineer ends, for the present, and the computer calculates. This can take a few minutes or up to weeks or months, depending on the machine, the number of cells and whether it is a steady or transient simulation. Following completion of the simulation, the engineer starts with the post-processing, which is mostly done by drawing sections of the interpolated variables of interest within the fluid body (e.g. velocity profiles). These are the colorful pictures and well known from CFD analysis. They can also be animated.

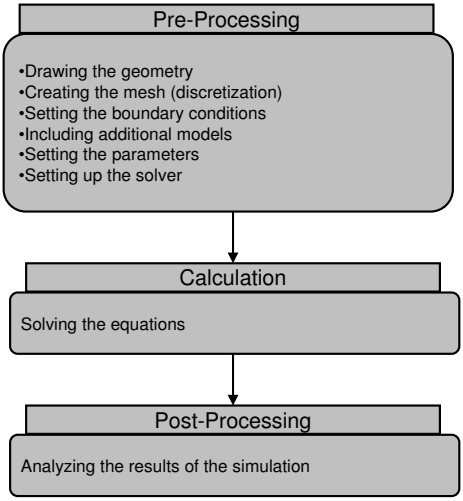

Figure 14: General work flow of computational fluid dynamics

3.3 Basic Equations for Sludge Modeling with CFD

Basically, there are two major equations that describe the flow of a fluid: mass conservation and momentum conservation (Navier-Stokes equation). Depending on the application, further equations, such as the energy equation, species transport, or turbulence models, can be added. The most important equations for the application of single-phase sludge modeling are presented in this Chapter and can be found, in German, in DWA-M 544 and the ANSYS FLUENT user's guide.

3.3.1 Mass Conservation

The mass conservation equation considers the different mass flows in a control volume. For incompressible fluids, the balance of all mass flows equals zero. For compressible fluids, the difference between inflow and outflow influences the density within the control volume. Because the density is not constant, due to the sludge model, sludge is regarded as a compressible fluid (see Figure 15 and Equation 61).

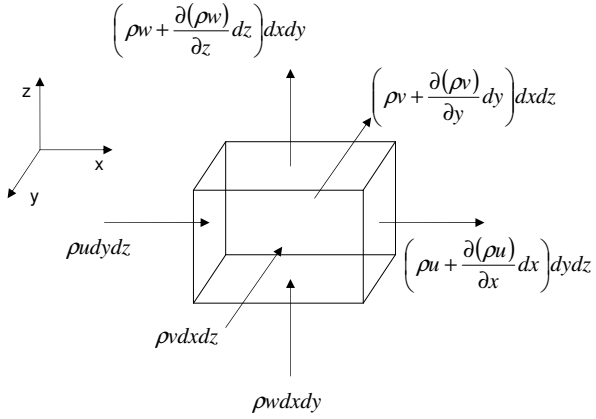

Figure 15: Mass flows in a control volume

$$\frac{\partial \rho}{\partial t} + \frac{\partial}{\partial x}(\rho u) + \frac{\partial}{\partial y}(\rho v) + \frac{\partial}{\partial z}(\rho w) = 0 \qquad (61)$$

3.3.2 Momentum Conservation

The Navier-Stokes equation describes the balance of forces for a fluid control volume. The forces are: momentum, pressure, shear, and gravity.

$$\underbrace{\frac{\partial}{\partial t}(\rho u_i)}_{transient} + \underbrace{\frac{\partial}{\partial x_j}(\rho u_i u_j)}_{momentum} = \underbrace{\rho g_i}_{gravity} - \underbrace{\frac{\partial p}{\partial x_i}}_{pressure} + \underbrace{\frac{\partial}{\partial x_j}\left(\eta\left(\frac{\partial u_i}{\partial x_j} + \frac{\partial u_j}{\partial x_i}\right)\right)}_{shear} \tag{62}$$

In numeric flow simulation, the symbol μ is frequently used for the viscosity. In the field of rheology and in the DIN 53019, the symbol η is used for the viscosity. However in this thesis η is used.

Whereas the transient term, momentum, pressure, and gravity are iteratively determined by the boundary conditions and geometry of the fluid domain and need only the density ρ as parameter, the shear term needs the viscosity η of the fluid as an additional parameter. The density plays a major role when calculating shock waves, hydraulic shocks, or acoustics. For relatively slow flow velocities, such as those prevailing in most water treatment plants, it does not effect the calculation dramatically, because the variation of the density is relatively small. However, the viscosity plays a major role in most simulation applications and the main reason for this is that the turbulence is, in many cases, modeled with a turbulent viscosity. For simulations of water treatment plants, this is also important. The second reason why it is so important for sludge modeling is the specific rheological (viscoplastic) behavior of highly concentrated sludge, which occurs preferably at places in which the turbulent viscosity becomes low. The correct modeling of the viscosity is therefore crucial for modeling the flow of concentrated sludge, which is sometimes completely different from the bulk flow (Schumacher 2006 and Armbruster 2004). The gravity term is important when multi-phase approaches are applied or in density driven flows. More details can be found in the ANSYS FLUENT user's guide.

3.3.3 Species Transport

The species transport equation describes the behavior of dissolved species in a bulk fluid (e.g. salt in water). Basically, there are two main phenomena: advection and diffusion (see Figure 16).

Advection means that the species moves with the velocity of the bulk fluid. Diffusion refers to the spreading of the species along the concentration gradient. A vivid example of diffusion is the spreading of perfume in a room, even if the air in the room does not move.

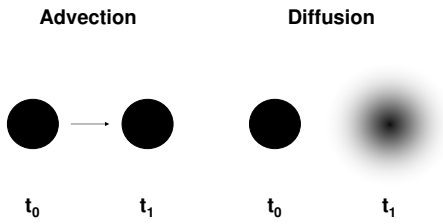

Figure 16: Advection and diffusion (according to Kinzelbach 1987)

The species transport equation is defined as:

$$\underbrace{\frac{\partial c}{\partial t}}_{transient} + \underbrace{\frac{\partial (uc)}{\partial x} + \frac{\partial (vc)}{\partial y} + \frac{\partial (wc)}{\partial z}}_{advection} = \underbrace{\frac{\partial}{\partial x}(D\frac{\partial c}{\partial x}) + \frac{\partial}{\partial y}(D\frac{\partial c}{\partial y}) + \frac{\partial}{\partial z}(D\frac{\partial c}{\partial z})}_{diffusion} + \underbrace{S}_{sourceterm} \tag{63}$$

The equation for species transport requires the flow velocity to calculate the advection. Therefore, most CFD codes solve the species transport equation sequentially, after the mass and momentum conservation equations. A new parameter appears: the diffusion coefficient D. When the Reynolds-averaged Navier Stokes (RANS) approach is used to model turbulence, as in this thesis, the very small turbulent vortices are not resolved. Because they play a major role in the distribution of a species in a fluid, the best way to model this is to couple the diffusion coefficient D with the turbulent viscosity η_t (the laminar diffusion coefficient is neglected for sludge):

$$D = \frac{\eta_t}{\Gamma \rho} \tag{64}$$

The turbulent Schmidt number Γ is an empirical parameter that is, in most cases, 0.7 (ANSYS FLUENT user's guide). The diffusion coefficient is isotropic and not constant. Detailed explanations about the turbulent viscosity η_t follow in Chapter 3.3.5.

There is no source term S in the hybrid sludge model, but one of the characteristics of sludge is its tendency to settle. The settling velocity v_s is included in the transport equation as follows (when the gravity vector $\vec{g}$ is in the negative y direction):

$$\begin{aligned}&\frac{\partial c}{\partial t}+\frac{\partial(uc)}{\partial x}+\frac{\partial(vc)}{\partial y}+\frac{\partial(wc)}{\partial z}-\frac{\partial(v_s c)}{\partial y}\\&=\frac{\partial}{\partial x}(D\frac{\partial c}{\partial x})+\frac{\partial}{\partial y}(D\frac{\partial c}{\partial y})+\frac{\partial}{\partial z}(D\frac{\partial c}{\partial z})\end{aligned} \tag{65}$$

3.3.4 Density

The density of sludge is not constant but depends on the sludge concentration.

$$\rho=\rho_w+(\rho_s-\rho_w)\frac{c}{\rho_s} \tag{66}$$

Therefore, the fluid is regarded as compressible. The density of dry sludge ρ_s is, according to Schumacher 2006, approximately 1470 kg/m^3. For organic material, van Rijn 1993 reports a range between 1200 and 1500 kg/m^3. Keudel 2002 measured 1400 kg/m^3 for dry sludge.

In most settling processes, a clearly defined sludge interface is visible. In other words, there is a steep concentration gradient and therefore a steep density gradient, which leads to a reduced exchange of momentum and sludge at the interface. This is modeled by reducing the generation of turbulent kinetic energy as a function of the density gradient. Thus, the turbulent viscosity (viable for the exchange of momentum) and the diffusion coefficient (viable for the distribution of sludge) are suppressed at the interface, where a steep density gradient prevails and stratified flow occurs (for details see the following chapter).

3.3.5 Turbulence

Turbulence is a chaotic phenomenon. Eddies of all length scales occur and finally convert kinetic energy into heat energy. It is possible to model turbulence only with the mass and momentum conservation equations (referred as direct numerical

simulation: DNS). But this requires a tremendous computational effort to resolve even the smallest eddies on a sub-millimeter scale. Even with larger computer clusters, the application is limited to very small geometries and scientific applications.

The next step is to resolve only eddies of a certain range of length scale (referred as large eddy simulation: LES). The smallest eddies are modeled roughly; only the larger eddies are resolved. This saves a lot of computational effort, in comparison with DNS, but the computational effort is still high.

For most practical applications, such as the modeling of water treatment plants, the Reynolds-Averaged-Navier-Stokes (RANS) approach is used. The eddies are not resolved, but the higher inner friction they cause is modeled as turbulent viscosity. First of all, the basic flow variables, such as velocity, are decomposed into time-averaged quantities $\overline{u}$ and fluctuating quantities u'.

$$u = \overline{u} + u' \tag{67}$$

After inserting them into the Navier-Stokes equation, one obtains the mass-weighted RANS:

$$\frac{\partial}{\partial t}(\rho\overline{u_i}) + \frac{\partial}{\partial x_j}(\rho\overline{u_i}\,\overline{u_j}) = \rho\overline{g_i} - \frac{\partial\overline{p}}{\partial x_i} + \frac{\partial}{\partial x_j}\left(\eta\left(\frac{\partial\overline{u_i}}{\partial x_j} + \frac{\partial\overline{u_j}}{\partial x_i}\right) - \rho\overline{u_i'u_j'}\right) \tag{68}$$

The same can be done with the mass conservation equation:

$$\frac{\partial\rho}{\partial t} + \frac{\partial}{\partial x_i}\left(\rho\overline{u_i}\right) = 0 \tag{69}$$

However, in the mass conservation equation, all fluctuating quantities disappear, due to averaging. Nevertheless, nine unknown variables, which are located in the Reynolds stress tensor, remain in the RANS:

$$\overline{u_i'u_j'} = \begin{pmatrix} \overline{u'u'} & \overline{v'u'} & \overline{w'u'} \\ \overline{u'v'} & \overline{v'v'} & \overline{w'v'} \\ \overline{u'w'} & \overline{v'w'} & \overline{w'w'} \end{pmatrix} \tag{70}$$

The tensor finally describes the loss of kinetic energy due to turbulence. How much energy is converted into heat energy depends on the velocity and the viscosity. Analog to the subtraction of kinetic energy from the flow through the molecular viscosity η, a turbulent viscosity η_t is defined. In turbulent flows, the turbulent viscosity is usually several orders of magnitude higher than the molecular viscosity. In

contrast to the molecular viscosity, the turbulent viscosity is not a material property. Usually, it is regarded as isotropic (Boussinesq approximation). Therefore, the Reynolds stress tensor can be written as follows:

$$\overline{u_i' u_j'} = -\frac{\eta_t}{\rho}\left(\frac{\partial \overline{u_i}}{\partial x_j} + \frac{\partial \overline{u_j}}{\partial x_i}\right) + \frac{2}{3}\delta_{ij}k \tag{71}$$

The Reynolds stress tensor is symmetric, a function of space and time, unknown, and the problem is to close the RANS equation for solving. The definition of the turbulent viscosity reduces the unknown quantities from six to one (η_t). Several semi-empirical approaches were developed to close the RANS equation, which are introduced in the following paragraphs.

Spalart-Allmaras

This approach solves the transport equation for the turbulent viscosity. There are damping functions for the near wall treatment. It is suitable for low Reynolds numbers and robust. But it is rarely used for open channel flows (see Nezu et al. 1993) and other simulations, since the Reynolds numbers are high in most cases.

Reynolds Stress Model

The Reynolds stress model (RSM) is the most accurate approach for closing the RANS equation. It denies the assumption of an isotropic turbulent viscosity (Boussinesq approximation) and calculates the transport equation for all components of the Reynolds stress tensor. Additionally, a transport equation is calculated for the dissipation rate. Because the tensor is symmetric, this means, for 3-D simulations, seven additional variables and equations that require solving (see Oertel et al. 1999). The computational effort is relatively high, divergence is often a problem, and the results are not always better than approaches with two equations.

k-ω Model

There are two wide-spread approaches to closing the RANS equation: the k-ϵ model and the k-ω model. The advantage of these models are a wide range of practical application, better results than approaches with one equation, and relatively low computational effort. Therefore, there are several versions of each approach. Both approaches are quite similar; the main difference is that, in the k-ω model, the turbulent viscosity is not only a function of turbulent kinetic energy k and dissipation rate ω but also of the Reynolds number. This leads to better results near the wall and wall functions are not required. However, inside the flow, the results are worse than in the k-ϵ model.

k-ϵ Model

The standard k-ϵ model is a wide-spread approach closing the RANS equation. It is very efficient (only two equations must be solved) and validated by many measurements. Launder and Spalding (1974) developed this approach. The turbulent viscosity is calculated as follows:

$$\nu_t = \frac{\eta_t}{\rho} = C_\eta \frac{k^2}{\epsilon} \tag{72}$$

For the turbulent kinetic energy k and the dissipation rate ϵ, the transport equations are solved:

$$\frac{\partial(\rho k)}{\partial t} + \frac{\partial(\rho u_i k)}{\partial x_i} = G + G_b - \rho\epsilon + \frac{\partial}{\partial x_j}\left(\left(\nu + \frac{\nu_t}{\sigma_k}\right)\frac{\partial k}{\partial x_j}\right) \tag{73}$$

$$\frac{\partial(\rho \epsilon)}{\partial t} + \frac{\partial(\rho u_i \epsilon)}{\partial x_i} = \frac{\epsilon}{k}\left(C_{\epsilon 1} G - C_{\epsilon 2}\rho\epsilon\right) + \frac{\partial}{\partial x_j}\left(\left(\nu + \frac{\nu_t}{\sigma\epsilon}\right)\frac{\partial \epsilon}{\partial x_j}\right) \tag{74}$$

This leads to a quadratic profile of the turbulent viscosity in open channel flows (see Figure 17) and a logarithmic velocity profile in open channel flows (see Figure 18), which has been validated by measurements performed by Nezu et al. 1993. The five empirical parameters C_η, $C_{\epsilon 1}$, $C_{\epsilon 2}$, σ_k and σ_ϵ must be derived from measurements. In this thesis the default parameters are used. In summary, the k-ϵ model is a complex interaction between the generation of turbulent kinetic energy k and the dissipation of the turbulent kinetic energy ϵ.

Stratified Flow

The generation of turbulent kinetic energy G is generally defined as:

$$G = -\overline{u_i' u_j'}\frac{\partial \overline{u_i}}{\partial x_j} \tag{75}$$

Because the velocity gradient is very steep near the wall (logarithmic velocity profile), the generation of turbulent kinetic energy is greatest here. As mentioned in Chapter 3.3.4, the sludge interface causes steep density gradients $\frac{\partial \rho}{\partial x_i}$. Because the turbulent viscosity and the diffusion are suppressed at the interface, very little exchange of momentum or species occurs. The concentrated sludge moves nearly independently of the clear water above, which is called stratified flow. To include

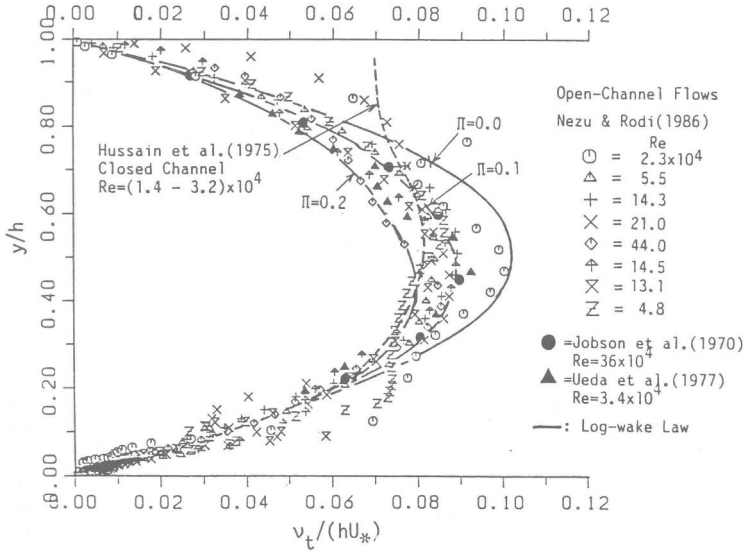

Figure 17: Distribution of turbulent viscosity ν_t in open and closed channel flows, Nezu et al. 1993

this phenomenon in the k-ϵ model, an additional term in Equation 73 is taken into account:

$$G_b = -g_i \frac{\nu_t}{Pr_t} \frac{\partial \rho}{\partial x_i} \tag{76}$$

Enhanced Wall Function

The results for the flow velocities inside the flow are quite well modeled with the k-ϵ model. However, near the wall this becomes difficult. There are some options for modeling turbulence near the wall. At the wall, the no-slip condition is valid. Due to the logarithmic velocity profile, there are steep velocity gradients near the wall. In order to obtain good simulation results, two options are available:

1. Use high grid resolution near the wall (i.e. inflation layers) to resolve the large gradients.

2. Use a wall function.

The first option is more accurate; the second option needs less computational effort. The original wall function, according to Launder and Spalding 1974, is:

$$\frac{u}{u^*} = \frac{1}{\kappa} ln(y^+ E_r) \tag{77}$$

where u is the velocity at the distance y^+ from the wall. The shear stress velocity u^* is derived from the wall shear stress or the turbulent kinetic energy k:

$$u^* = \sqrt{\frac{\tau}{\rho}} = C_\mu^{0,25} k^{0,5} \tag{78}$$

The non-dimensional wall distance y^+ is defined as:

$$y^+ = \frac{y_w u^*}{\nu} \tag{79}$$

y_w is the distance from the cell center to the wall. In Figure 18, the non-dimensional shear stress velocity $\frac{u}{u^*}$ is displayed against the non-dimensional wall distance y^+. The velocity profile is divided into four zones. Near the wall, the velocity profile is laminar (it depends only on the molecular viscosity) and is called the viscous sub layer, where $\frac{u}{u^*} = y^+$. At a greater distance from the wall, the velocity profile is logarithmic ("Log-Law", Equation 77). Between the two zones, there is

a buffer layer that can be considered with a blending function. Nezu et al. 1993 suggest that the blending zone should lie between $5 < y^+ < 30$, but other values are used as well (Rodi 1993). For very high Reynolds numbers, the velocity profile differs from the Log-Law near the surface of the open channel flow; thus, a "Log-Wake-Law" is introduced. But the Log-Wake-Law is not valid for transient, stratified flows, and is thus not considered in this thesis (see Nezu et al. 1993).

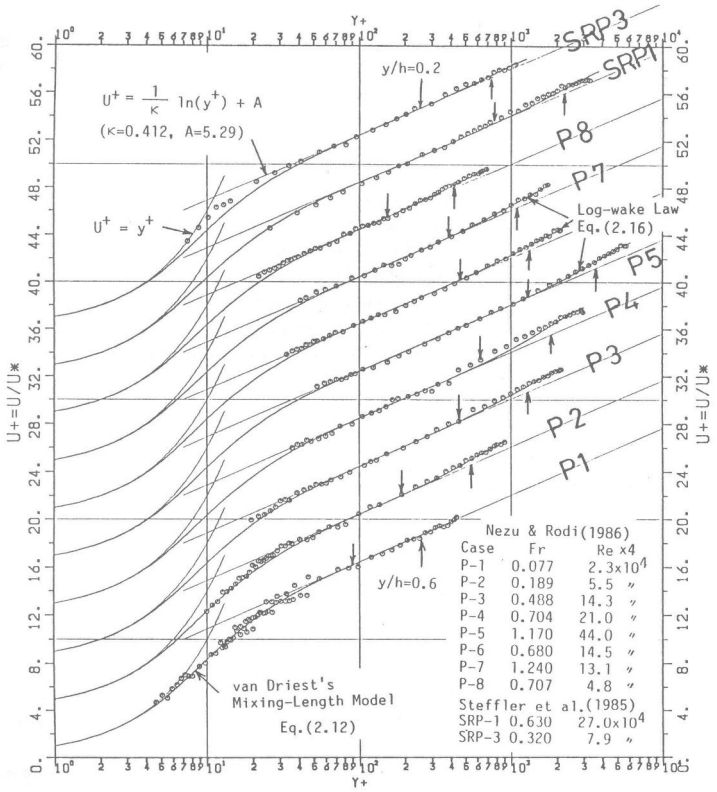

Figure 18: The four zones for the velocity profile of open channel flows with different Froude and Reynolds numbers, comparison of measured and calculated values, Nezu et al. 1993

The Enhanced Wall Treatment used in most simulations in this thesis combines both approaches. If the mesh near the wall is fine enough to resolve the laminar viscous sub layer, it calculates turbulence without using wall functions. If the mesh

is too coarse, it uses wall functions. The main advantage of this method that it is not necessary to check the y^+ values for each simulation, whether or not a wall function is needed. It automates this process (ANSYS FLUENT User's Guide 2014).

4 Results

For the characterization of sludge, two major properties have to be defined: settling velocity and viscosity. Starting with activated sludge from the communal WWTP Eberstadt, the measurement of the settling velocity is presented (Chapter 4.1.1), followed by the numerical modeling of the settling tests (Chapter 4.1.2). Hybrid sludge modeling means achieving the best possible agreement between measurements and simulation results. In a next step, the viscosity is measured with a process-viscometer, which will be introduced in Chapter 4.2.1. The procedure and the results will be described in Chapter 4.2.2. Since this approach is novel, a detailed numerical analysis of viscometers follows, in order to derive the viscosity of sludge from the measurements (Chapter 4.2.3). Finally, a lamella clarifier was operated with activated sludge from the WWTP Eberstadt and the measurements were compared with the simulation results of the lamella clarifier (Chapter 4.3) to confirm the transferability of the hybrid sludge model to complex water treatment plants.

In Chapter 4.4, the properties of other sludges are presented. Digested sludge and thickened digested sludge from the WWTP Eberstadt were compared with the activated sludge, to examine the influence of the digestion process on the sludge properties (settling velocity: Chapter 4.4.1 and viscosity: Chapter 4.4.3). Sludges from another WWTP in Griesheim were compared with the sludges from the WWTP Eberstadt as well as the results from the flocculation sludge and lime sludge from a DWTP in Langenau (settling velocity: Chapter 4.4.2 and viscosity: Chapter 4.4.4).

4.1 Settling Velocity

4.1.1 Measuring the Settling Velocity

There are simple but effective settling tests, described in the DIN 38414 standard, for examining the settling velocity of sludge. However, there are limitations for low concentrations (<1 g/l, where it is initially difficult to define the height of the sludge interface) and high concentrations (>5 g/l, due to wall effects), as described previously. Therefore, the settling tests are also modeled with CFD, in order to adjust the parameters for the numerical sludge model.

The settling tests are conducted at a communal WWTP in Eberstadt on 12 and 13 June 2012. The aeration tank from which the activated sludge probes are taken has a sludge concentration of 4.2 g/l. For the measurements, 31 samples of activated sludge are investigated. The range of concentration lays between 1 and 7 g/l, which is achieved by dilution and thickening by settling. The 1 l cylinder has a diameter of 6 cm and the sludge level is observed for 30 min. The settling curves are shown in Figure 19.

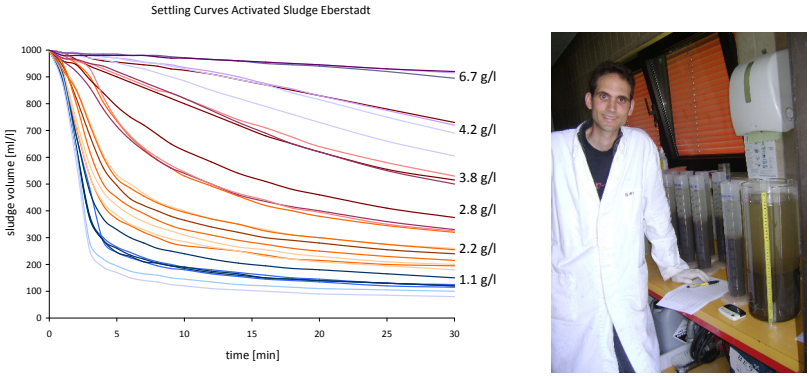

Figure 19: Settling curves (left) and measuring the settling velocity (right)

The maximum settling velocity, which usually occurs in the first few minutes, is plotted over the initial sludge concentration (see Figure 20). In a next step, the approach of Takács is fitted to the measurements (similar to Vesilind's "Direct Method"). The standard curve (red line) fits best for all values. For conventional sludge modeling, this curve would have been implemented for simulation. Hybrid sludge modeling, however, goes one step further and first simulates the settling tests, in order to calibrate the sludge model with the measurements. Several variations are tested, in order improve the results of the simulated settling tests. Variation 3 (green line) yields better results than the standard curve and, in variation 4 (dashed line), a break point is introduced at 3.5 g/l, which results in the best approximation of the measured settling curve for the entire range of concentrations. For lower sludge concentrations, the curve follows the standard curve, for higher concentrations it is fitted to only the values above 3.5 g/l.

4.1.2 Modeling Settling Tests

As explained in Chapter 4.1.1, the settling curves are transformed into a model that relates the sludge concentration to the settling velocity according to Takács, with compression. Simulations are conducted with several variations of this model. The simple geometry of a cylinder with a diameter of 6 cm and a height of 35 cm resulted in a mesh with 26,078 cells. The size of a cell was 3 mm, which is similar to the size of the 10 ml graduation of the measurement cylinder. A special feature is the usage of a k-ϵ turbulence model, even though there is no flow. However, there is a good reason for doing this. After the sludge is poured into the

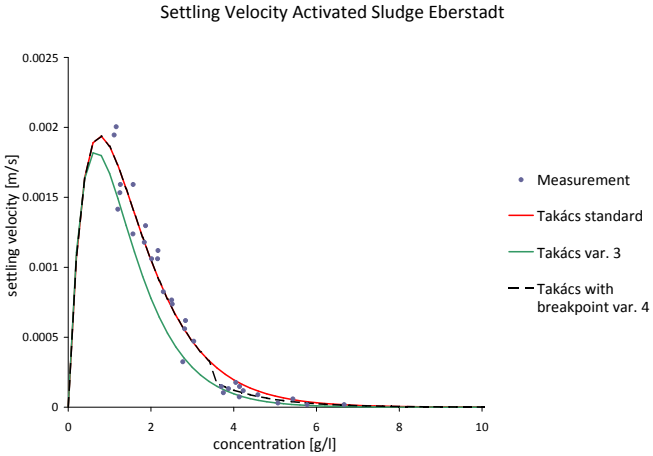

Figure 20: Settling curves of activated sludge from the WWTP in Eberstadt

cylinder, the fluid moves and it takes some minutes until it comes to rest. In the settling curve (see Figure 2 in Chapter 2.3), this results in the flocculation phase. Thus, settling does not start immediately, but only after a certain delay. To model this delay, an initial turbulence is modeled. The coupling of the turbulence with the diffusion coefficient of the sludge model (see Chapter 3.3.3) prevents settling until the turbulent viscosity is reduced to nearly zero. Another effect of including the turbulence model is the slight bowing of the sludge interface, due to wall effects. It should be mentioned that ANSYS FLUENT provides accurate results for a zero-flow simulation. The velocity is always exact zero. A few years ago, it was not possible to conduct exact zero-flow simulations with FLUENT. Nevertheless, because of numerical inaccuracies, slightly negative concentrations can occur.

In order to compare the simulation with the measurements, three different initial sludge concentrations were simulated:

1. low sludge concentration (1.87 g/l)
2. medium sludge concentration, close to the original sludge concentration of activated sludge (3.70 g/l)
3. high sludge concentration (5.43 g/l)

The results for the simulation with the variation 4 model (Takács, with compression) are shown in Figure 21. As in the real situation, it is initially difficult

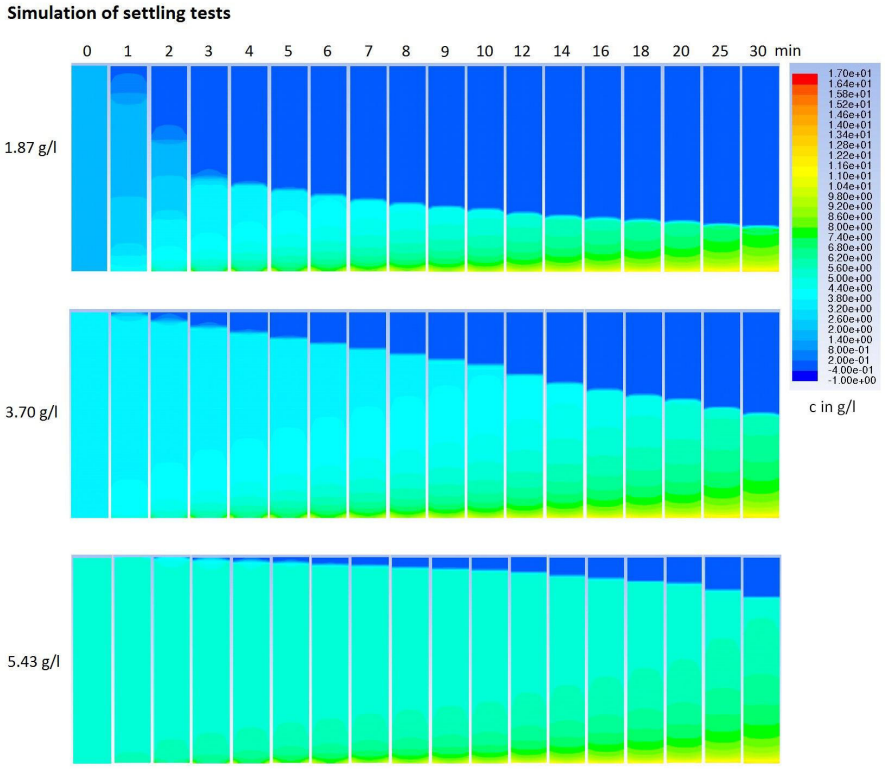

Figure 21: Simulation of settling tests with three different initial sludge concentrations (variation 4, Takács with compression)

to distinguish the height of the sludge level for low sludge concentrations. Subsequently, the sludge level becomes clearly visible. Because ANSYS FLUENT is based on the Finite Volume Method, the value for the sludge concentration is situated in the cell center. Therefore, the sludge interface cannot be thinner than the size of a cell (3 mm). But, as mentioned above, because the graduation on the real measurement cylinders is of the same size as the cells in the simulation, the measurement accuracy is the same. In Figures 22 to 24, the results of measurements and simulations are compared. The results of the simulations of different variations of the parameters for the model are shown according to the explanation in Chapter 4.1.1. For reasons of comparability, not only the measurements of the corresponding sludge concentrations are shown, but also measurements of similar sludge concentrations are displayed. This already reveals a certain range of settling curves for one specific sludge concentration, which was also described by Häck and Lange 2003. Therefore, it is not helpful to vary the parameters of the model until it fits best to one curve, because the variances of the measurements themselves are already high. The best model parameter set shows a good agreement for low, medium and high sludge concentrations.

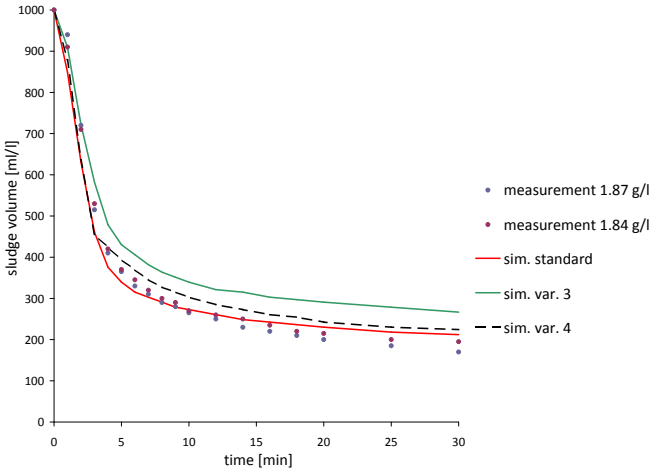

Figure 22: Comparing simulation and measurement of a settling test with an initial sludge concentration of 1.87 g/l

The standard model parameter set (red line) shows a good agreement for low sludge concentrations (correlation coefficient R^2 between 0.986 and 0.988); however, for the medium sludge concentration (R^2 between 0.792 and 0.880) and the

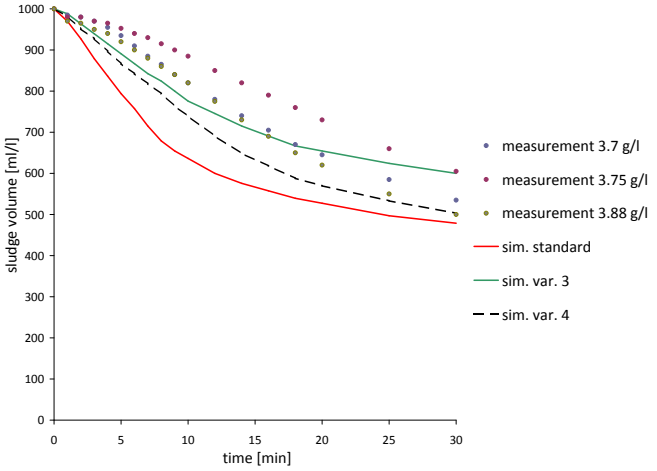

Figure 23: Comparing simulation and measurement of a settling test with an initial sludge concentration of 3.70 g/l

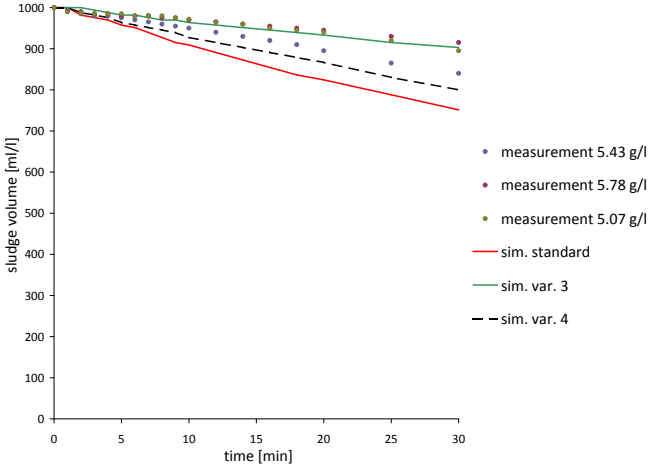

Figure 24: Comparing simulation and measurement of a settling test with an initial sludge concentration of 5.43 g/l

high sludge concentration (R^2 between 0.950 and 0.985), it underestimates the measured settling curve. Accordingly, the parameters are varied (the settling velocity was reduced) to obtain a better performance for the medium and high sludge concentrations. This is variation 3 (green line) in the Figures. For low sludge concentrations, it overestimates the measured curves (R^2 between 0.998 and 0.999), for medium and high concentrations it fits better (R^2 between 0.905 and 0.980). These results make it obvious why the introduction of a break point is necessary. Firstly, a reasonable fit for low and high sludge concentrations is only possible if compression is included in the model, as described by Merkel 1971, Armbruster 2004, and Zhang et al. 2006. Secondly, the physics of settling changes at the break point. At low sludge concentrations, hindered settling prevails: the sludge flocs do not contact each other. In the compression phase, which is the dominant process for medium and high sludge concentrations, the sludge flocs form a matrix in which the water is pressed out slowly. The question is how to determine the break point. Merkel 1971 defined his break point at a sludge volume $SV = 480\ ml/l$; Armbruster 2004 at 6 g/l and Zhang et al. 2006 at 5.84 g/l. A closer look at the prevailing sludge concentration during the simulation reveals that, even for the simulation of low sludge concentrations, a concentration of 4 g/l is rapidly achieved (see Figure 21). This means that the major part of the settling curves is determined by concentrations between 4 and 8 g/l. The measurement from the WWTP in Eberstadt indicates a break point close to 3.5 g/l, as can be seen in Figure 25 with a logarithmic scale.

Therefore, variation 4 (dashed line) includes a break point at 3.5 g/l. For lower sludge concentrations, it is identical with the standard model; for concentrations above 3.5 g/l, the curve was fitted only to the values with a higher sludge concentration.

$$v_s = \begin{cases} 0.008e^{-0.92c} - 0.008e^{-1.80c} & \text{for } c < 3.5\ g/l \\ 0.003e^{-0.80c} & \text{for } c \geq 3.5\ g/l \end{cases} \tag{80}$$

This model shows a reasonable fit with low, medium, and high sludge concentrations (R^2 between 0.920 and 0.991). A heuristic approach that varies the break point or the parameters of the model did not improve the results. As a recommendation for the curve fitting, it can be said that the measurements should first be plotted on a logarithmic scale and then the parameters of the exponential functions, which appear linear in the logarithmic scale, should be determined (see also the “Direct Method“, Veselind 1969). The break point is then determined visually and, finally, the Takács approach for the lower sludge concentrations is integrated (the maximum settling velocity is about 2 mm/s and usually appears at concentrations between 1 and 2 g/l). For the simulation of water treatment plants, the

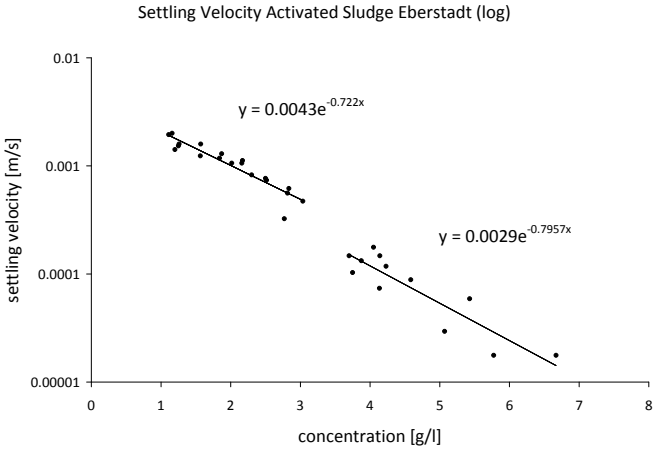

Figure 25: Measurements with a logarithmic scale

low settling velocities at low concentrations are important for modeling residual turbidity in the outflow. The significant influence of the break point on simulation results for more complex flows is described in Chapter 4.3.

4.2 Viscosity

4.2.1 Set-up of the Process-Viscometer

In this thesis, a completely new method is developed to measure the viscosity of sludge. To avoid settling, there is a vertical flow through the process-viscometer (see Figure 26). Figure 27 displays the advantage of this set-up. It shows the measured moment over time with activated sludge. During pumping, the measured moment is relatively constant, because the vertical flow prohibits settling. When the flow stops, the flocs settle and the moment decreases continually. To understand the moment due to pumping, it is necessary to first describe the flow field in the annulus.

The flow in the annulus is completely different and therefore the DIN 53019 standard cannot be applied to derive the shear rate from the angular velocity, or the shear stress from the moment. The set-up of the process-viscometer and the schematic flow in the annulus is shown in Figure 28.

The horizontal flow profile is not linear, as for Couette flows. Because the vertical flow already applies a certain shear rate to the fluid, the bob needs more power

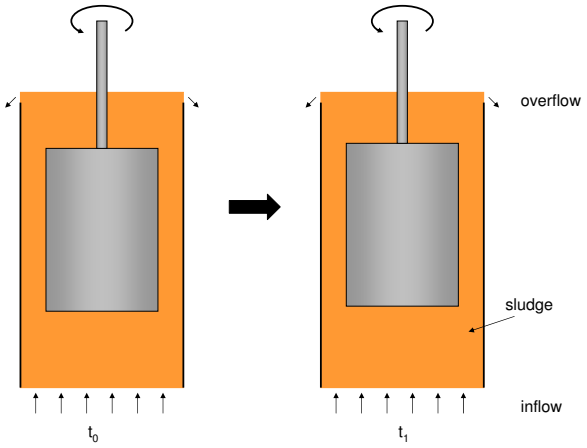

Figure 26: Prevent settling with a vertical flow in a process-viscometer

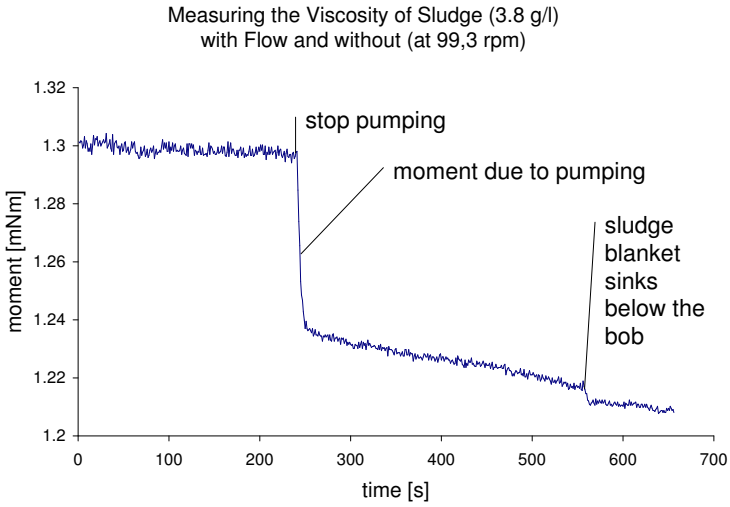

Figure 27: Measurement with a process-viscometer (with flow) compared to standard conditions (without flow)

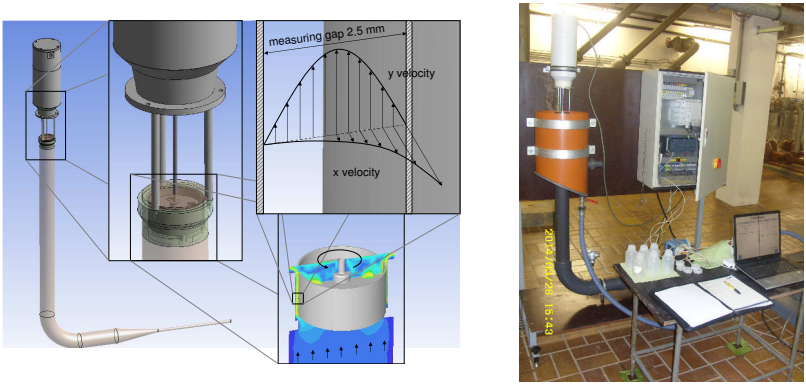

(a) (b)

Figure 28: The process-viscometer and the flow within the annulus (measuring gap)

to achieve the same rotational speed as without vertical flow. This explains the moment due to pumping in Figure 27 and the non-linear horizontal velocity profile. The same set-up, but without a vertical flow, would result in a Couette flow with a nearly linear velocity profile (details in Chapter 4.2.3).

Another interesting effect of the vertical flow is that it prevents Taylor vortices (details also in Chapter 4.2.3). Because of the vertical flow, thixotropic effects cannot occur, because the pump applies a constant shear to the sludge and prevents the formation of a structure in the sludge matrix.

The use of a process-viscometer to investigate rheological properties of sludge in combination with CFD is the core of the hybrid sludge modeling approach presented in this thesis. As discussed in this Chapter, this has some advantages but also disadvantages; these are summarized in Table 2. Bornholdt and Kleinjans 2001 state that a process-viscometer is only used in industrial processes for control reasons, never for designing plants. This is true if the complex flow within the annulus is unknown and the measured values indicate changes in the process, but the viscosity cannot be derived from the measurements. However, if the flow and the corresponding shear rates are known (modeled with CFD), the situation changes and it becomes possible to derive the viscosity from the measurements. The first reason why the measurements with the process-viscometer are modeled with CFD is to understand and quantify the flow within the measuring gap and to derive the viscosity from the measurements. The second reason for modeling is to adjust and calibrate the parameters of the rheological model until the simulation agrees

with the measurement; the hypothesis is that this is the “fundamentally justified“ physical viscosity of sludge.

	Measuring the viscosity of sludge	
	Standard viscometer	Process-viscometer with flow
Advantages	• Using DIN 53019 standard calculations to interprete measurements possible • Temperature constant (±0.1°C)	• No settling → constant measuring signal over time • No thixotropic effects due to pumping • No occurence of Taylor vortices at higher rotational speeds
Disadvantages	• Settling of sludge leads to non-constant measuring signal over time • Undefined thixotropic effects possible • Maximum rotational speed limited because of Taylor vortices • c_L factor not constant for non-Newtonian fluids and must be defined	• Simulations necessery to interprete measurements • Temperature rises because of the closed circuit (±1°C)

Table 2: Summary of advantages and disadvantages of standard viscometers and process-viscometers

4.2.2 Measuring the Viscosity of Sludge

The viscosity of activated sludge from a communal WWTP in Eberstadt is measured on 26 September 2013. The sludge concentration in the aeration tank from which the sludge was taken is 4.4 g/l. Approximately 100 l of sludge are taken and filtered with a screen (mesh size 1 mm), to prevent coarse grains from clogging the viscometer, because the plant operates without primary sedimentation. Moshage 2004, Battistoni 1997 and others describe the positive effect of prior sludge filtration on measurements. The sludge was concentrated by sedimentation. The concentrated sludge was poured into the viscometer. This initial concentration (dry matter) was 8.83 g/l. Subsequently, the sludge was diluted with effluent from the plant to 6.25 g/l, 4.52 g/l, 2.92 g/l, and, finally, 1.52 g/l. The temperature of the sludge was close to $20°C$. Because the sludge in the process-viscometer (approx. 30 l volume) is pumped in a circuit flow, the temperature increases by between 1 and $2°C$ in half an hour, which is the time required for measurement of a certain sludge concentration. This temperature difference does not have a significant effect on the sludge viscosity, because the changes in viscosity due to the sludge concentration are much greater. Special attention should be paid to the ambient temperature because the viscometer is very sensitive to it.

The process-viscometer - Covimat 205 TO - is produced by the German company proRheo. It is a Searle-type process-viscometer with a flow rate of 10 l/min. The measuring gap (thickness of the annulus) has a width of 2.5 mm to meet the requirement that the gap should be 5 times greater than the particle size of the flocs (DIN 53019). The bob has a radius of 32.5 mm and a height of 35 mm. The rotational speed varies between 10 and 99.3 rpm. Starting at 99.3 rpm the rotational speed is decreased stepwise (59.4, 34.7, 19.5 and 10) and increased again. The speed level is constant for 3 minutes at a certain rotational speed but, occasionally, a step lasts longer than 3 minutes (see Figure 29).

Following acceleration, the signal only becomes constant again after a certain time interval; therefore, only the values for the last 90 seconds are used to calculate the mean value of the moment for a given rotational speed (see Figure 30). The differences between the moments measured while decreasing the rotational speed and the moments measured while increasing the rotational speed are usually below 10% (average 7.1%).

These curves need to be transformed into real flow curves, to obtain the viscosity of sludge. Thus, it is necessary to derive a mathematical relationship between the moment and the shear stress, as well as between the rotational speed and the shear rate, based on the given flow conditions inside the process-viscometer. As explained above, the DIN 53019 does not help in this context because of the vertical flow. Therefore, CFD analyses were necessary to interpret the measurements.

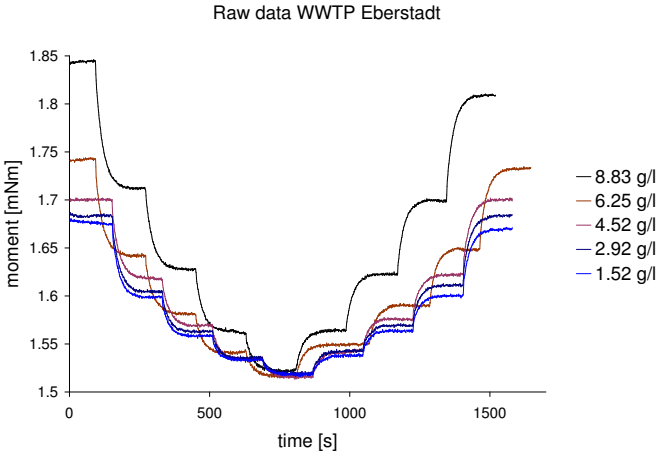

Figure 29: Raw data of rheological measurements at the WWTP Eberstadt with different sludge concentrations and angular velocities

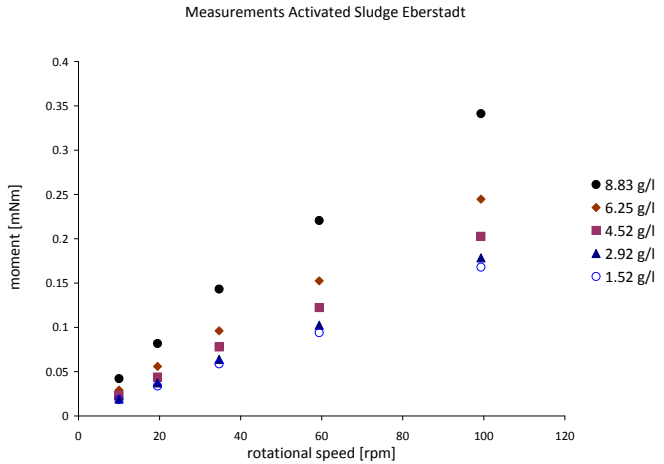

Figure 30: Summary of the measurements with the process-viscometer from activated sludge with different concentrations from the WWTP in Eberstadt

4.2.3 Modeling Viscometers

Prior to simulating the complex process-viscometer, some theoretical investigations are conducted in order to understand how viscosity is implemented in the numerical code of ANSYS FLUENT and how turbulence models or grid resolutions influence the results of the simulation. Starting with a simple 3-D viscometer, the complexity of the simulation is increased until the process-viscometer is modeled. Initially, only the Newtonian fluid water is considered, since the viscosity of water is well known and is therefore best suited for comparisons.

Comparison of various Turbulence Models

In order to test several turbulence models, wall functions, and solver configurations, a relatively simple geometry was created and the fluid was simply water. In fact, only the annulus of a simple viscometer was modeled, using a rotating bob in a cup. The geometry consists of a bob ($R_i = 32.5\ mm$) and a cup ($R_a = 35.0\ mm$) with a height of $L = 35.0\ mm$, which results - according to Equation 27 - in $k_\nu = 296.5\ m^{-3}$. The rotation speed was 10 rpm and the rotation was modeled with a moving reference frame approach (MRF) in which the geometry does not move but the velocity resulting from the rotation is set within a cell domain (details provided later in this chapter). Similar to the process-viscometer, there is an additional vertical flow of 0.17 m/s. The mesh uses a finer resolution near the walls (inflation layers) and the tested result is the moment that affects the bob. The moment is calculated by ANSYS FLUENT by integrating the shear stress over the area of the wall of the bob. Therefore, it is important to have an accurate velocity distribution near the wall to obtain an accurate shear stress distribution. Because the flow is laminar, the laminar solution serves as a reference; the other configurations and their results are given in Table 3.

The inclusion of gravity, as well as the use of the simple or coupled solver, has no effect in this kind of simulation. The simple pressure-based solver is a segregated or sequential solver that inverts the matrices for the unknown variables - flow velocity and pressure - sequentially. The coupled solver inverts one matrix with all the unknown variables and therefore needs more RAM memory. Convergence usually is better, and experience have shown that, because of the non-constant density in the sludge model, the coupled solver is usually the first choice. The density-based solver is always a coupled solver and usually preferred for simulations in which the change of the density is dominant (shock-waves, acoustics, etc.). For the k-ϵ model, only the enhanced wall treatment yields good results. All other wall functions deviate from the laminar solution. The worst is the scalable wall function, which produces a logarithmic velocity profile for a laminar flow. Normally, logarithmic velocity profiles appear at turbulent flows, whereas laminar flows have a parabolic

Turbulence Model	Near Wall Treatment	Gravity included	Solver	Result (Moment) [Nm]
Laminar	-	No	Coupled Pressure based	1.58602 E-5
Laminar	-	Yes	Coupled Pressure based	1.58602 E-5
Laminar	-	Yes	Simple Pressure based	1.586036 E-5
k-ε	Enhanced wall treatment	Yes	Coupled Pressure based	1.586208 E-5
k-ε	Scalable wall function	No	Coupled Pressure based	2.5031 E-7
k-ε	Standard wall function	Yes	Coupled Pressure based	2.10132 E-5
k-ε	Non equilibrium wall function	Yes	Coupled Pressure based	3.435305 E-5
k-ω	-	Yes	Coupled pressure based	1.588528 E-5
Reynolds-stress	Enhanced wall treatment	Yes	Coupled pressure based	1.5862 E-5

Table 3: Comparing different turbulence models, wall functions and solver configurations. Green: small deviation from reverence value; yellow: medium deviation; red: great deviation

shape. As expected, the k-ω model produces good results. Because it is optimized for flows near walls and does not need a wall function, it can be regarded as nearly as good as the k-ϵ model with enhanced wall treatment. The Reynolds stress model also yields good results but needs more computational effort and the solution converges much more slowly. In order to achieve convergence, the simulation should first be started with a k-ϵ model and then switched to the Reynolds stress model.

For the simulations within this thesis, in which relatively slowly, sometimes even laminar flows occurre, the k-ϵ model with enhanced wall treatment or the laminar solution is preferred. When simulating viscometers, some backflow appears because of a vortex at the free overflow; that is also observed in the real process-viscometer. For this reason, every turbulence model requires boundary conditions for k and ϵ at the outlet. Since the outlet is near the fluid domain of interest, this might have a negative effect on the results. Therefore, wherever possible, the simulation was laminar and the turbulent simulation was added only for comparison. It is interesting that the turbulent simulation converges faster than the laminar simulation. Gravity can be neglected, because the settling of sludge and stratified flow effects are already included in the sludge model otherwise. The coupled pressure-based solver is preferred, because of the non-constant density and the better convergence behavior.

Simulation of a Simple Viscometer

It is not possible to construct an infinite viscometer for which end effects do not occur. Simulation, however, provides this possibility. A 3-D simulation of the flow in the annulus of a simple viscometer was conducted with water ($\eta = 1.000\ mPas$). The geometry is the same as that described in the previous paragraph, in which the turbulence models were compared. The only difference in this simulation is that there is no vertical flow. To avoid end effects, the boundaries at the top and the bottom were treated as symmetry planes. Inflation layers were used to increase the accuracy of the laminar flow near the walls. For a rotational speed of $\Omega = 10\ rpm = 1.047\ rad/s$, the simulation calculates a moment of $M = 3.56E{-}6\ Nm$. Backward calculation of the viscosity results in

$$\eta = k_\nu \frac{M}{\Omega} = 1.009\ mPas \tag{81}$$

The difference to the constant input parameter for the viscosity of 1.000 mPas is rather small and can be explained by discretization errors.

Simulation of a Standard Viscometer

In order to use rotational viscometers to measure viscosity in practice, one has to deal with the end effects. The DIN 53019 standard therefore defines a standard

geometry for the Searle-type viscometer as follows: $L/R_i = 3$; $L'/R_i = L''/R_i = 1$; $R_s/R_i = 0.3$; $\delta = R_a/R_i = 1.0847$; $\beta = 120°$ (see Figure 31).

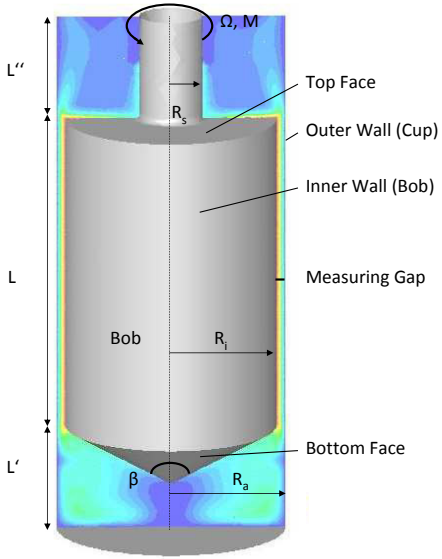

Figure 31: Standard geometry for Searle-type viscometers according to DIN 53019 with velocity contours of the surrounding fluid

Choosing the inner radius at $R_i = 32.5\ mm$, the geometry is defined with $k_v = 115.9\ m^{-3}$.

There is a limitation for Searle-type viscometers, because Taylor vortices appear at higher rotational speeds. The DIN standard 53019 defines the maximum speed as:

$$\left(\frac{\rho\Omega_{i,crit}}{\eta}\right)^2 = \frac{\pi^4(\delta+1)F_0}{2(\delta-1)^3R_i^4} \tag{82}$$

$$F_0 = \frac{1-0.652(\delta-1)}{0.00056+0.0571[1-0.652(\delta-1)]^2} \tag{83}$$

Simulating water ($\eta = 1.003\ mPas$) with the chosen inner radius, the maximum rotational speed is $\Omega_{i,crit} = 18.2\ rpm$. Simulation confirms this. The process-viscometer was simulated without flow and water but with similar geometry; thus, it is comparable to the standard geometry discussed here. The riffles in the velocity contours in the measuring gap in Figure 32 represent the Taylor vortices, which occur at higher rotational speeds.

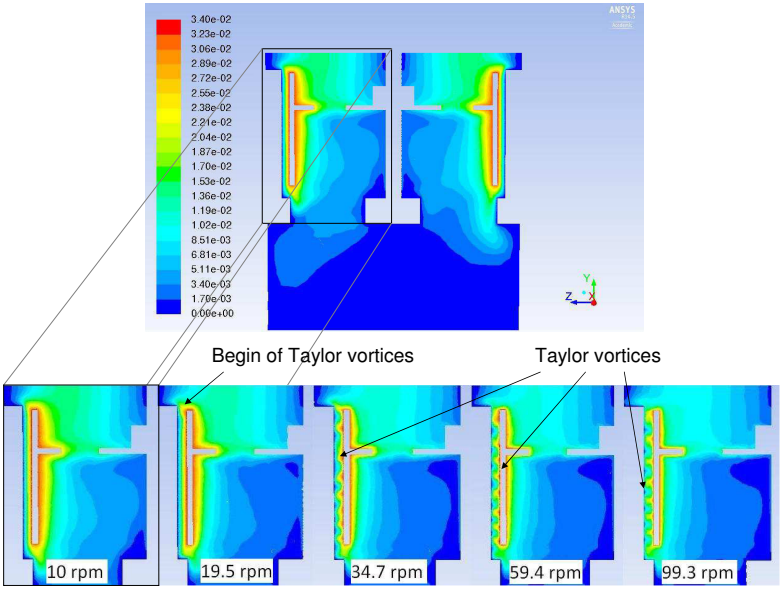

Figure 32: Velocity contours [m/s] in the viscometer without vertical flow for different angular velocities. The first Taylor vortex starts at 19.5 rpm at the top of the bob, at 34.7 rpm the Taylor vortices already cover the entire annulus (riffles in the velocity contours). Figure 36 might help to understand the geometry of the viscosimeter better.

A rotational speed of $\Omega = 10\ rpm$ is chosen to prevent Taylor vortices and turbulence. Even though turbulence should not occur, the simulations are conducted laminar and with a k-ϵ turbulence model, to enable comparisons. Because the results of both simulations are relatively similar, only the results of the laminar simulation are presented here and compared with the DIN 53019 standard. Surprisingly, the laminar simulation is more time-consuming than the turbulent one, because the

convergence behavior is worse. This demonstrates, once again, that the turbulence models currently available can deliver good results, even for laminar flows. The maximum turbulent viscosity ($2.2E-10\ Pas$), which appears in the measuring gap, is several orders of magnitude lower than the molecular viscosity and can therefore be neglected. To have at least 8 cells in the measuring gap (2.75 mm), a high grid resolution is necessary ($11.2E+6$ cells).

From the simulation, one obtains the moment for the rotating cylinder: $M = 0.0125\ mNm$ (for the turbulent simulation: $0.0120\ mNm$). It becomes obvious at this point that a high precision viscometer is required to measure the viscosity of water. The DIN standard derives a representative shear stress τ from the moment considering the bottom and the top of the bob that also contributes to the moment. Therefore, the factor c_L is introduced, which is 1.10 for the standard geometry.

$$\tau = \frac{1+\delta^2}{2\delta^2}\frac{M}{2\pi L R_i^2 c_L} = 0.0163\ Pa \tag{84}$$

From the rotational speed, a representative shear rate $\dot{\gamma}$ is calculated.

$$\dot{\gamma} = \Omega\frac{1+\delta^2}{\delta^2-1} = 12.9\ s^{-1} \tag{85}$$

For Newtonian fluids, the viscosity is simply

$$\eta = \frac{\tau}{\dot{\gamma}} = 1.261\ mPas \tag{86}$$

Interestingly, the result differs from the constant input parameter for viscosity ($\eta = 1.003\ mPas$). Even for the turbulent simulation there is a remarkable difference ($\eta = 1.204\ mPas$; the main difference between both simulation is the shear rate near the wall, due to the enhanced near-wall treatment of the turbulence model; see Chapter 3.3.5). Therefore, it is necessary to consider at the assumptions and preconditions of the DIN 53019 standard and the simulation itself in more detail.

1. The flow must be laminar. In this simulation, this is true, as described above.

2. The measurement or simulation must be conducted under ambient pressure in order to neglect the influence of pressure on the moment. The simulation takes the ambient pressure into account, but the resulting moment due to pressure

Moments Standard Geometry	Pressure		Viscosity		Total	
	[Nm]	share	[Nm]	share	[Nm]	share
Inner wall	2.96359 E-11	0%	-1.01894 E-05	81%	-1.0189 E-05	81%
Top face	2.31454 E-11	0%	-1.27728 E-06	10%	-1.2773 E-06	10%
Bottom face	-4.52031 E-12	0%	-1.06959 E-06	9%	-1.0696 E-06	9%
Sum	4.82611 E-11	0%	-1.25362 E-05	100.00%	**-1.2536 E-05**	100.00%

Table 4: Moments due to pressure and viscosity of different faces and their share of the total moment

($M_p = 4.8\ E-11\ Nm$) is six orders of magnitude below the moment due to viscosity ($M_\eta = 1.25\ E-5\ Nm$); thus, pressure contributes virtually nothing to the moment (see Table 4).

3. The flow within the measuring gap should approximate a Couette flow. Therefore, the measuring gap should be narrow in order to have a nearly linear velocity distribution; for a broad measuring gap, the velocity distribution is hyperbolic; see Figure 33 and the following mathematical expression from the DIN 53019. Apart from the velocity tangential to the bob (u), all velocity components in the vertical direction (v) should be zero.

$$u = r\Omega \frac{\delta^2 R_i^2 - r^2}{\left(\delta^2 - 1\right) r^2} \tag{87}$$

The simulation confirms this, but there are small velocity components in the vertical direction as well (max 4 E-5 m/s, which is three orders of magnitude lower than the prevailing velocity). In Figure 34, the results from the laminar and turbulent simulation are displayed; as mentioned earlier, the differences are small, because turbulence does not occur. The line represents the theoretically calculated values according to DIN 53019, which is basically derived from the Margules equation (Equation 24).

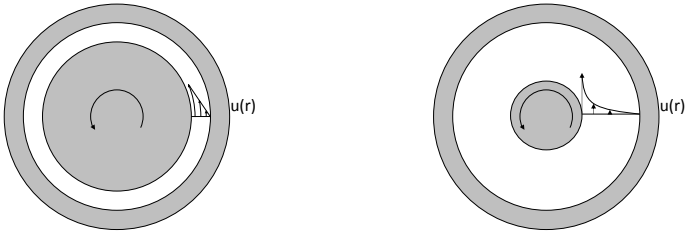

(a) (b)

Figure 33: Velocity distribution in a narrow (a) and broad (b) measuring gap

4. The shear rate distribution is almost linear for narrow measuring gaps and hyperbolic for broad measuring gaps. The representative shear rate is the average of the shear rate at the outer and inner wall, which, for a nearly linear distribution, is more or less the shear rate at the middle of the measuring gap. The DIN 53019 defines the shear rate in the measuring gap as

$$\dot{\gamma} = \Omega \frac{2R_i^2 \delta^2}{\left(\delta^2 - 1\right) r^2} \tag{88}$$

Here, the simulation paints a slightly different picture (Figure 35a). The shear rate of only the x-velocity component (du/dz) differs from the total shear rate (square root of the second invariant of the shear rate tensor), because the other velocity components are small but not zero.

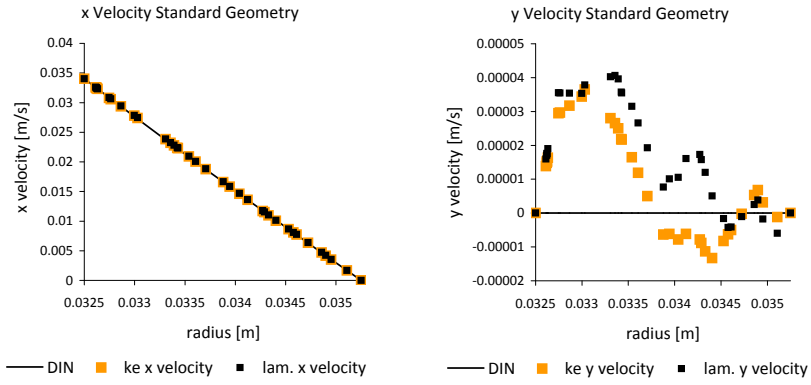

(a) (b)

Figure 34: Flow velocities in x (horizontal) and y (vertical) directions in the measuring gap

5. The shear stress distribution is also nearly linear for narrow measuring gaps and hyperbolic for broad measuring gaps. Again, the representative shear stress is the average of the shear stress at the outer and inner wall, which is approximately the shear stress at the middle of the measuring gap for a nearly linear distribution. The DIN 53019 defines the shear stress in the measuring gap as

$$\tau = \frac{M}{2\pi L r^2} \tag{89}$$

Note that end effects are not included in this consideration. Unfortunately, ANSYS FLUENT does not provide the components of the shear stress tensor within the fluid domain. It is therefore calculated by multiplying the shear rate with the molecular viscosity (rough approximation). However, ANSYS FLUENT does provide the wall shear stress for walls, which returns zero for the fluid domain. At the walls, it corresponds well with the values according to the DIN 53019 standard (Figure 35b).

6. The c_L factor actually describes the ratio between the moment for the entire rotating cylinder and the moment of the inner wall only, in order to consider end effects. It cannot be measured directly. For the standard geometry, it is known from

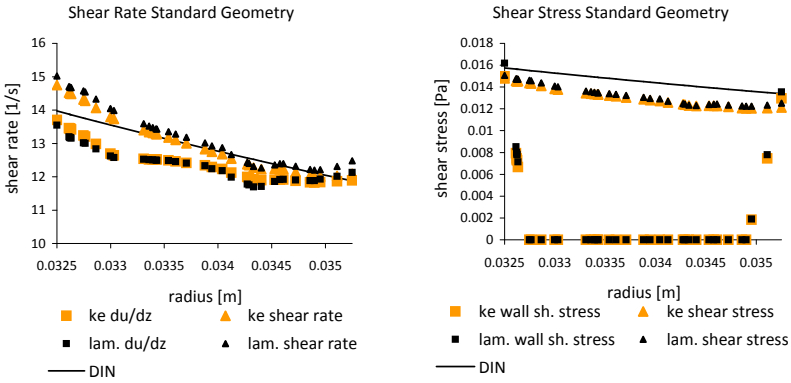

(a) (b)

Figure 35: Shear rate and shear stress in the measuring gap

experience and comparisons of various measurement methods. The simulation is able to distinguish between the moments resulting from the different walls (see Table 4). It demonstrates, again, that the pressure does not contribute to the total moment; the top and bottom faces do, however (in total: 19%). The $c_L = 1.10$ factor for the standard geometry does not fit to the results of the simulation. It must be set to 1.38 in order to obtain the viscosity of 1.003 mPas, which is already considered as unrealistically high.

7. The simulation provides the shear rate and the shear stress directly for the inner wall (wall of the bob without bottom or top faces). Using the area weighted average of the shear rate for the inner wall ($\dot{\gamma} = 15.8\ s^{-1}$) and the shear stress ($\tau = 0.0151\ Pa$) to calculate the viscosity result in $\eta = \tau/\dot{\gamma} = 1.006\ mPas$, which is close to the constant input 1.003 mPas. Multiplying the shear stress with the area of the inner wall and the radius matches the moment resulting from the inner wall well. This shows that the simulation is independently consistent. The viscosity in every cell of the mesh is 1.003 mPas (ignoring small numerical inaccuracies).

Summary and Discussion about Simulating Viscometers

The conclusion from this investigation is that it is difficult to measure the viscosity of water exactly with this kind of device. The difficulties cover not only the

inaccuracies within the measurement device or numeric inaccuracies but are inherent to the measurement system itself, because it does not produce a plane Couette flow but, instead, something close to it.

From own measurements and observations, which are described below, it is clear that the simulation overestimates the moments for some unknown reasons, as is the case even in this theoretical consideration. The simulation is consistent on its own but the moments are too high, compared with the measurements. A more realistic total moment would have been 0.00999 mNm rather than 0.0125 mNm. Only the simulation of a geometry without end effects matches the theory. This fact underlines the necessity for hybrid sludge modeling, which would make it possible to calibrate the simulation and the measurements to the known viscosity of water.

Nevertheless, the simulation provides a better understanding of the flow within such a device and, as it has been demonstrated, it differs somewhat from the theoretical calculations (without end effects). For a standard geometry and water, this might be an interesting exercise, but if fluids, such as sludge, have to be measured for which the standard geometry and standard conditions from DIN 53019 are no longer applicable, it is necessary to conduct simulations in order to interpret the measuring results and to derive a viscosity from the measurements.

Simulation of the Process-Viscometer with Newtonian fluids

The geometry of the process-viscometer is similar to the viscometers described above. The radius of the bob is also $R_i = 32.5\ mm$, the radius of the cup is $R_a = 35.0\ mm$, the height is $L = 35.0\ mm$. The interior of the bob is also different: there is only a disc with four holes (see Figure 36); the rest is hollow. A pipe is mounted under the cup (diameter 80 mm) and is connected to the pump. At the top of the cup, there is a free overflow into a reservoir, where the sludge is collected and pumped back again in a closed circuit.

The mesh of the process-viscometer consists of $3.7E + 6$ cells, with a maximum skewness of 0.87. The shape of the cells is predominantly a hexahedron, but some tetrahedrons also appear. Within the measuring gap, so-called inflation layers are used to refine the mesh near the wall. For laminar calculations, it is important to have a high mesh resolution near the walls to obtain good results for the shear stress and shear rate at the wall. All together, there are 18 cells in the measuring gap between the cup wall and the outer wall of the bob (see Figure 37). Other mesh configurations have been tested (coarse tetrahedrons, fine tetrahedrons with and without inflation layers), but the results were not very different, so that one can say that the solution is independent of the mesh. The hexahedron mesh has the advantage that it requires fewer cells for a mesh with the same resolution as with tetrahedrons and, therefore, less computational effort. In a pre-study, Weyand

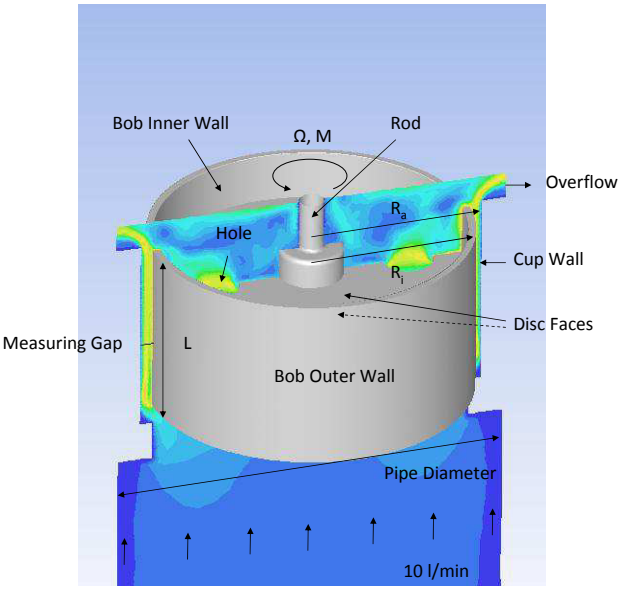

Figure 36: The geometry of the process-viscometer in detail with velocity contours of the surrounding fluid

2012 finds that a minimum of 6 cells in the measuring gap is necessary to generate mesh-independent velocity profiles in the measuring gap.

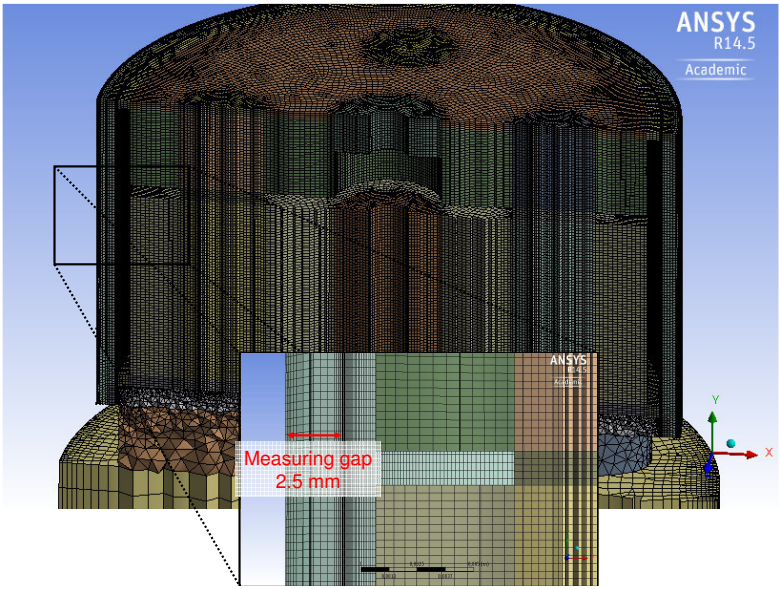

Figure 37: Mesh of the fluid body of the process-viscometer

Within ANSYS FLUENT, the pressure-based coupled solver is used. Several methods for the discretization are tested, but the results are more or less the same. For pressure, the standard method is applied and, for momentum, the 2^{nd} order method. The simulations are laminar. They are also compared with simulations with k-ϵ turbulence models but, as mentioned earlier in this chapter, the results did not differ greatly. The rotation was modeled with the so-called moving reference frame (MRF). This model simply applies an additional source term in the momentum equation to the fluid zone enclosing the bob, according to following equation:

$$u = \omega r \tag{90}$$

This means that the bob does not move and the geometry remains the same, but the fluid assumes the shape it would have, if the bob was rotating. ANSYS FLUENT also provides a sliding mesh model. Here, the bob and its mesh are really moving

over time. A simulation is conducted with this model as well, but the results are the same as for the MRF model. Since the computational effort for the sliding mesh is much greater, the MRF model is used. The second advantage is that, with the MRF model, steady simulations can be conducted, which again reduces computational effort. Transient simulations are also conducted; they do not produce different results, but are more time-consuming. In a pre-study, Weyand 2012 also compares laminar simulations with MRF and sliding mesh, and finds no major differences in the results.

The inlet is a velocity inlet at the pipe with 0.034 m/s, which corresponds to 10 l/min. The overflow is a pressure outlet. Since the simulations are laminar, no adverse effects occur when, at some faces of the outlet, a reverse flow occurs. When turbulence models are used, attention should be paid to the values for the turbulence model at the outlet. The boundary conditions of the walls enclosing the bob are adjusted to the MRF model. All simulations are conducted on a Linux machine with 12 Intel Xeon cores (3.4 GHz). One steady simulation of the process-viscometer requires about half an hour.

In order to develop a detailed understanding of the flow within the process-viscometer, some preliminary simulations with Newtonian fluids are conducted. The initial constant value for the viscosity is 1 mPas, which corresponds to water at $20°C$. Then, five simulations were performed at different rotational speeds (10.0, 19.5, 34.7, 59.4 and 99.3 rpm, the same as for the real process-viscometer), in order to obtain a flow curve. Therefore, it is first necessary to calculate the shear stress and the shear rate. Because ANSYS FLUENT only provides the shear stress at walls, the shear stress from the outer wall of the bob is taken into account, as well as the corresponding shear rate. The flow velocity contours of the simulation with 10 to 99.3 rpm are displayed in Figure 38. The maximum velocity in the measuring gap is 0.29 m/s because of the vertical flow. Compared to the value of 0.034 m/s at the inlet, this increase corresponds to the reduction of the flow cross section, due to the bob of the viscometer. At a rotational speed of 10 rpm, the horizontal x velocity at the outer wall of the bob is only 0.03 m/s; thus, the vertical flow dominates. At a rotational speed of 99.3 rpm, the horizontal velocity at the outer wall of the bob is 0.34 m/s, which is somewhat higher than the vertical velocity.

The vertical flow is required to avoid settling, but, on the other hand, it also contributes to the shear rate and the shear stress. As Figure 39 demonstrates, the shear stress is not constant over the outer wall of the bob. Especially at the bottom, it is highly influenced by the change of the flow direction. The rest of the outer wall face is more or less constant, but some stripes appear, which are nearly vertical for low rotational speeds and diagonal for high rotational speeds. From the simulations without flow, where Taylor vortices appear (Figure 32), the stripes are also present, but more distinct. Thus, at 99.3 rpm, the flow starts to become unstable. At 10 rpm,

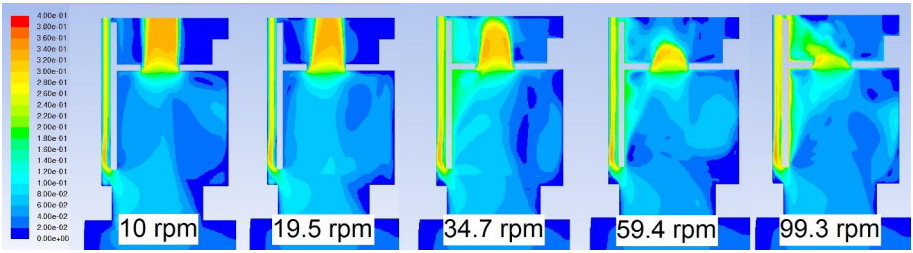

Figure 38: The velocity contours [m/s] within the left half of the process-viscometer (see also Figure 32). The effect of decreasing velocity with increasing rotational speed is most vivid over the hole. This effect can also be observed in the real process-viscometer.

the stripes appear only at the three points where the mount of the bob is connected to the cup. Comparing Figure 39 (shear stress τ) with Appendix Figure 108 (shear rate $\dot{\gamma}$), one can see that the viscosity η is 0.001 Pas in every cell ($\eta = \tau/\dot{\gamma}$) and the simulation is consistent on its own. In fact, the pictures are identical; only the magnitude of the values in the legend is different (factor 0.001).

To find the relationships between the moment and the shear stress, as well as between the rotational speed and the shear rate, due to the rotation of the bob, the influence of the vertical flow must be eliminated. For this reason, only the shear stress and shear rate in the horizontal direction (x-z-plane, tangential to the bob, see Figure 40 and Equations 91 and 92), averaged over the whole outer wall of the bob, are considered, according to the following formulae. As one can see in Figure 40, the tangential shear stress is lower but more evenly distributed over the area.

$$\tau = \sqrt{\tau_x^2 + \tau_z^2} \tag{91}$$

$$\dot{\gamma} = \sqrt{2\left(\frac{du}{dx}\right)^2 + 2\left(\frac{dw}{dz}\right)^2 + \left(\frac{du}{dz} + \frac{dw}{dx}\right)^2} \tag{92}$$

A closer look to the measuring gap reveals the prevailing kind of flow. For low rotational speeds (10 rpm), the horizontal x velocity is small, compared to the vertical y velocity (see Figure 41). For the vertical flow, a typical parabolic velocity profile occurs, as is expected for laminar flows. For higher rotational speeds

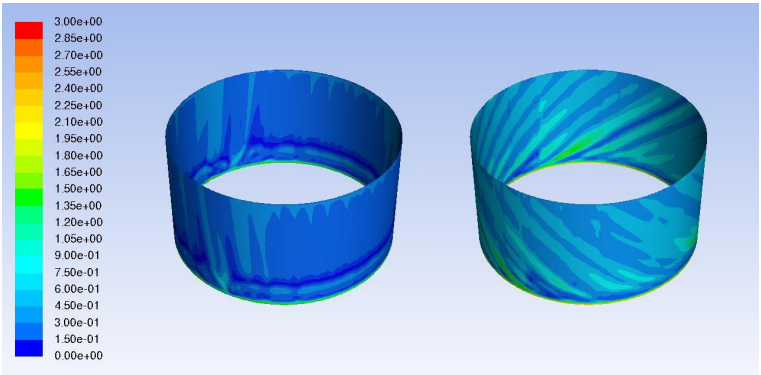

Figure 39: Total shear stress [Pa] at the outer wall of the bob for rotational speeds of 10 rpm (left) and 99.3 rpm (right)

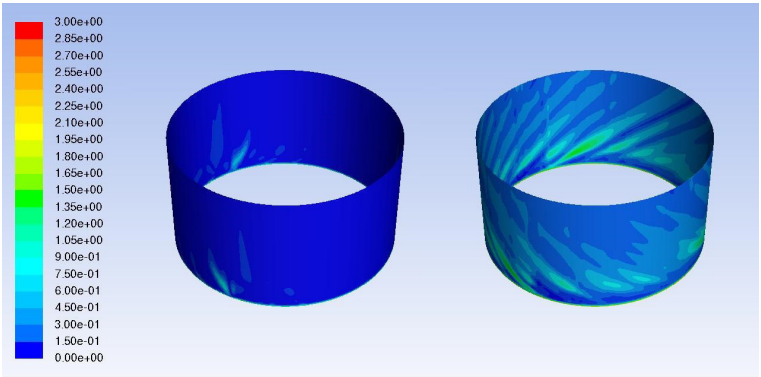

Figure 40: Shear stress [Pa] only in the horizontal (tangential) direction at the outer wall of the bob for rotational speeds of 10 rpm (left) and 99.3 rpm (right)

(99.3 rpm), the horizontal x velocity profile is hyperbolic (see Figure 42). The maximum velocity at the outer wall of the bob is $u = \omega R_i = 0.34 m/s$.

Without the vertical flow, the shape would have been nearly linear for narrow gaps (compare with Figure 34), but the vertical flow changes its shape and becomes hyperbolic. In the half near the cup wall (right half in the diagram), the horizontal flow becomes slightly negative. Figuratively spoken, the vertical flow does not allow the horizontal flow to develop over the entire width of the measuring gap. The vertical flow profile remains constant, no matter which rotational speed is applied (compare Figure 41b to Figure 42b).

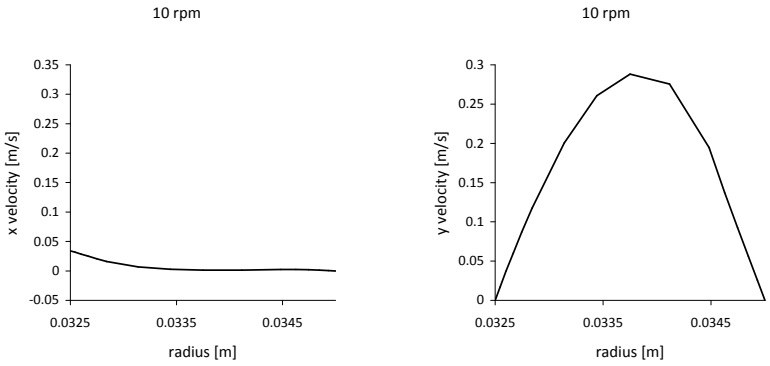

(a) (b)

Figure 41: Flow in the measuring gap at a rotational speed of 10.0 rpm: horizontal velocity profile (left), vertical velocity profile (right)

Up to this point, only theoretical considerations and simulations have been considered. In a further step, the simulations are compared with the measurements. ANSYS FLUENT can calculate the moment by integrating the shear stress over the wall areas and multiplying it with the distance to the moment center, which is the middle of the bob in this case. Taking into account the outer and inner wall of the bob, the disc faces, the holes, and the rod, the total moment resulting from the rotation of the bob is calculated. This can be compared with the moment measured by the process-viscometer, which is displayed in Figure 43.

It should be noted that the measurements with the process-viscometer do not allow one to distinguish between flushing water (nearly 0 g/l) and sludge with low sludge concentrations (up to 2 g/l). The measurements can be considered as

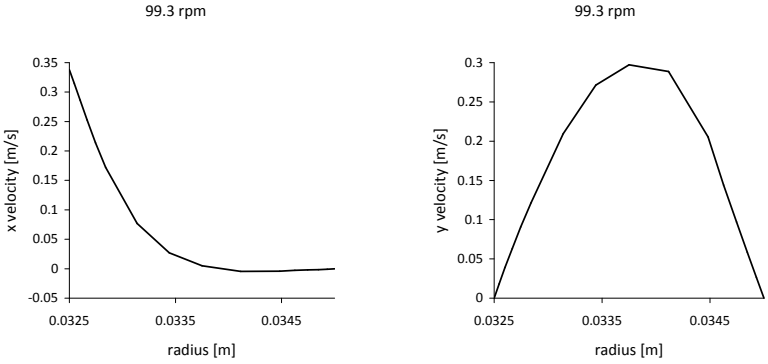

(a) (b)

Figure 42: Flow in the measuring gap at a rotational speed of 99.3 rpm: horizontal velocity profile (left), vertical velocity profile (right)

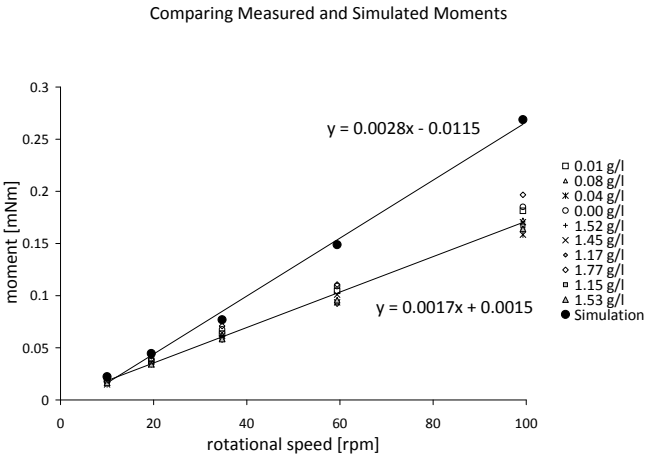

Figure 43: Comparing the measured moments with the simulated moments

identical with the measurements of water within a certain range, as displayed in Figure 43. Note, further, that only the moment over the rotational speed is displayed, which is not equal to a flow curve (where the shear stress is displayed over the shear rate). The most interesting part of the functions is the gradient. For the measured curves, it varies between 0.0016 and 0.0019; the average is 0.00172. The gradient of the simulated curve, however, is 0.00280. Thus, it is obvious that there is a systematic deviation between simulation and measurements. As stated previously in this chapter, when investigating the standard geometry, the simulation overestimates the total moment for some reasons, but is consistent on its own. In every cell of the fluid domain, the quotient of shear stress and shear rate is 1.0 mPas. Because different mesh-, time-step- and solver-configurations did not yield a solution that is closer to the measurements, it can be considered as a mesh- and solver-independent solution, which must be calibrated to the viscosity of water. Fortunately, the deviation is constant and does not vary for the given geometry. Therefore, a calibration factor is introduced, in order to make the simulations comparable to the measurements:

$$\text{calibration factor} = \frac{0.00280}{0.00172} = 1.63 \tag{93}$$

The total moment from the simulation must be divided by this factor, in order to obtain the calibrated moments for further considerations. As will be shown below, due to the fact that the simulation is consistent on its own, the calibration provides reasonable results for the viscosity of sludge and water. The mathematical relationship between the moment and shear stress, as well as between the rotational speed and the shear rate, can be derived from the simulation. Correlating the calibrated moments from the simulation with the shear stress and the rotational speed with the shear rate, one obtains Figure 44.

The DIN 53019 standard suggests a linear relationship between the moment and the shear stress that depends only on the geometry (see Equation 84). The vertical flow prohibits the use of DIN 53019 and it seems that there is a nonlinear relationship for the process-viscometer, which fits better (Figure 44a). Considering the relationship between shear rate and rotational speed, a linear relation is more evident, similar to the DIN 53019 standard (see Equation 84 and Figure 44b). The only difference is a small offset caused by the vertical flow. In a first attempt, these relationships are used to evaluate the measurements with these two curves, to fit a rheological model to the measured curves, and to create a relationship between the parameters of the rheological model and the concentration. With this sludge model, the process-viscometer is simulated again, but the results from the simulations do not fit the measurements. Thus, further investigations are undertaken with Newtonian fluids but with higher viscosities.

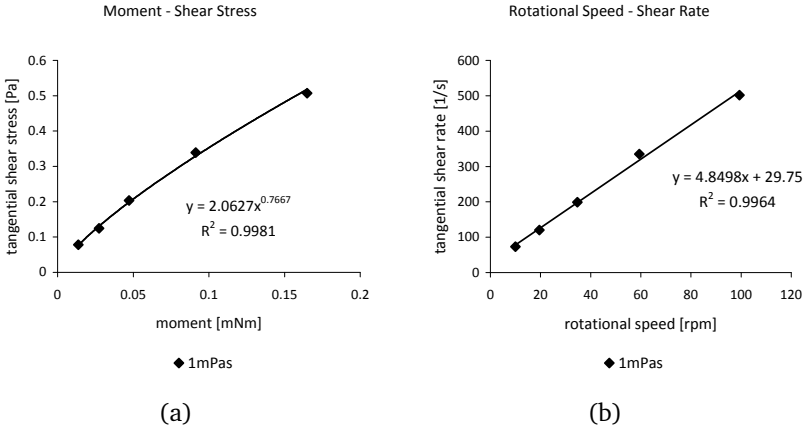

Figure 44: Correlation of shear stress and moment (left) and shear rate and rotational speed (right)

What happens when the viscosity increases but still remains Newtonian? According to the DIN 53019 standard, nothing would change. The geometry remains the same, the fluid is still Newtonian; therefore, an extrapolation of the linear relationships is expected. But is this true for the process-viscometer? Further simulations are conducted with a constant viscosity of 2, 3, and 4 mPas (fictive Newtonian fluids). Inspection of the velocity profiles reveals changes in the situation. The horizontal velocity and the vertical velocity change their shape and, accordingly, their shear rate (which is the gradient of the velocity profile; see Figures 45 and 46). The vertical velocity decreases with increasing viscosity, because the higher inner friction removes kinetic energy from the flow. Again, the vertical flow is independent of the rotational speed of the bob. The maximum value for the horizontal velocity remains the same but, with increasing viscosity, the extent of the nearly linear part of the velocity profile increases. Figuratively spoken, the higher viscosity allows the horizontal velocity profile to develop further and the influence of the vertical flow decreases. For the curves with rotational speeds of 19.5, 34.7, and 59.4 rpm, see Appendix Figures 98 to 102. There the profiles for the horizontal shear rates and the total shear stresses are also available.

What does this mean for the relationships between shear stress and moment and shear rate and rotational speed? Figure 47 makes it clear that the relationships change significantly with the prevailing viscosity. A constant factor between the

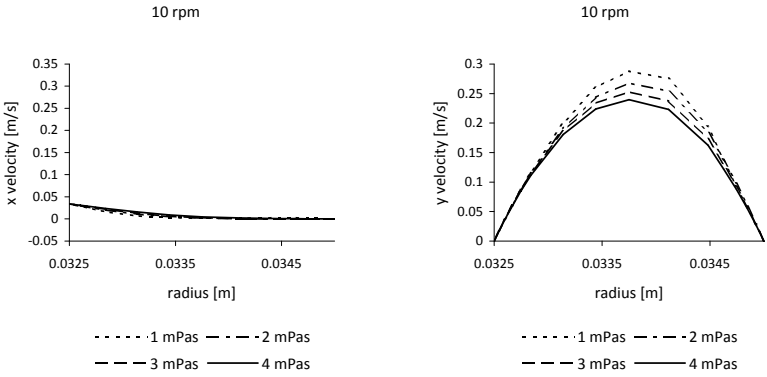

(a) (b)

Figure 45: Flow in the measuring gap at a rotational speed of 10.0 rpm for different viscosities: horizontal velocity profile (left), vertical velocity profile (right)

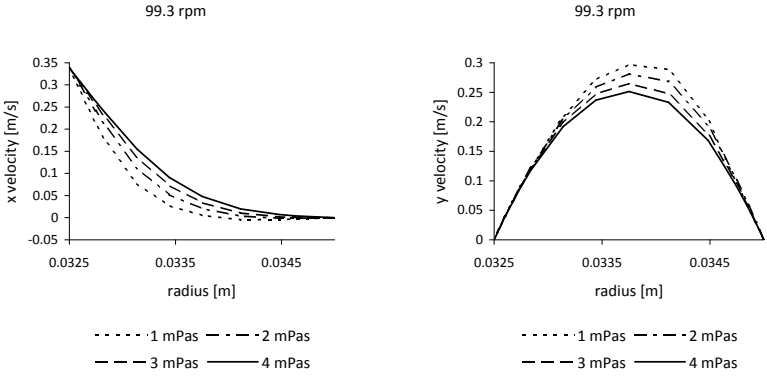

(a) (b)

Figure 46: Flow in the measuring gap at a rotational speed of 99.3 rpm for different viscosities: horizontal velocity profile (left), vertical velocity profile (right)

moment and the shear stress is not apparent; the shear stress is a function of the geometry parameters (which remain the same here), the moment, and the viscosity. Especially at higher moments, the related shear stress deviates from a linear function. Even more obvious is the change in the function for the shear rate, due to viscosity. Even though there is a linear relation with a small offset, the function changes completely with increasing viscosity.

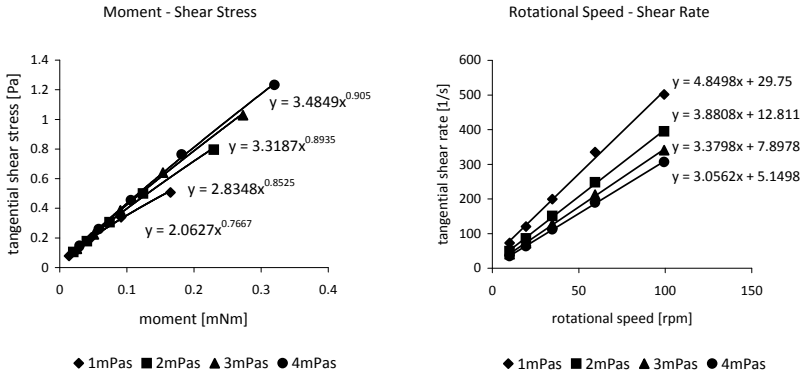

(a) (b)

Figure 47: Correlation of shear stress and moment (left) and shear rate and rotational speed (right) for Newtonian fluids with viscosities between 1 and 4 mPas

Thus, for standard viscometers, there is a constant factor that depends only on the geometry of the viscometer to calculate the shear stress or the shear rate. For non-Newtonian fluids, this factor is not constant, and the DIN 53019 suggests changing the c_L factor. For the process-viscometer, the viscosity also influences the factor.

As the simulations demonstrate, for the process-viscometer there is a non-linear relationship between the shear stress and the moment that depends, furthermore, on the viscosity, even for Newtonian fluids. The relationship between the shear rate and the rotational speed is linear, but with a small offset, and it depends strongly on the viscosity, even for Newtonian fluids. It is now necessary to define the relationship between these functions and the viscosity (see Figure 48). The relationship is also non-linear, and a power law fits best.

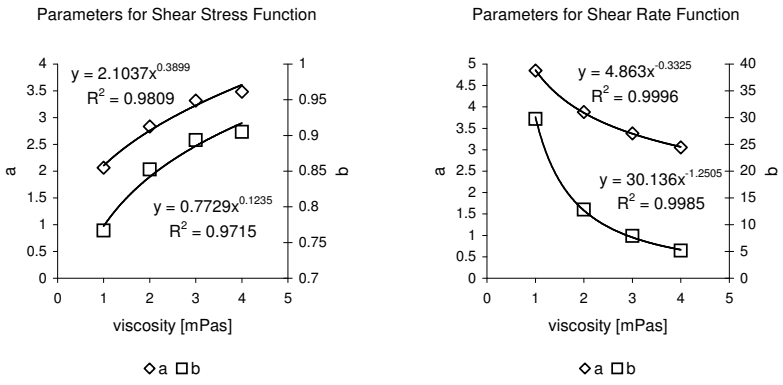

(a) (b)

Figure 48: Correlation of the parameters for shear stress and moment (left) and shear rate and rotational speed (right) and viscosity

Merging the functions of Figures 47 and 48 for the shear stress results in

$$\tau = \left(2.1037\eta^{0.3899}\right) M^{\left(0.7729\eta^{0.1235}\right)} \tag{94}$$

and the shear rate is

$$\dot{\gamma} = \left(4.863\eta^{-0.3325}\right)\Omega + 30.136\eta^{-1.2505} \tag{95}$$

Note that η has the dimension [mPas] in these formulae. Now, functions are derived to calculate the shear stress from the measured moment and the shear rate from the measured rotational speed. Note that these functions are only valid for the given geometry ($R_i = 32.5\ mm$, $R_a = 35.0\ mm$, $L = 35.0\ mm$) and the given operating conditions (flow rate = 10 l/Min). A final validity check of the simulations is shown in Figure 49, in which the flow curves of the simulations with varying viscosity are displayed. The gradients of the linear trend lines reflect the defined viscosity with very good agreement. This underlines the fact that the simulation is consistent on its own. However, it also clearly shows that the shear rate is different from the rotational speed, depending on the viscosity. The rotational speeds are always 10.0, 19.5, 34.7, 59.4, and 99.3 rpm. But for 99.3 rpm, for example, the corresponding shear rate varies between 501 s^{-1} for 1 mPas and 307 s^{-1} for

4 mPas. This is important to understand when evaluating the measurements and the derivation of the rheological model.

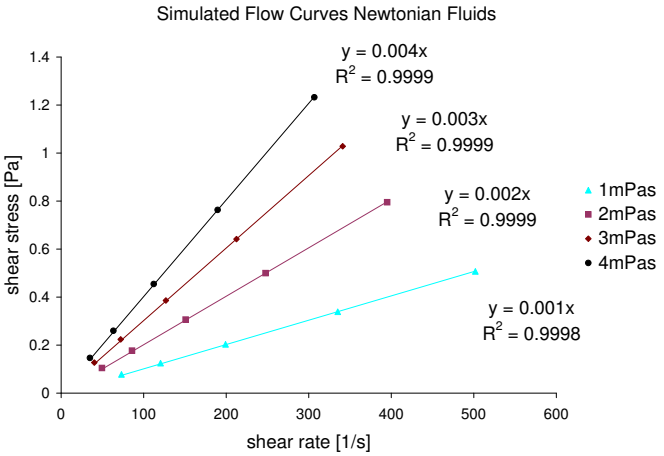

Figure 49: Simulated flow curves of Newtonian fluids with varying viscosity

Analysis of the Measurements with the process-viscometer

The measurements provide the moment and the rotational speed for different sludge concentrations (see Figure 30 in Chapter 4.2.2). The unknown variable is the non-Newtonian viscosity. In the previous paragraphs, functions were derived to calculate the shear stress from the measured moment and the shear rate from the measured rotational speed. Finally, the measured viscosity is derived. This raises some questions:

1. Since the viscosity is unknown, how can the shear stress and shear rate be calculated, for which the viscosity is required as input parameter?

2. How can the functions derived from simulations of Newtonian fluids be applied to non-Newtonian fluids?

The first question leads to an iterative process, where an initial value for the viscosity is estimated and varied until the calculated rheological model fits best to the measured values. The second question is somewhat more difficult to answer but it is fundamental for the entire sludge model.

As mentioned earlier, the process-viscometer is not able to measure the yield stress directly or indirectly. Because it also cannot be modeled in the simulation, it is set to zero. Therefore, there are three parameters left to fit the rheological model to the measurements: η_0, η_∞ and τ_B. To recall the rheological model of Worrall and Tuliani 1964 (for $\tau_y = 0$):

$$\tau = \frac{(\eta_0 - \eta_\infty)\dot{\gamma}}{1 + \frac{(\eta_0 - \eta_\infty)\dot{\gamma}}{\tau_B}} + \eta_\infty \dot{\gamma} \tag{96}$$

For the iterative process, there are three ways in which viscosity could be considered as the input parameter:

1. η_0
2. η_∞
3. something different

η_0 describes the viscosity (gradient of the flow curve) for low shear rates, whereas η_∞ describes the viscosity for high shear rates (an asymptotic value). Considering the simulations conducted with water, it becomes clear that, due to the vertical flow, a very high shear rate prevails in the measuring gap, independent of the rotational speed. Therefore, the viscosity considered in the functions for calculating the shear stress and the shear rate is η_∞.

In an iterative process, the rheological model is fitted to the measurements (see Figure 50). The square correlation coefficients R^2 are between 0.995 and 0.998 and the mean square residuals are between 0.0002 and 0.0018. The flow curve for water is also displayed, for comparison, because the functions are calibrated to the viscosity of water. As mentioned above, the viscosity for sludge up to a concentration of 2 g/l does not differ significantly from that of water. As Günder 1999 already reported, the flow curve of sludge up to a concentration of 5 g/l (prevailing sludge concentration in aeration tanks) is nearly Newtonian. Plastic behavior (curvature in the flow curve) starts at round about 5 g/l. This means that the assumption that sludge is a Newtonian fluid, which was stated by Bokil and Bewtra 1972, Hanel 1982, and partly Armbruster 2004 is correct when considering low sludge concentrations. The antithesis - sludge is a non-Newtonian fluid - is correct for higher sludge concentration. However, because higher and lower sludge concentrations occur in aeration tanks and particularly in secondary clarifiers and thickeners, the synthesis of modeling sludge with a shear thinning approach is preferable. It reproduces a nearly linear flow curve for low sludge concentrations and a non-linear, plastic flow curve for higher sludge concentrations. Please note: in the

rheological model of Worrall and Tuliani (Equation 96), a linear function appears when $\eta_0 = \eta_\infty$; then, only the term $\tau = \eta_\infty \dot{\gamma}$ remains, which is exactly the flow curve for Newtonian fluids. The greater the difference between η_0 and η_∞, the more distinct the curvature in the flow curve is (shear thinning). Mathematically, the function of Worrall and Tuliani can model Newtonian and shear thinning fluids exactly. Attention should be paid to the fact that η_0 is always greater than η_∞ and τ_B is never zero (division by zero).

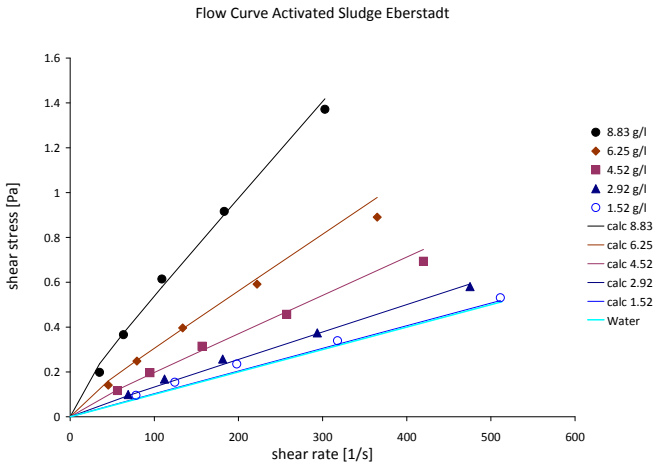

Figure 50: Measured and calculated flow curves for different sludge concentrations

The next step of the analysis is to correlate the three parameters of the rheological model (η_0, η_∞ and τ_B) with the sludge concentration (see Figure 51). Since many similar figures will follow, it will be explained in detail. The parameters η_0 (initial viscosity) and η_∞ (viscosity for high shear rates) have the dimension [Pas] and refer to the left axis. The parameter τ_B (Bingham yield stress) has the dimension [Pa] and refers to the right axis. Note that both axes have a logarithmic scale. The formulae for the trend lines are also displayed in the diagram and in Equations 97 to 99. As all investigators cited in Chapter 2.5 mention, there is a non-linear relationship between the parameters of the rheological model and the sludge concentrations. The investigators use three different types of functions: polynomial, power, and exponential. For the measurements of activated sludge, the polynomial functions show the best fit.

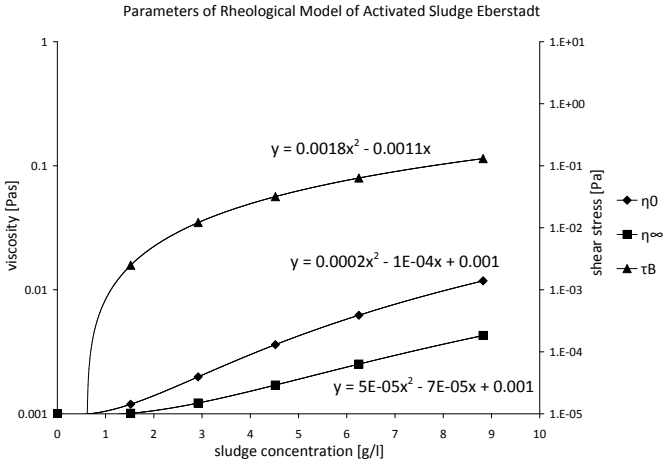

Figure 51: Correlating the parameters of the rheological model to the sludge concentrations

From the curve fitting (Figure 51), it is possible to derive the final formulae required to complete the hybrid sludge model as follows:

$$\eta_0 = 0.00015c^2 - 0.0001c + 0.001 \tag{97}$$

$$\eta_\infty = 0.00005c^2 - 0.00007c + 0.001 \tag{98}$$

$$\tau_B = 0.0018c^2 - 0.0011c \tag{99}$$

$$\eta = \frac{d\tau}{d\dot{\gamma}} = \eta_\infty + \frac{\left(\eta_0 - \eta_\infty\right)\left(1 + \frac{(\eta_0 - \eta_\infty)\dot{\gamma}}{\tau_B}\right) - \frac{(\eta_0 - \eta_\infty)^2\dot{\gamma}}{\tau_B}}{\left(1 + \frac{(\eta_0 - \eta_\infty)\dot{\gamma}}{\tau_B}\right)^2} \tag{100}$$

Some remarks about the fitting of the parameters and transferring it to a numerical sludge model are appropriate here. For η_0 and η_∞, the values should be 0.001 Pas (the viscosity of water) for a sludge concentration of 0 g/l (clear water).

The values can become slightly lower than 0.001 Pas for sludge concentrations between 0 and 1 g/l. This is not a problem for the solver, but it can be easily handled by setting the value to 0.001 Pas in this case. The value for τ_B should be zero for clear water. Because a problem for the solver arises when division by zero occurs, the viscosity should be set to 0.001 Pas in this case.

In the final step of the evaluation, all measurements made with the process-viscometer are simulated with the hybrid sludge model. The results are displayed in Figure 52 and fit well to the measured and calculated values of the rheological model (R^2 between 0.994 and 0.997, square residuals between 0.0004 and 0.0011). Note: it is possible to obtain a better fit between the measured and the calculated flow curves by increasing the plastic characteristics (increase the values for τ_B and η_0), because the measurements indicate a distinct plastic behavior above 5 g/l. However, as a consequence, η_∞ is then lower. If the simulation is conducted with these values, the results are far away from the other curves. Hybrid sludge modeling means achieving an optimum of agreement with all the three components: measurements, rheological model, and simulation. This is considered as the "fundamentally justified" physical viscosity of sludge.

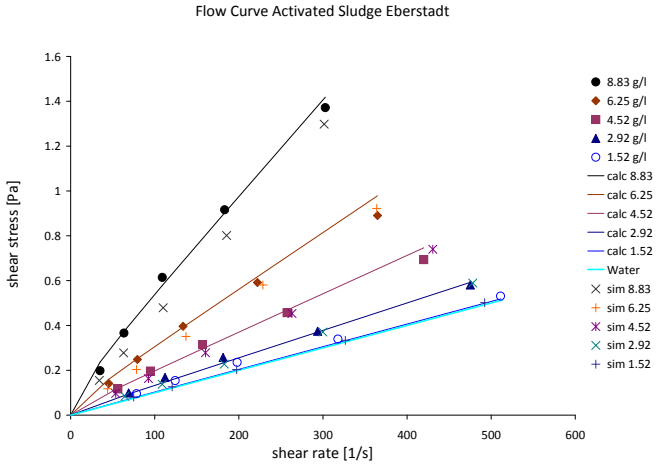

Figure 52: Comparing the measured flow curves for different concentrations with the calculated (fitted) rheological models and the simulated flow curves

As mentioned above, the higher shear rates prevail in the annulus of the process-viscometer. Figure 53 shows the distribution of the viscosity in the measuring gap at 10 rpm and 99.3 rpm for different concentrations. At least for 10 rpm and higher

sludge concentrations, the viscoplastic behavior of sludge in the annulus is obvious. For the other simulations, it is more or less constant. More details about the viscosity distribution and the corresponding shear rates can be found in Appendix Figures 114 to 118. In addition, the velocity profiles can be found in Appendix Figures 109 to 113.

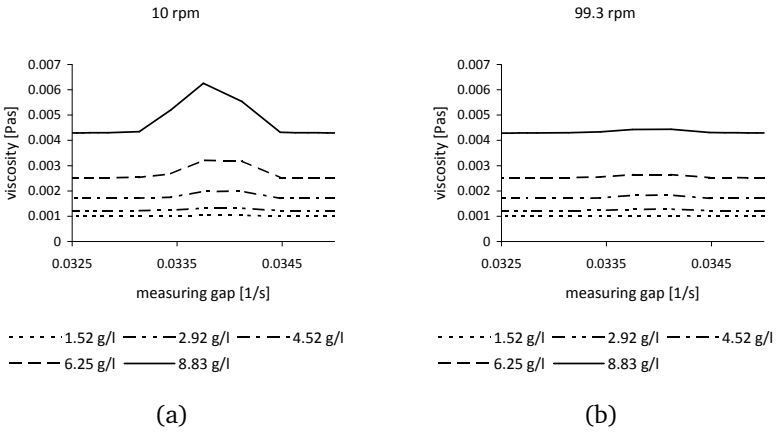

Figure 53: The viscosity in the measuring gap at a rotational speed of 10.0 rpm (left) and 99.3 rpm (right) for different sludge concentrations

Another strong argument for the plausibility of these flow curves for sludge is the flow curve of water. As mentioned previously, low-concentrated sludges have a viscosity close to that of water and then the viscosity begins to increase. Above 5 g/l, the viscoplastic properties become significant and, because the relationships between the parameters of the rheological model are non-linear related to the concentration, the viscoplastic properties (curvature) develop disproportionately.

To answer the ultimate question - what is the viscosity of sludge - with numbers: activated sludge from the communal WWTP in Eberstadt with 5 g/l has a viscosity between $\eta_0 = 4.3$ mPas and $\eta_\infty = 1.9$ mPas. This is significantly higher than water (1.0 mPas) but not as high as measured by other investigators with standard viscometers. Sludge with 10 g/l has a viscosity between $\eta_0 = 15.0$ mPas and $\eta_\infty = 5.3$ mPas. The accuracy of the process-viscometer is about 0.1 mPas. This is already sufficient to distinguish between water at $10°C$ (1.3 mPas) and at $20°C$ (1.0 mPas), which the process-viscometer actually does.

Attention should be paid to the basic values of the measurements and simulations (moment and rotational speed) in Figure 54. The moments of the simulation are calibrated with the same factor (1.63), as explained earlier. The agreement between the simulated and measured values is good (R^2 between 0.989 and 0.998, square residuals between 0.00004 and 0.00046) and shows that the calibration factor is still valid, even for non-Newtonian fluids.

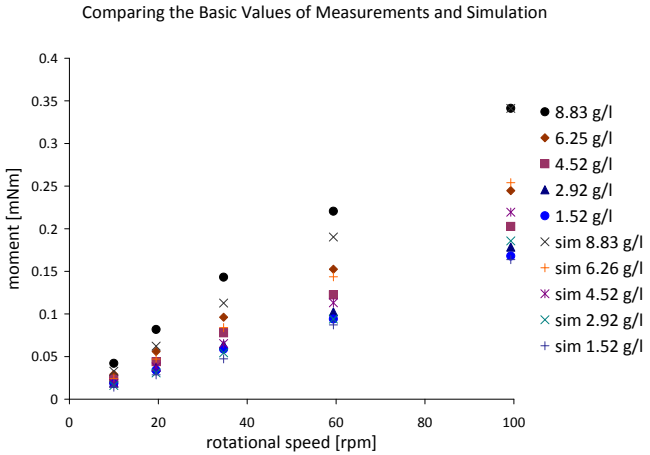

Figure 54: Comparing moments of measurements and simulation

4.3 Validating the Sludge Model with a Lamella Clarifier

Following the derivation of the parameters for the hybrid sludge model, it is necessary to test the model in a real treatment plant with complex flow conditions. Here, it can be seen whether or not the hybrid sludge model is able to predict flows, sludge levels, or even outflow concentrations. In particular, outflow concentrations are difficult to predict with acceptable accuracy. Schumacher 2006 states: "It should be stated that every simulation is only conditionally able to predict absolute outflow concentrations. The outflow concentrations of the simulations have a rather relative character in order to compare different geometric or operational set-ups"(p. 39, translated). For water treatment plants, it is still state-of-the-art to compare different set-ups rather to predict outflow concentrations.

4.3.1 Design and Set-Up of the Lamella Clarifier

The testing plant is a small lamella clarifier, made of Plexiglas, in order to allow visual comparison of the testing plant with the simulation. Its height is 2 m, the length is 1.6 m and the width is 0.6 m. The volume is 1.17 m^3. The inlet is a small pipe (diameter 1/2") on top of the clarifier (the inlet has been modified later on, so that the flow is from the top down into the clarifier). There are 6 lamellas with a total effective area of 2.3 m^2. The perpendicular distance between the lamellas is 5 cm (see Figure 55). During the tests, sludge is not withdrawn to achieve a breakthrough. The sludge is taken from the aeration tank of the WWTP in Eberstadt, which has a concentration of approximately 5 g/l. For operational reasons, it is not possible to keep the inlet concentration exactly constant (see Figure 56). The flow is 20 l/min or 1.2 m^3/h, which has been measured with a magneto-inductive sensor located at the pipe to the inlet; thus, the volume of the plant is exchanged, theoretically, in one hour.

Two tests are conducted, one on 27 March 2013 the other on 11 April 2013. The sludge concentration on these two days differs slightly. During the tests, sludge samples are taken every 15 min from the inlet, the outlet and from underneath the lamellas. During the second test, a photo of the plant is made every minute, to visualize the distribution of sludge within the lamella clarifier. During this second test, the flow velocity near the inlet in the stream is measured with a magneto-inductive flow sensor.

Two simulations are also conducted. The first one involved a relatively fine mesh (7,089,881 cells, max. skewness 0.889) with 20 cells between the lamellas to resolve secondary flows. The inlet concentration remains constant at 4.6 g/l (the average of the inlet concentration of the test conducted on 27 March 2013). In this simulation, only a rudimentary sludge model is included. The settling velocity is modeled with the variation 3 curve without considering a break point (see Chap-

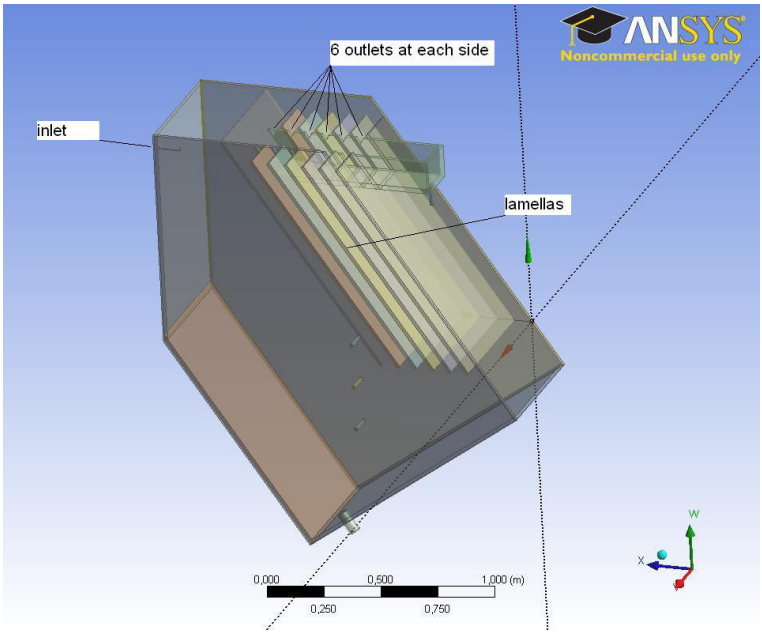

Figure 55: Geometry of the lamella clarifier

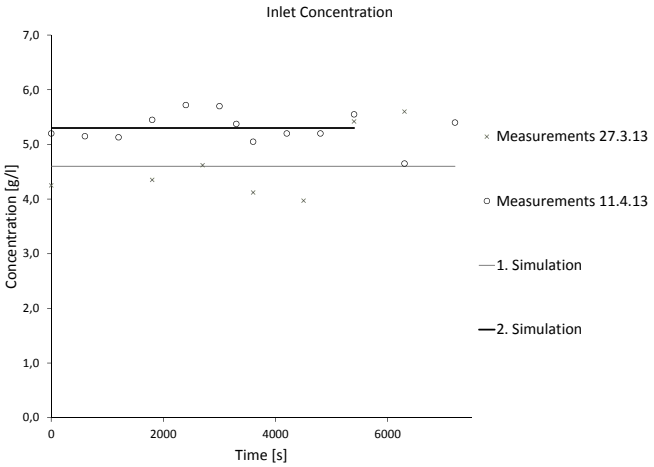

Figure 56: Measured and simulated inlet concentration of the testing plant

ter 4.1.1). The viscosity is constant at 1 mPas, without considering shear thinning, or the dependency on sludge concentration. The diffusion of sludge is coupled with the k-ϵ turbulence model (see Chapter 3.3.3), and the density varies with the sludge concentration, to enable stratified flow effects (see Chapter 3.3.4). The time step size is increased to 0.05 s. Due to the high velocity at the inlet (1.7 m/s) and the fine mesh, it is not possible to calculate with a higher time step size. In the end, approximately 300,000 iterations are necessary to simulate a flow time of two hours (7,200 s), which takes 5 weeks with a 12-core machine.

The second simulation has a coarse mesh (1,730,254 cells, max. skewness 0.892) with 15 cells between the lamellas. The inlet concentration remains constant at 5.3 g/l (the average of the inlet concentration of the test conducted at 11 April 2013). In this simulation, the full sludge model is included. The settling velocity is modeled with the variation 4 curve with break point. The viscosity is modeled according to the measurements presented in Chapter 4.2.3. Again, the diffusion of sludge was coupled with the k-ϵ turbulence model, and the density varies with the sludge concentration, to enable stratified flow effects. The time step size is increased to 0.01 s, and about 1,000,000 iterations are necessary to simulate a flow time of only 89 min (not the 120 min for which the test lasted). The 12-core machine required 2 months for the simulation. The time step size was kept small to avoid any inaccuracies caused by the time step size during the calculation.

4.3.2 Comparing the Results from the real Lamella Clarifier and the Simulation

For the main result of the simulation - a comparison of the outlet concentration of the simulation with the measurements - significant differences, as displayed in Figure 57, are apparent. The first simulation should fit the measurements of the test conducted on 27 March 2013, but it barely does. The outlet concentration is, at first, nearly zero, as expected, and approaches the inlet concentration, as in the test. But the breakthrough starts far too early. Already after 16 min (960 s), the outlet concentration increases, whereas, during the test, it starts to increase after 45 min (2,700 s). Even though both tests are not identical, due to differences in the inlet concentrations, the breakthrough after 45 min is the same. This shows that the test is reproducible. The second simulation with the full sludge model reveals a different picture. Since the constant inlet concentration is the average of the test conducted on 11 April 2013, it should fit the measured values of this test, and it does this very well. The breakthrough starts after 45 min, as it did during the test. The simulated outlet concentration follows the course of the measured values well until it ends after 89 min (5,342 s). After this time span, the measured outlet value decreases slightly, probably because the inlet concentration also decreased at this

time, since a new batch volume with activated sludge was connected to the testing plant (this was necessary every 40 min). However, due to time constraints, it was not possible to simulate the last 31 min, but the greatest part of the breakthrough was simulated and predicts well what happens in the real testing plant. In this case, one can say that this is already beyond state-of-the-art for predicting outlet concentrations and the time of the breakthrough. In terms of real WWTPs, it is different, because a breakthrough should not occur, but changes in the outflow concentrations, due to rainfall or changes in operation would be interesting. Because the outflow concentration is some orders of magnitudes lower than that of activated sludge within the plant, this is quite challenging to grasp, but would be interesting to simulate with the hybrid sludge model.

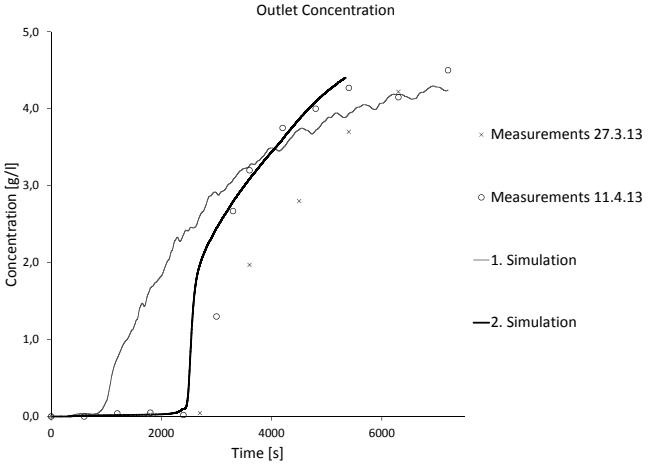

Figure 57: Measured and simulated outlet concentration

The flow through the testing plant is measured with a magnetic inductive sensor located at the pipe to the inlet of the testing plant. This can be compared with the flow at the outlet of the simulation (the inlet flow is a constant boundary condition with 20 l/min). Figure 58 shows the measured and simulated values. During the first iterations of the simulation, there is as always an overshoot but, after a few seconds, it is more or less constant at 20 l/min. During the test, it also takes a few seconds until the pump reaches its designated value, but it remains relatively constant throughout the test.

As already mentioned, there are 6 lamellas and 6 interspaces between the lamellas. Each interspace has two overflows that drain into an open channel (see Figu-

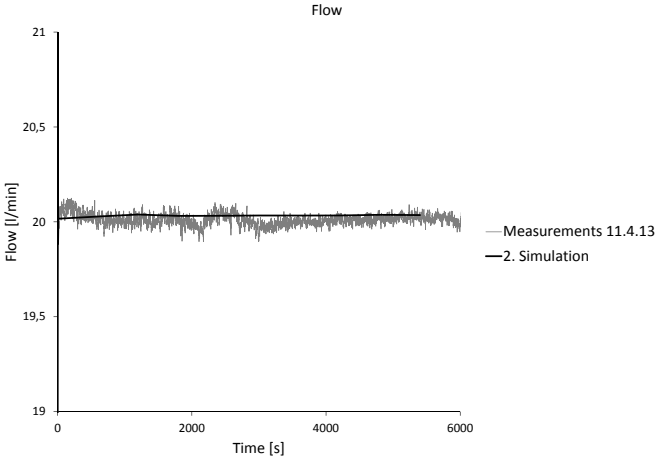

Figure 58: Measured and simulated flow through the testing plant (the flow axis appears boldly because of the overshoot in the first milliseconds of the simulation)

re 60). To evaluate whether or not the flow through each interspace is identical, the overflow has a triangular shape. The height of the overflow h_o was measured with a simple ruler (between 16 and 17 mm). The flow is calculated as follows:

$$Q = h_o^{2.5} \left(\frac{8}{15} 0.64 \tan\left(\frac{60^\circ}{2} \right) \sqrt{2g} \right) \tag{101}$$

This value is, of course, not very accurate but it is a good approximation. As shown in Figure 59, the flow through the outer interspaces is slightly lower than for the rest, whereas the simulations show a nearly uniform flow through all interspaces. One explanation might be that the testing plant is not exactly horizontal but, as one can see, the differences are small and should not be overemphasized, because the measurement with the ruler is also not very exact.

The flow velocities in the testing plant are small (<5 cm/s, see Figure 61). One large vortex appears at the edge, near the bottom. The mesh becomes fine near the inlet and underneath the lamellas; therefore, the vectors are very dense in this region. Actually, the flow appears as would be expected and as it is also encountered at the real testing plant.

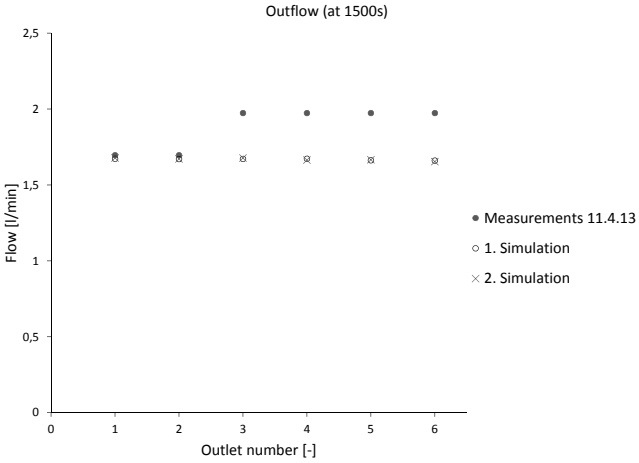

Figure 59: The measured and simulated flow through each interspace between the lamellas

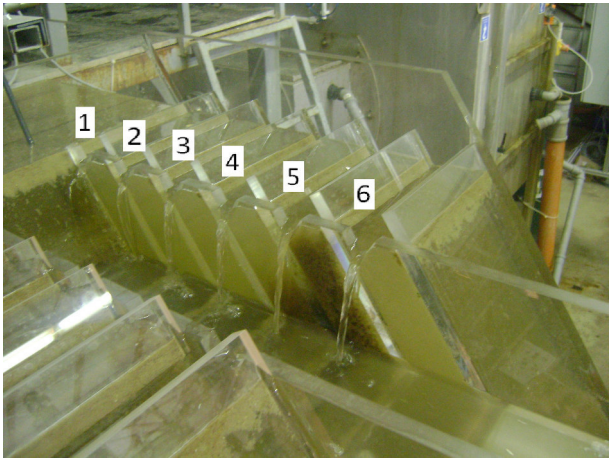

Figure 60: The outflow of the testing plant

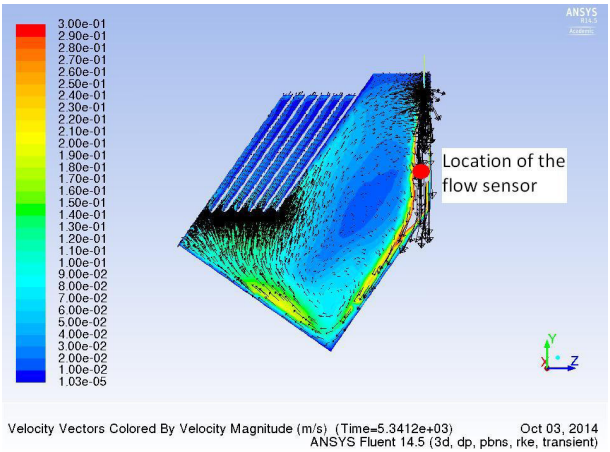

Figure 61: Flow velocity [m/s] inside the testing plant and location of the flow sensor. The high velocities at the inlet are not displayed, but can be seen in Appendix Figures 119 to 121

As mentioned previously, the flow is measured in the stream from the inlet, because the accuracy of the magneto-inductive sensor is at its limit below 5 cm/s. In Figure 62, the measured and averaged velocity is compared with the velocity during the simulation at one point. Due to the averaging of the measured values, less scattering occurs and a decreasing velocity becomes visible. The simulation, however, shows a relatively constant velocity over the time period with some fluctuation. A possible explanation is that the position of the sensor changed slightly during the test. As shown in Figure 61, the velocity gradients along the inlet streams are very high. If the sensor changes its position by only a few millimeters, the velocity changes significantly. The magneto-inductive flow sensor at the pipe to the inlet indicates no change of the flow rate during the test (see Figure 58); therefore, it is not plausible that the velocity near the inlet decreases.

It is more interesting to consider the flow field in the interspaces between the lamellas in more detail (Figure 63). Because the outflow is on top of the interspaces, the flow must move upwards. ANSYS FLUENT shows strange vectors at walls, when the sludge model is used. There is no flow through the walls and the results confirm this. This seems to be a problem with the display function and not with the results, because similar observations have been made in other simulations with the sludge model. However, at the bottom of each lamella, the sludge concentration is relatively high, due to settling. Therefore, the density is also higher and a density gradient

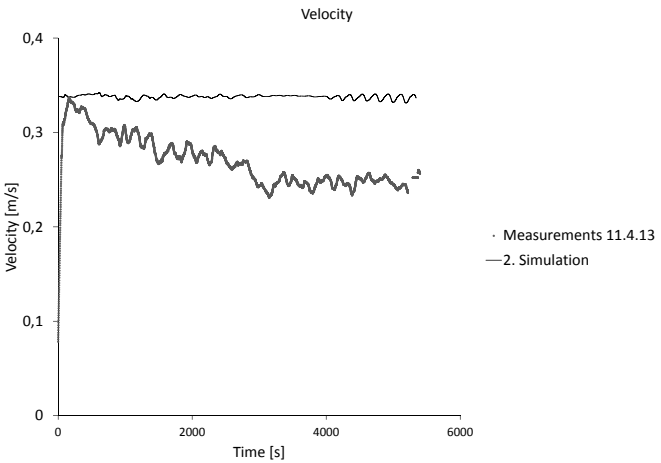

Figure 62: Measured and simulated velocity at a point in the inlet stream 37 cm under the inlet

occurs. (The density is linked linearly to the sludge concentration; therefore, the appearance of the contours is the same - only the values are different.) Because the turbulent viscosity is already low in the interspaces between the lamellas (in the range of the molecular viscosity; see Figure 65), the exchange of momentum is low and the concentrated sludge can move independently of the bulk flow. Because of the higher density and the slope of the lamellas, it moves downwards. The less concentrated sludge moves upwards and, at the top of the interspace, there is a thin layer of relatively clear water. This is the stratified flow effect explained in Chapter 3.3.4 and 3.3.5. A comparison of Figures 65 and 66 reveals that the molecular viscosity for concentrated sludge is already two orders of magnitude higher than the turbulent viscosity.

When standing in front of the real testing plant, one can observe the movement of the sludge, which confirms the simulation results. Even though the photo (Figure 64) only gives a faint impression, one can recognize indications of the presence of a thin clear water layer at the top of the interspaces. The first simulation presents a completely different picture (see Appendix Figure 121). There is no distinct backflow at the bottom of the lamellas and no upflow in the clear water zone at the top of the lamellas. This, together with the sludge concentration, contradicts the observations made at the real testing plants. This demonstrates, again, the importance of a realistic rheological model and the necessity for small time step sizes. To

simulate the effects mentioned above, a minimum of 10 cells between two lamellas is needed, which usually results in a high cell number, especially when there are more than 6 lamellas.

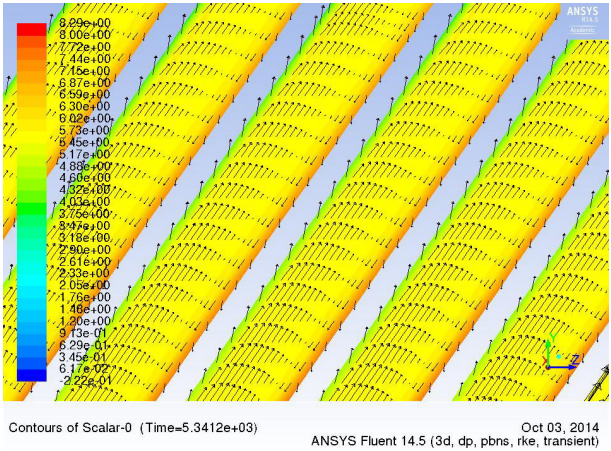

Figure 63: The vectors show the flow velocity, the color shows the sludge concentration [g/l] in the interspaces between the lamellas of the 2. simulation

Even though the flow velocity field cannot be shown in photos from the real plant, the development of the sludge interface or of the sludge level over time can be shown and compared with the simulation (see Figures 67 to 74). After 5 min, a diffuse sludge distribution can be seen, but not a clear sludge interface. After 10 min, a sludge interface becomes visible at the bottom of the lamellas. It is highlighted in the photo from the real plant. In the following minutes, the sludge moves up. In the real plant, the sludge level in each interspace is different; it is more or less uniform in the simulation. However, in total, the height of the sludge level correlates well. After 30 min, the sludge level is in the middle of the lamellas, both in the simulation and in the real testing plant. After 40 min, the sludge level in the simulation is a bit higher than at the real plant. Recalling Figure 57, the breakthrough starts after 45 min. After 50 min, the sludge level in the simulation reaches the outflow; in the real plant, the sludge level in only 3 of the 6 interspaces reaches the outflow. After 60 min, the simulation and the real plant paint the same picture and the outlet concentration approaches the inlet concentration. The situation does not change any more and, after 89 min, it is still the same. A small difference can be seen on the right side of the lamellas, where the real plant shows a distinct clear water zone at the top, which does not occur in the simulation.

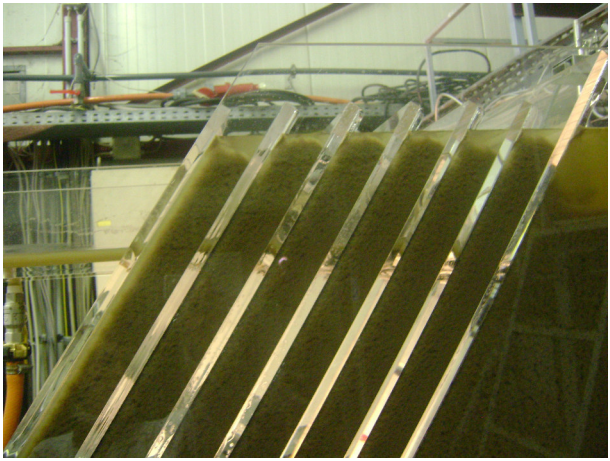

Figure 64: The interspaces between the lamellas in the real testing plant after the breakthrough

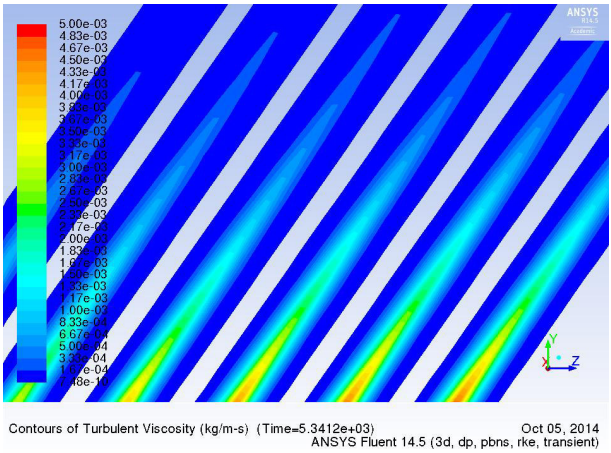

Figure 65: The turbulent viscosity [Pas=kg/(ms)] between the lamellas of the 2. simulation

Summary and Discussion

In summary, the hybrid sludge model predicts the behavior of sludge in a complex treatment plant such as the lamella clarifier quite well. The breakthrough is predicted very well and the visual comparison of the sludge movement underlines this fact, even though small differences occur, as is the case with every simulation or model. However, it is also demonstrated that the introduction of a break point in the settling velocity, to describe compression, as well as the introduction of a realistic rheological model is essential for good simulation results (comparing the first and second simulation). In settling tanks, in particular, where the turbulent viscosity is low and the molecular viscosity becomes high, it is of major importance to have a realistic rheological model to describe the viscosity as a function of shear stress and sludge concentration. There are two reasons why the breakthrough of the second simulation starts later than in the first simulation. First, the settling velocity for low concentrations (below the break point) is higher. Second, the higher viscosity, caused by the sludge concentration, removes kinetic energy from the flow and transforms it into heat energy. Both factor leads to a later breakthrough, which is more realistic. These two differences seem to be small but, as has been shown, they have a major impact on the quality of the results. This confirms what is already stated by Armbruster 2004 and Schumacher 2006: changes in the rheological model have a significant influence on the flow velocity field in secondary clarifiers. With the new approach of measuring the viscosity of low concentrated sludge, which is presented here, it is now possible to have a more realistic rheological model and, therefore, an improved quality in the results of the simulation.

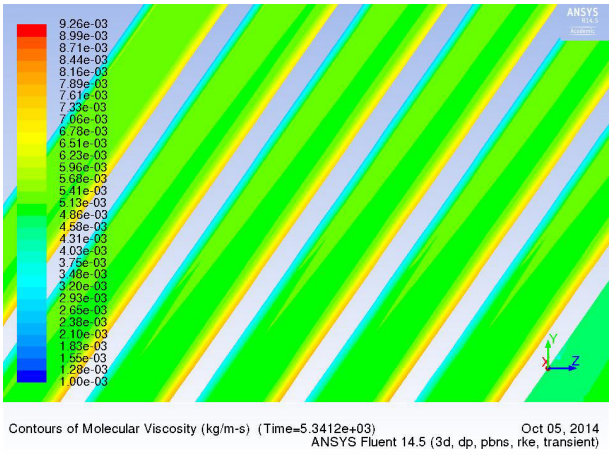

Figure 66: The molecular viscosity [Pas=kg/(ms)] between the lamellas of the 2. simulation

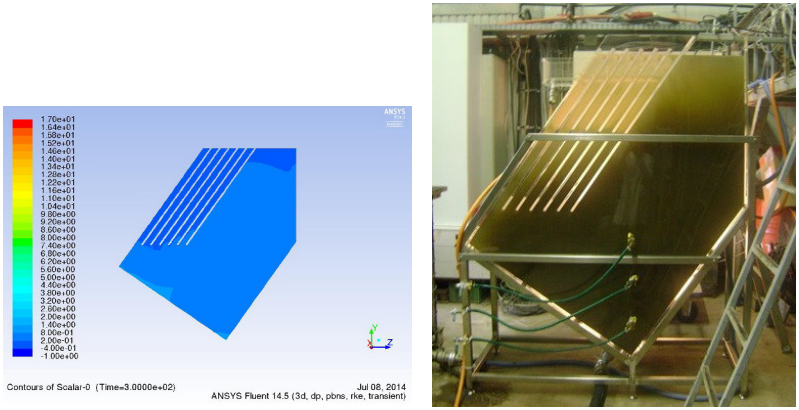

(a) (b)

Figure 67: Sludge concentration [g/l] in the simulation (left) and the real testing plant (right) after 5 min

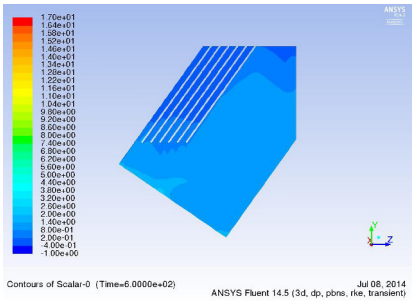

(a) (b)

Figure 68: Sludge concentration [g/l] in the simulation (left) and the real testing plant (right) after 10 min

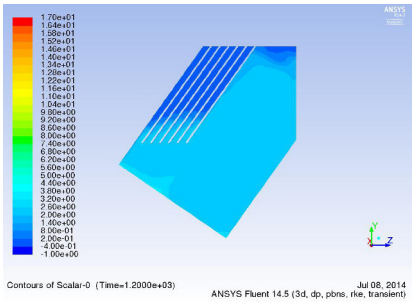

(a) (b)

Figure 69: Sludge concentration [g/l] in the simulation (left) and the real testing plant (right) after 20 min

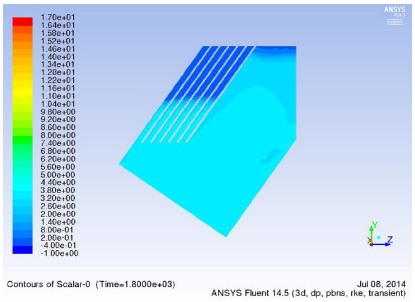

(a)

(b)

Figure 70: Sludge concentration [g/l] in the simulation (left) and the real testing plant (right) after 30 min

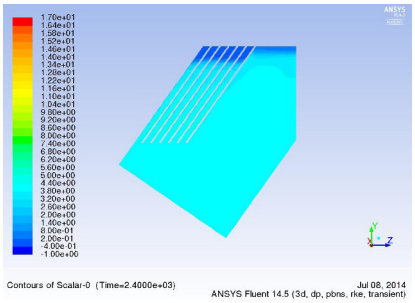

(a)

(b)

Figure 71: Sludge concentration [g/l] in the simulation (left) and the real testing plant (right) after 40 min

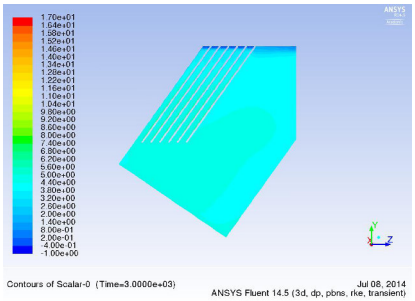

(a) (b)

Figure 72: Sludge concentration [g/l] in the simulation (left) and the real testing plant (right) after 50 min

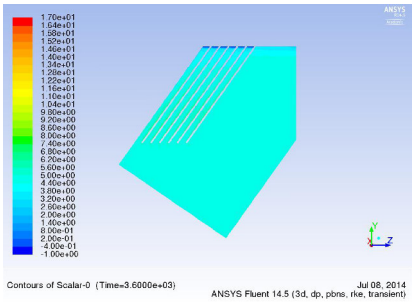

(a) (b)

Figure 73: Sludge concentration [g/l] in the simulation (left) and the real testing plant (right) after 60 min

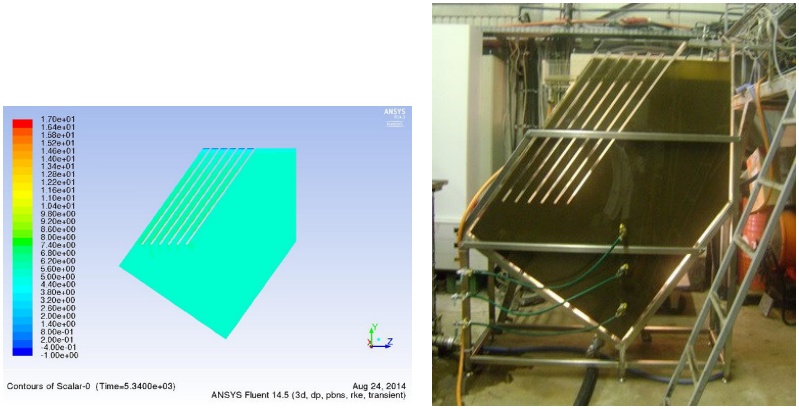

(a) (b)

Figure 74: Sludge concentration [g/l] in the simulation (left) and the real testing plant (right) after 89 min

4.4 Comparing the Properties of Different Sludges

Up to this point, the focus is on activated sludge from the WWTP in Eberstadt. But how does digestion change the properties of sludge? And how do sludge properties differ between other WWTPs or even between WWTPs and DWTPs? This will be discussed in this chapter.

4.4.1 Influences of Digestion on Settling Velocity

Conducting settling tests with digested sludge is more difficult than with activated sludge, for several reasons. First, the turbidity of the “clear water“ from digested sludge is much higher than that of activated sludge and, therefore, the sludge level can be seen only when strong illumination is present behind the cylinders. Second, floating sludge creates a problem. Settling of digested sludge occurs in two directions because of the gas production resulting from anaerobic digestion. The analysis of this thesis considers only the “down settling“. The results for digested sludge from the WWTP in Eberstadt are shown in Figure 75. It has also been modeled numerically by Knecht 2013.

Thickened digested sludge, which is older than digested sludge and therefore tends to produce less gas, the problem with floating sludge disappears. Only the issue with the high turbidity remains. The results for thickened digested sludge from the WWTP in Eberstadt are shown in Figure 76.

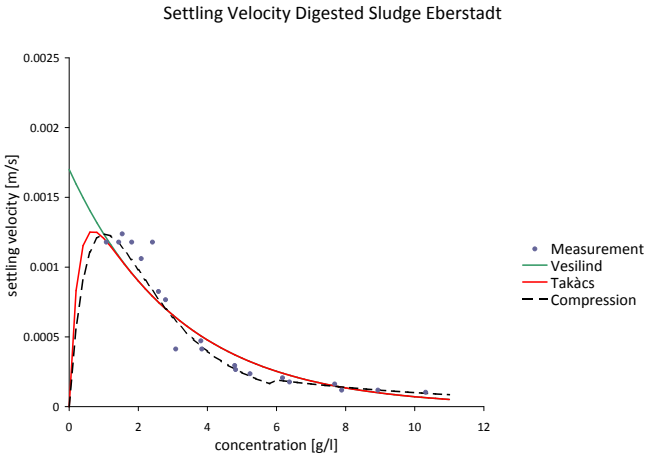

Figure 75: Settling velocity depending on sludge concentration for digested sludge in Eberstadt

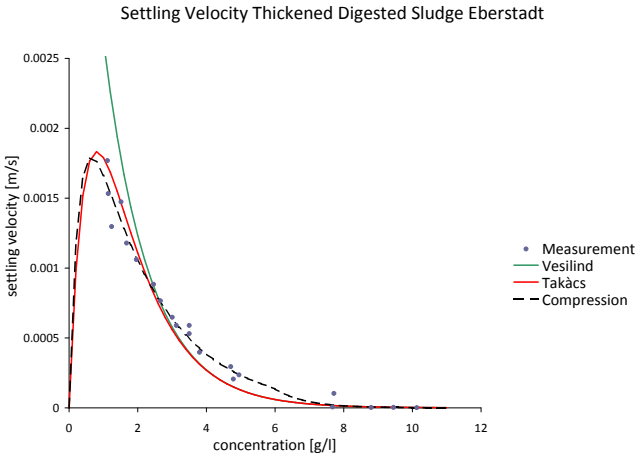

Figure 76: Settling velocity depending on sludge concentration for thickened digested sludge in Eberstadt

A comparison of the settling behavior of sludge during the treatment process reveals significant differences (see Figure 77). For higher sludge concentrations, the settling velocity of digested sludge is higher, compared to activated sludge; for lower concentrations, the settling velocity of digested sludge is lower. The differences can reach two orders of magnitude for sludge concentrations above 7 g/l. Only the maximum settling velocities are similarly high.

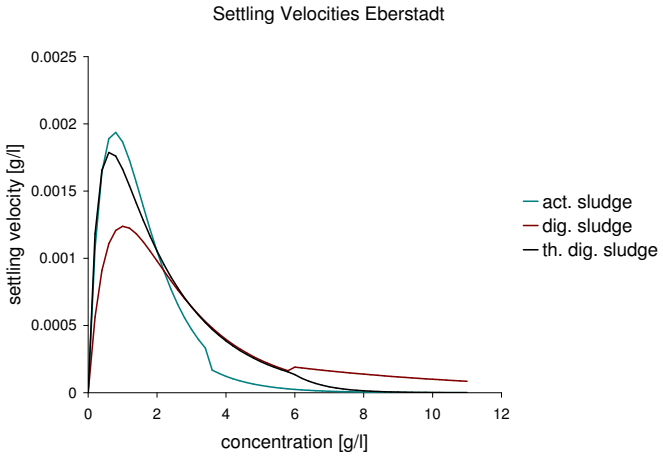

Figure 77: Comparing the settling behavior during the treatment process

Summary and Discussion

The treatment process, especially digestion, has a marked influence on settling behavior and cannot be neglected. In particular, the gas production makes it difficult to measure the settling velocity for digested sludge. In terms of simulations, further research is necessary to model the settling and floating velocity as a function of gas production.

4.4.2 Comparing the Settling Velocity of Sludges from Different Treatment Plants

The settling tests were repeated on a second WWTP in Griesheim. A comparison of activated sludges from both plants (Figure 78) makes it obvious that there is no significant difference, either in the fitted curves or in the measured datasets. The measurements in Griesheim were also numerically modeled; see Bickert 2013.

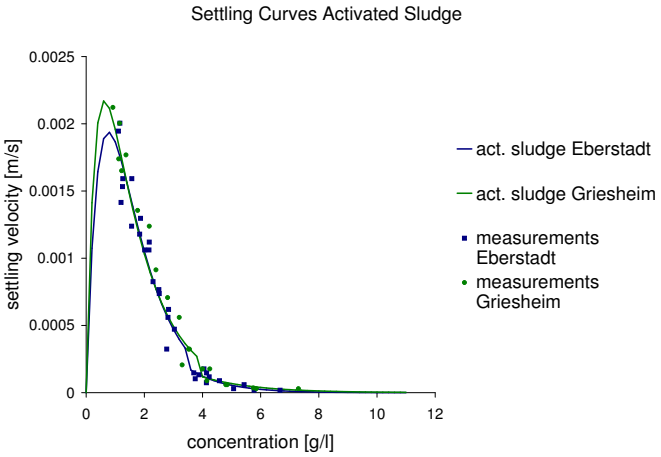

Figure 78: Comparing the activated sludges from Eberstadt and Griesheim

Comparing the curves with curves found in the literature for activated sludge reveals significant differences. They are in the same range and comparable but, as explained earlier, especially the settling velocity of more highly concentrated sludge has a major impact on simulation results, and there are large differences that cannot be neglected. Furthermore, it should be remembered that Härtel and Pöpel 1982 and Wahlberg and Keinath 1980 related the parameters of the settling velocity to the sludge volume index (SVI). For the given sludges in Eberstadt, the SVI for undiluted activated sludge ranged between 124 and 144 ml/g. Taking into account all thickened and diluted samples, it ranges between 70 and 177 ml/g, with an average of 119 ml/g. This also affects the resulting curves.

Interestingly, the settling velocity for digested (Figure 80) and thickened digested sludge (Figure 81) is significantly higher in Griesheim.

Attention will now be paid to the DWTP in Langenau. There, water from the Danube River and ground water is treated. Whereas the bacteria from activated sludge have a density slightly higher than that of water, the dry matter from flocculation sludge has a much higher density, which results in a wider range of concentrations. It is important to understand that there are two flocculation plants in Langenau. The older one is called Accelator the newer one is called compact-flocculation plant. The different processes affect the sludge properties. The settling velocity is, in general, much higher in the compact-flocculation plant than in the Accelator. The difference is obvious in Figure 82. This is remarkable, because it is the same raw

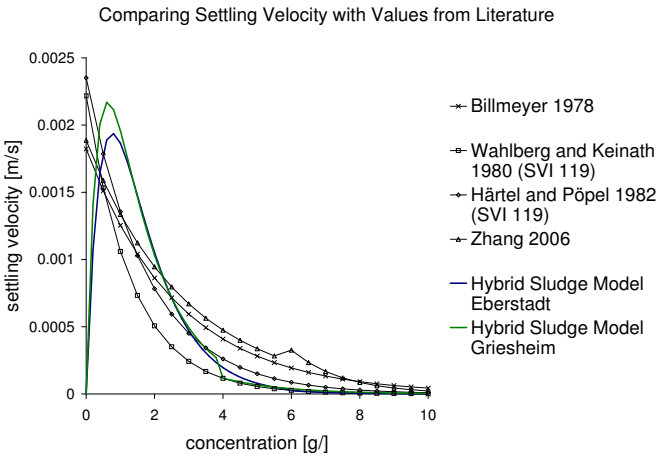

Figure 79: Comparing the settling velocities from both WWTPs in Eberstadt and Griesheim with curves found in Literature

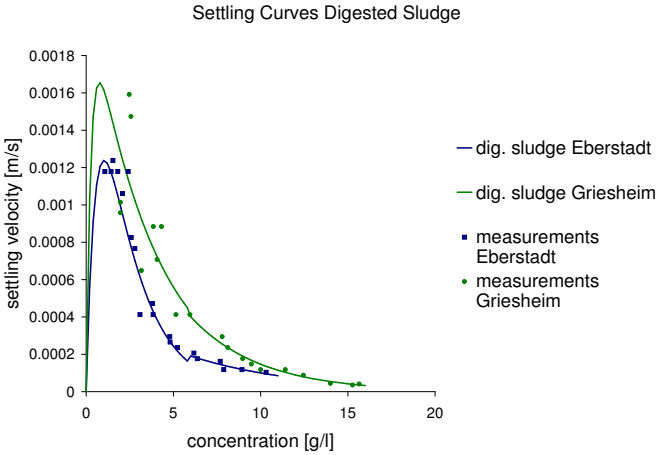

Figure 80: Comparing the digested sludges from Eberstadt and Griesheim

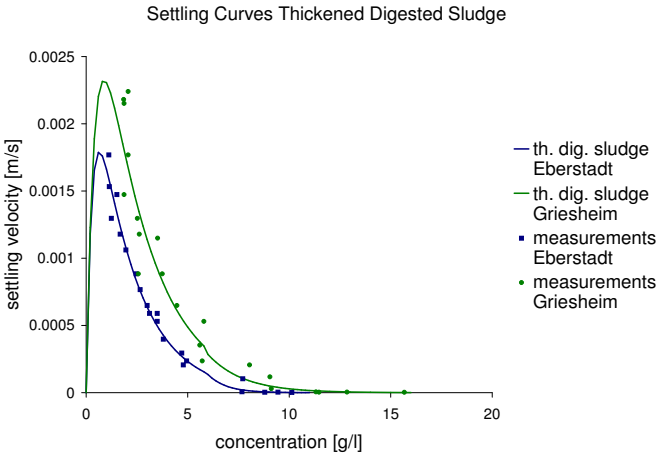

Figure 81: Comparing the thickened digested sludges from Eberstadt and Griesheim

water, the same flocculants but a different process. For flocculation processes, in particular, the speed with which flocculants are mixed in the raw water flow plays a major role. In the Accelator, this occurs in a pre-mixer, which has a relatively high volume and therefore the mixing process is slow. Other types of mixers have been therefore investigated with CFD (Brenda, Sonnenburg and Urban 2009). In addition, the sedimentation plant is also different. Within the Accelator, flocculation and sedimentation takes place in the same plant. In the compact-flocculation plant, there are separate chambers. In several chambers, slowly rotating mixers allow the flocs to grow until the mixture reaches the lamella clarifier, where the sludge is separated from the clear water. Building a lamella clarifier within the Accelator, in order to increase capacity, has been investigated (Brenda 2012). This is possible but the lower settling velocities would remain. In the end, it was decided to dismantle the Accelator completely to make room for a decarbonization plant.

Both plants, the Accelator and the compact-flocculation plant, are, in fact, two-line plants. One line of each plant is used for the flocculation, treating water from the Danube, and the other line is used for the decarbonization of ground water. The lime sludge from the compact-flocculation plant is also investigated; the results are shown in Figure 83. The picture is similar to the one before, but the range of concentration is even broader. Interestingly, the maximum settling velocity remains at about 2 mm/s, as is the case for all other investigated sludges. The scattering

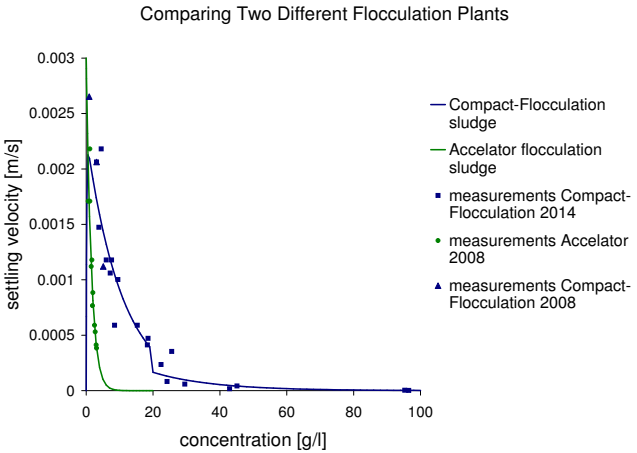

Figure 82: Comparing the settling velocity of two different flocculation processes

of the measured values with lime sludge is higher than with the other investigated sludges.

In any case, this kind of decarbonization will be replaced by a process in which lime pellets will be produced, instead of lime sludge. The main reason behind this decision is the deposition of the lime sludge. Only few factories, for instance, in the paper industry, can use lime sludge. The contracts with a nearby paper factory end soon; therefore, using a different decarbonization process, which produces lime pellets, is investigated. Due to the raw water quality, the lime pellets have a high quality and can be sold to different kinds of industry, such as cosmetics. Consequently, the Accelator will be dismantled and replaced by a new decarbonization plant and the two lines of the compact-flocculation will be used for flocculation (Holmer 2014). This is in line with a trend that is followed by quite a number of DWTPs in the Netherlands and Germany (Urban 2014 and Koppers 2014). Incidentally, CFD helped to optimize the new decarbonization plant in the planning and testing stages and also delivers valuable insights into the complex multi-phase flow with water and pellets inside the new plant.

Summary and Discussion

Even though settling velocities from sludge types from different treatment plants are in a comparable range, the differences are significant. Interestingly, the maximum settling velocity for all investigated sludges is about 2 mm/s. However, at

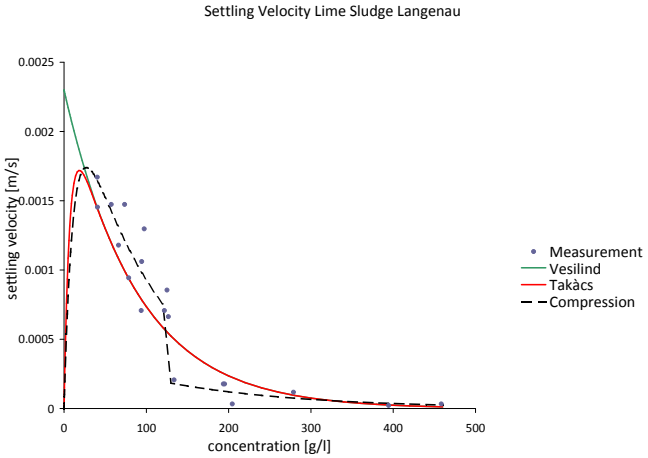

Figure 83: Settling velocity of the lime sludge in Langenau

higher sludge concentrations, when the settling velocity is low and compression starts, there are differences of several orders of magnitude and this leads to remarkable differences in the simulation results. It is therefore recommended to conduct settling tests for every water treatment plant of interest. Nevertheless, averaged curves can be useful for rough estimations for pre-designs.

4.4.3 Viscosity Changes due to Digestion

During the process of anaerobic digestion, the organic matter of the activated sludge (71.6-74.3% of the dry matter) is gradually transformed into inert matter (only 56.4-58.2% glowing loss in the digested sludge). That means that the ability of the bacteria to form flocs and to build up certain structures diminishes. This should have an impact on the viscosity. Figure 84 shows the flow curves of digested sludge from the WWTP in Eberstadt. The concentration of digested sludge (23.7 g/l) is much higher than that of activated sludge (4-5 g/l); therefore the values are also higher. In principle, however, the flow curve has the same shape as for activated sludge with the shear thinning effect. For higher concentrations, the shear thinning effect (non-linear flow curve) is even more apparent. The sample was diluted stepwise, as described in Chapter 4.2.2. When the concentration approaches zero, the viscosity is similar to the viscosity of water, as before.

To make the rheological model of digested sludge comparable to the other rheological models, it is necessary to display the three parameters of the rheological

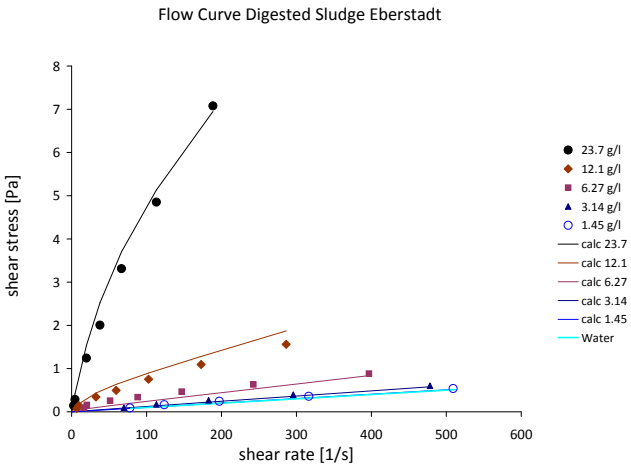

Figure 84: Flow curves of digested sludge with different concentrations from WWTP Eberstadt

model that depend on sludge concentration (see Figure 85). As before, the relation is non-linear, but it shows a greater spread of concentrations. A remarkable difference is the approximation of the Bingham shear stress τ_B. It was not possible to fit this parameter with a polynomial trend line of 2^{nd} order (square function), as it is the case with activated sludge. Therefore, a power function was applied. In fact, the power function would also fit quite well to the data from the activated sludge, because the difference, up to a concentration up to 10 g/l, is relatively small. However, when the sludge concentration exceeds 10 g/l, it is necessary to use a power function.

As a third type of sludge, thickened digested sludge is measured. The organic fraction is the same as for the digested sludge, the concentration is somewhat bit higher, but the age is greater. In terms of viscosity, large differences, compared to the digested sludge, are not expected. In Figure 86, the flow curves for different sludge concentrations are displayed. The shapes and the values are similar to those of digested sludge.

The parameters of the rheological model that depend on the concentration are displayed in Figure 87. The curves are quite similar to the curves of the digested sludge, as expected.

Keeping in mind all the different flow curves and parameter curves, the question is, how different are they? The advantage of the curve fitting is that it is now

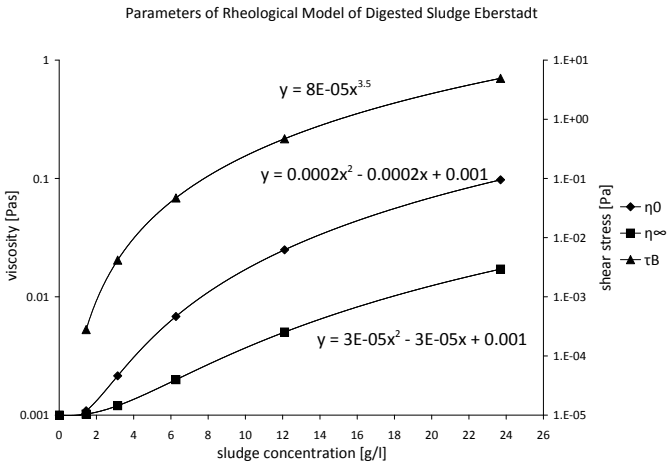

Figure 85: Parameters of the rheological model of digested sludge from WWTP Eberstadt depending on sludge concentration

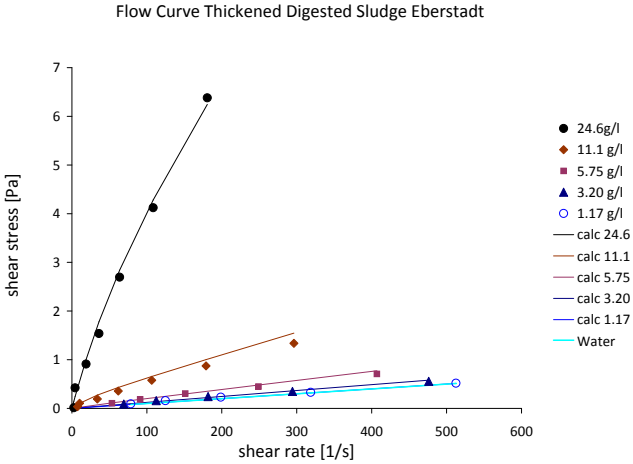

Figure 86: Flow curves of thickened digested sludge from WWTP Eberstadt with different concentrations

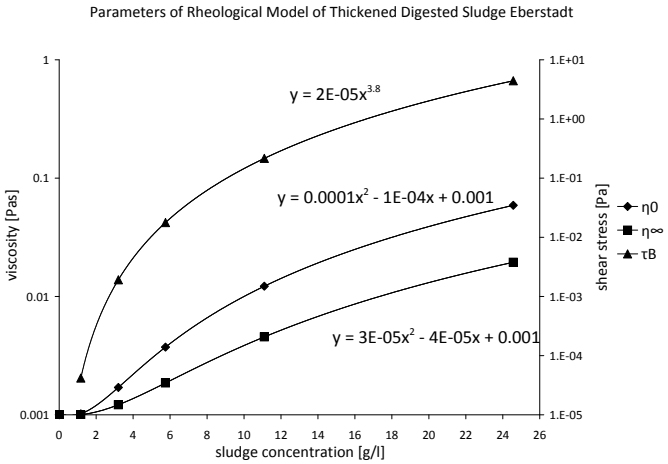

Figure 87: Parameters of the rheological model of thickened digested sludge from WWTP Eberstadt depending on sludge concentration

possible to compare the different sludge types, irrespective of concentration of the measured sludge. Figure 88 shows all the parameters of the different sludge types. Even at a first glance, it is obvious that each parameter is close to the corresponding parameter from the other sludge types. Thus, the differences related to the viscosity of sludge during the process seem to be small. As mentioned earlier, the Bingham shear stress τ_B differs, due to the different approximation functions, but it would also be possible to apply the power function to the activated sludge; therefore, this difference is negligible. Inspection of the initial viscosity η_0 reveals remarkable differences. However, the accuracy of the measurement is not very high at low shear rates, so this should not be overemphasized. Most interesting is the most sensitive parameter of the viscosity: η_∞. Here, one can see that the digested and the thickened digested sludge are close to each other but both are significantly lower than the activated sludge. In other words, the process of digestion of organic matter to inert inorganic matter (lowering the glowing loss) decreases the viscosity.

This becomes more obvious when comparing the flow curves for the same concentration (see Figure 89). Here, it is obvious that the viscosity (slope of the flow curve) of activated sludge is higher than the viscosity of digested and thickened digested sludge for a concentration of 10 g/l or 5 g/l, whereas the differences of initial viscosity and the Bingham shear stress are negligible, because the accuracy of the measurements at low shear rates is limited.

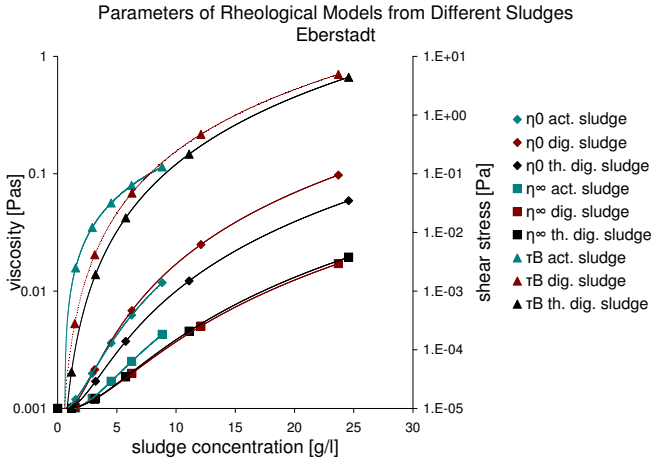

Figure 88: Parameters of the rheological models of three different sludge types from the same WWTP in Eberstadt

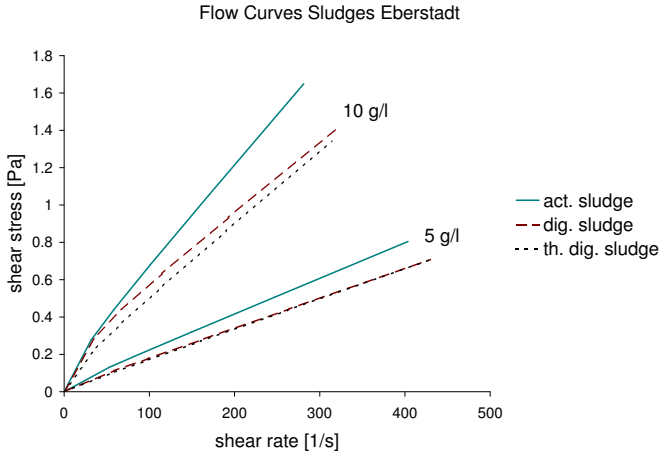

Figure 89: Comparing the flow curves of the three different sludge types with a concentration of 5 g/l and 10 g/l

Summary and Discussion

In summary, the viscosity of sludge changes significantly during the treatment process. As already described Monteiro 1997, the viscosity decreases due to digestion. An explanation is the decrease of the organic matter in the sludge, due to digestion.

4.4.4 Comparing the Viscosity of Sludges from Different Treatment Plants

A remaining question is, how different are sludges from different WWTPs? Rosenberger et al. 2002 considers activated sludge from nine different WWTPs equipped with membranes and state that the main parameter influencing the viscosity is the sludge concentration, independent of mode of operation or scale of the treatment plant. However, Moshage 2004 investigates digested sludge from 32 conventional WWTPs, and finds that the rheological properties vary significantly from plant to plant. For CFD applications, this question is of major importance. If there are no significant differences from plant to plant, it would be sufficient to measure the viscosity of a sludge type from a certain number of plants and to use this for simulations of any plant. If, however, significant differences do exist, it would be necessary to conduct rheological measurements at every investigated plant separately.

Figure 90 shows the flow curves for activated sludge from a different WWTP in Griesheim. The parameters, with their approximation functions, can be found in Appendix Figure 123. In Figure 91, the parameters of activated sludge from Griesheim are compared to the ones from Eberstadt. Again, there is a distinct difference in the viscosity η_∞; because the other parameters also deviate, the result is a different flow curve, as shown in Figure 92. For more details see Appendix Figures 128 to 133.

The flow curves and the parameters with their approximation functions from the digested and thickened digested sludge from Griesheim can be found in Appendix Figures 124 to 127. Furthermore, the differences between the digested sludge and the thickened digested sludge of both plants, together with the flow curves, can bee seen in Appendix Figures 128 to 133. In principle, the flow curves are similar to what has been previously shown with the activated sludge; the deviation between the digested sludges is even smaller. A point of interest here is the fact that the difference between the digested sludge and the activated sludge from the plant in Griesheim is of the same kind as in Eberstadt. In Figure 93, the parameters and the corresponding flow curves (see Figure 94) are displayed. Again, the most significant deviation is that of η_∞: the decrease of viscosity due to the digestion process. Again there is only a negligible difference between the digested sludge and the thickened digested sludge.

Results from investigations of several sludges from a DWTP will now be presented, namely: flocculation sludge from two different flocculation plants and lime

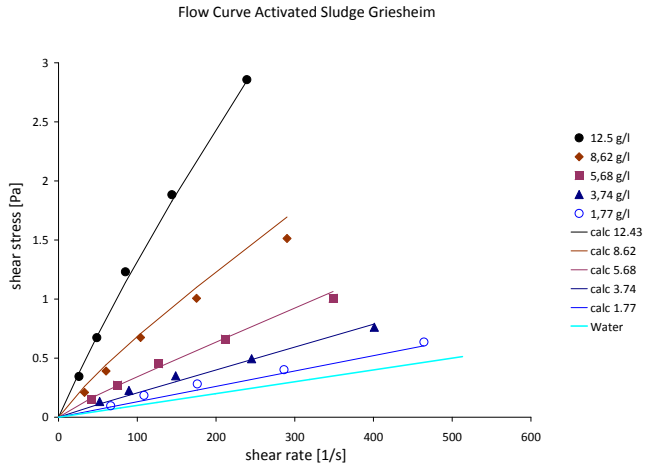

Figure 90: Flow curves of activated sludge from WWTP Griesheim with different concentrations

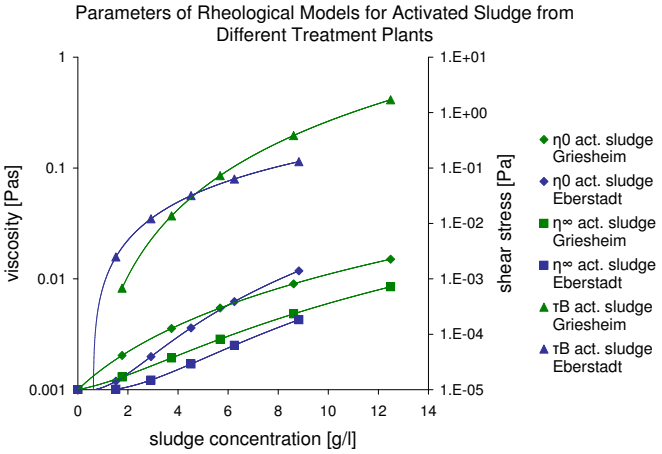

Figure 91: Comparing the parameters of the rheological model of activated sludge from two different treatment plants

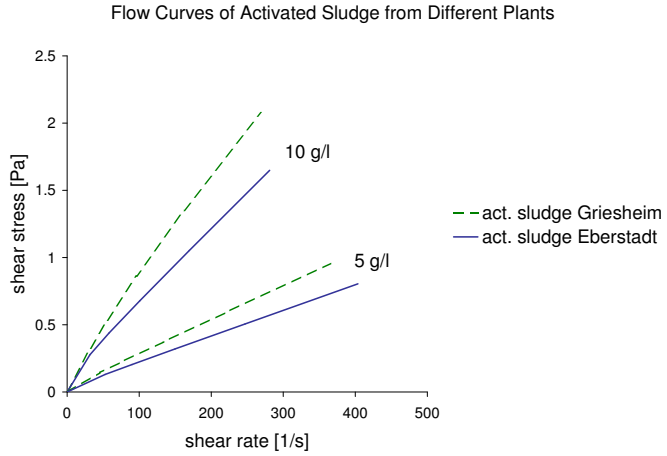

Figure 92: Comparing the flow curves of activated sludge from two different treatment plant for 10 g/l and 5 g/l

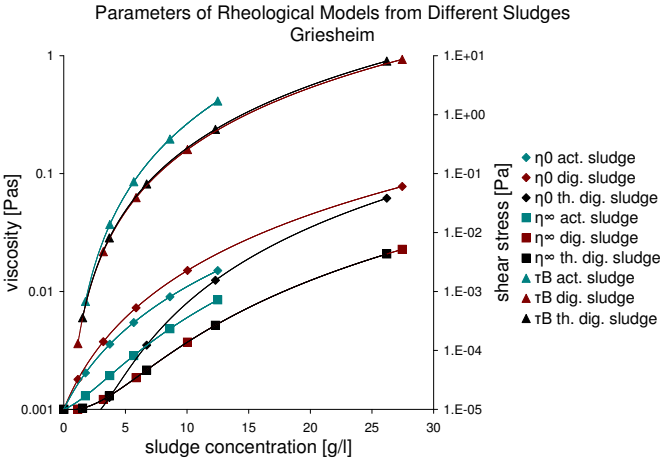

Figure 93: Parameters of the rheological models of three different sludge types from the WWTP in Griesheim

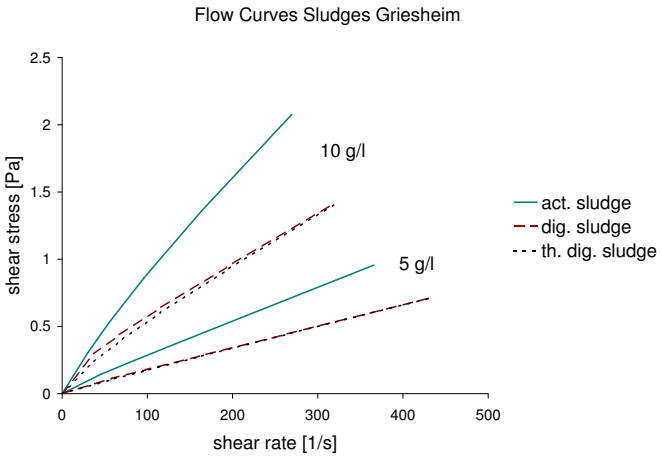

Figure 94: Comparing the flow curves of the three different sludge types with a concentration of 5 g/l and 10 g/l

sludge from a treatment plant in Langenau, treating water from the Danube River, and ground water. Whereas the bacteria from activated sludge have a density slightly higher than that of water, the dry matter from flocculation sludge (Fe^{3+}) has a much higher density, which results in broader range of concentrations. The flow curve of flocculation sludge at 76 g/l is similar to the flow curve of activated sludge at 15 g/l. Figure 95 shows the flow curves for flocculation sludge at different concentrations.

Closer inspection of the flow curves reveals that there is no distinct curvature in the flow curves, as it is the case with the sludges from WWTPs. In fact, the rheological behavior is Newtonian! The correlation between the viscosity and the concentration can be approximated with an exponential function (see Figure 96), in contrast to the other sludges, where polynomial and potential functions fit best. Sozanski et al. 1997 investigates flocculation sludge (with Al^{3+}) and also finds an exponential relationship between the water content and rheological parameters. The sludge shows a Bingham behavior there. This must not contradict the results of the process-viscometer, because, as explained previously, the process-viscometer cannot identify a yield stress. Wichmann and Riehl 1997 also investigate sludge from flocculation plants, but use a different method to measure the vane shear strength, which is an important parameter when it comes to the deposition of

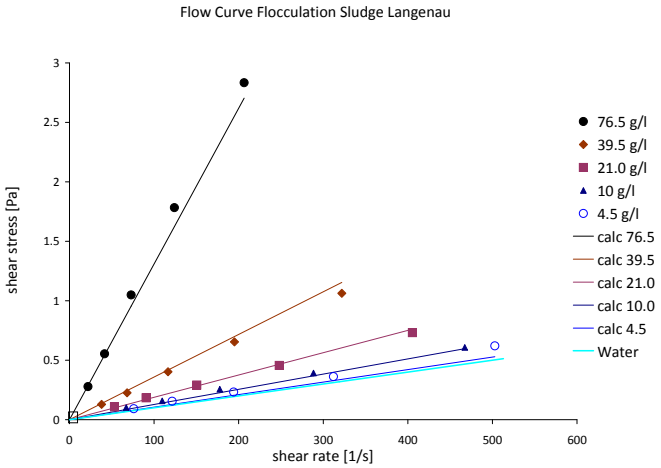

Figure 95: Flow curves of flocculation sludge with different concentrations from a water treatment plant

dewatered sludge. However, their results are not comparable to the rheological measurements conducted here.

Previous publications of the author (Brenda, Sonnenburg and Urban 2009, Brenda 2012) have demonstrated a distinct non-linear, visco-plastic behavior of flocculation sludge. It is important to understand that there are two flocculation plants in Langenau. The older one is called Accelator the newer one is called compact-flocculation plant. Even though both treat water from the Danube, the process is different and the sludge properties are also different, as has been shown with the results from the settling tests (Chapter 4.4.2). The other important difference is the investigated range of shear rates and shear stress, which has been some orders of magnitude lower (see the small box near zero in Figure 95). If there is any visco-plastic behavior in this range, it cannot be measured with the process-viscometer. And the old measurements has been conducted with a standard viscometer, with all the corresponding problems and inaccuracies described in Table 2. Unfortunately, the Accelator is dismantled in order to make room for a decarbonization plant, therefore further investigations cannot be conducted. In any case, some questions about the rheological behavior of flocculation sludge still remain unanswered and further studies are necessary.

The lime sludge is also investigated with the process-viscometer but, due to separation during the measurement, the signal was not constant and therefore

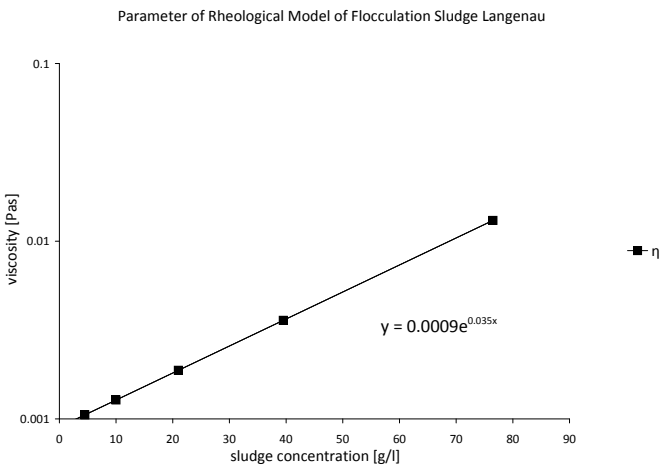

Figure 96: Parameter of the rheological model of flocculation sludge from the WTP in Langenau

unusable. The lime sludge differs in several aspects from all other investigated sludges. When it settles, it forms a stable structure that needs much higher shear stresses to remix than the other sludge types. This is especially clear during the cleansing of the system, which is quite exhausting. Several modifications of the process-viscometer are necessary to minimize this problem. Even then, it is doubtful whether this type of sludge can be investigated with the process-viscometer. This type of sludge marks the limitation of the process-viscometer in its present state.

Summary and Discussion

It is obvious that two different WWTPs is not a large number when making statistically supported statements. But it shows, at least for these two plants, that the differences in the rheological behavior between sludges of the same type are relatively small or even non-existent, even though the mode of operation and the used additives are different. More significant is the change of rheological behavior within the waste water treatment process, namely digestion. Again, the second plant in Griesheim shows a significant reduction of viscosity due to digestion. Flocculation sludge from a DWTP shows a totally different behavior: it is Newtonian. Lime sludge cannot be investigated with the process-viscometer. For practical applications of CFD, it can be stated that, for a first-guess simulation, it is sufficient

to use a rheological model that is based on measurements of the same sludge type from several different treatment plants. For more detailed investigations of a plant, especially when outflow concentrations should be predicted, which require a higher quality of simulation results, it is recommended to make measurements at the treatment plant concerned.

5 Conclusion

A single-phase hybrid sludge model is developed and tested and shows powerful performance. The main advantages of the single-phase hybrid sludge models are the savings in computational efforts and relatively easy measurement procedures. In fact, for a given sludge type, it takes about one day to measure the settling velocity and one day to measure the viscosity. The derivation of the parameters for the hybrid sludge model takes less than one day, according to the methods presented in this thesis. Only if the geometry or the mode of operation of the process-viscometer is changed, it is expensive to derive the new parameters for the hybrid sludge model. The goal of describing the behavior of sludge in water treatment plants with adequate accuracy and a minimum of computational and measurement effort is achieved.

The main advantages of the newly developed process-viscometer are the prevention of settling, Taylor vortices, and thixotropic effects. Because the measurement and simulation are calibrated to the viscosity of water, very plausible flow curves can be derived for sludge, with good reproducibility. Because there is a strong agreement between measured and simulated flow curves and the rheological model it can be stated that not an operational value for the viscosity of sludge is measured but, instead, the real physical viscosity. However, there is also room for improvements. The process-viscometer already has a good accuracy for high shear rates. To improve the accuracy for low shear rates, and especially for the initial viscosity η_0, it is necessary to increase the area of the bob. A height of 10 cm would already significantly improve the accuracy of the results at low shear rates, if the flow is simultaneously reduced to 5 l/min, which is still enough to avoid settling.

For the derivation of the parameters for settling, it can be stated that the consideration of compression by a break point in the settling velocity curve increases the accuracy of the hybrid sludge model, because the settling velocity for higher sludge concentrations determines the sludge level. The settling velocity for lower sludge levels influences the residual turbidity of the outflow sludge, which is also a parameter of interest in many investigations.

The simulation of a complex testing plant (lamella clarifier) confirms the ability and performance of the hybrid sludge model to describe the behavior of sludge in water treatment plants. The breakthrough of sludge in the simulation fits very well to the measured breakthrough. The comparison with a simulation with a rudimentary sludge model without considering viscoplastic behavior or compression shows that these two parts of the sludge model are of great importance. The hybrid sludge-modeling concept increases the accuracy of simulation results, compared to conventional sludge modeling concepts.

The hybrid sludge model can be applied to simulate aeration tanks or secondary clarifiers. Further research is necessary for the simulation of digestion towers. The hybrid sludge model has to be expanded to consider floating sludge, as well as reaction kinetics for gas production.

Figure 97 summarizes the components of the hybrid sludge model and the interaction with the CFD code from ANSYS FLUENT. The formulae are generally valid but the parameters for the sludge model depend on the sludge type and the treatment plant and treatment process. Here, only the parameters for the activated sludge from the WWTP in Eberstadt are displayed.

The comparison of different sludge types from different treatment plants demonstrates that the process itself has the greatest impact on the sludge properties. Digestion, in particular, dramatically changes the settling behavior, due to gas production and viscoplastic behavior. The differences between sludges of the same type from different WWTPs seem to be less distinct, but still significant, even though the number of investigated plants is limited. Also the comparison of two flocculation plants shows that the kind of process has a great impact on sludge properties, even though the raw water and additives are the same. For the practical application of CFD simulation in design processes, it is advisable to derive average sludge parameters for a greater number of treatment plants for pre-design simulations. Because these simulations take the specific hydraulics of a treatment plant into account, the results of such simulations are of higher quality than simple presumptions of e.g. plug flow conditions. Therefore the author strongly recommends the application of CFD simulation in the design process of water treatment plants. It delivers valuable insights into the prevailing flow conditions inside the treatment plant before it is built and thus prevents faulty designs that have to be redesigned expensively afterwards. A best practice example from the waterworks in Langenau, where a new decarbonization plant is planned using CFD as well, has been described. Simulation (CFD) should never replace hydraulic models (EFD) or proven standards, but it is a valuable complement (see the newly edited draft version of the DWA-A 131 for designing aeration tanks).

For the optimization of existing plants (or the redesign of faulty designs), CFD helps to achieve a detailed description at the hydraulics inside the plant (which is difficult to achieve only with on-site measurements). Here, it is possible to calibrate the hybrid sludge model to the existing sludge precisely and to evaluate various options for optimization and, therefore, reduce the number of constructed measures.

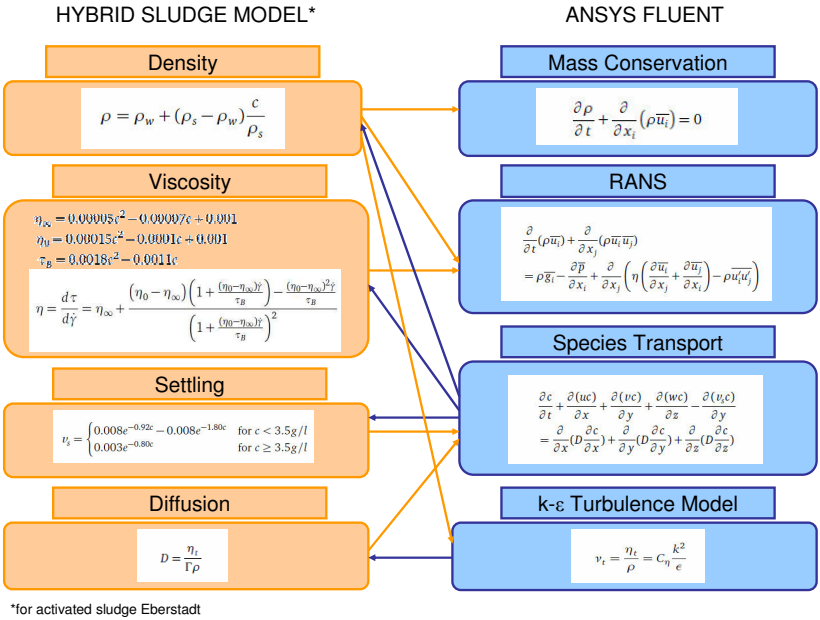

Figure 97: The components of the hybrid sludge model and the interaction with the ANSYS FLUENT CFD code: density (Equation 66), viscosity (Equations 97 to 100), settling (Equation 80), diffusion (Equation 64), mass conservation (Equation 61), momentum conservation (Equation 62), species transport (Equation 65) and k-ϵ turbulence model (Chapter 3.3.5)

List of References

Abu-Orf, M. and Dentel, K. (1997): Effect of mixing on the rheological characteristics of conditioned sludge: full-scale studies. Water Science Technology, Vol.36(No.11):51-60

ANSYS FLUENT, Software user's guide (2014)

Ardern, E. and Locket, W. (1914): Oxidation of sewage without filters. Society of the Chemical Industry, Vol.33:523-539

Armbruster, M. (2004): Untersuchungen der möglichen Leistungssteigerung von Nachklärbecken mit Hilfe numerischer Simulationen. Hydrograv, Dresden

ATV-DVWK (2003): Feststofftransportmodelle für Fließgewässer, Deutsche Vereinigung für Wasserwirtschaft, Abwasser und Abfall e.V.

Barnes, H. and Walters, K. (1985): The yield stress myth? Rheologica Acta, Vol.24:323-326

Battistoni, P. (1997): Pre-treatment, measurement execution procedures and waste characteristics in the rheology of sewage sludges and the digested organic fraction of municipal solid wastes. Water Science Technology, Vol.36(No.11):33-41

Bickert, C. (2013) Numerische Modellierung eines Absetzversuchs mit Belebtschlamm, assignment, Technische Universität Darmstadt (unpublished)

Billmeier, E. (1978): Verbesserte Bemessungsvorschläge für horizontal durchströmte Nachklärbecken von Belebungsanlagen. Berichte aus Wassergütewirtschaft und Gesundheitsingenieurwesen, No.21

Bokil, S. and Bewtra, J. (1972): Infulences of mechanical blending on aerobic digestion of waste activated sludge. In 6th IAWPRC Conference on Water Pollution Research

Bornholdt, J. and Kleinjans, W. (2001): Messtechnische Aspekte von Feststoffsuspensionen und Schlämmen hinsichtlich ihrer rheologischen Eigenschaften. HANSA. International Maritime Journal, Vol.138(No.6):87-88

Brenda, M. (2007): Erstellung und Anwendung eines numerischen Simulationsmodells zur Berechnung der Dynamik einer hochkonzentrierten Suspension kohäsiven Feinsediments, Diploma thesis, Technische Universität Darmstadt

Brenda, M. (2012): Optimization of a flocculation-sedimentation treatment plant with computational fluid dynamics (cfd). In Proceedings of 10th International Conference on Hydroinformatics 2012, Hamburg, TuTech Verlag

Brenda, M., Sonnenburg, A. and Urban, W. (2009): Nachweis des Einflusses der Schlammkonzentration und -viskosität auf das Flockenabsetzverhalten in einer Wasseraufbereitungsanlage mit Hilfe von cfd-Simulation. Das Gas- und Wasserfach. Ausgabe Wasser, Abwasser, Vol.150(No.5):348-354

Coe, H. and Clevenger, G. (1916): Methods for determining the capacity of slimesettling tanks. Trans AIME, Vol.55:356-385

Concha, F. and Bürger, R. (2002): A century of research in sedimentation and thickening. KONA, Vol.20:38-70

Cornel, P. and Krause, S. (2005): Rheologische Eigenschaften von belebtem Schlamm aus Membranbelebungsanlagen und deren Einflüsse auf den Sauerstoffeintrag. Fritz und Margot Faudi - Stiftung, Kennziffer 59. Technical report, Darmstadt (unpublished)

Dahl, C., Larsen, T. and Petersen, O. (1994): Numerical modelling and measurement in a test secondary settling tank. Water Science Technology, Vol.30(No.2):219-228

De Clercq, B. (2003): Computational Fluid Dynamics of Settling Tanks: Development of Experiments and Rheological, Settling and Scraper Submodels. PhD thesis, Ghent University

Dentel, S. (1997): Evaluation and role of rheological properties in sludge management. Water Science Technology, Vol.36(No.11):1-8

Dick, R. and Ewing, B. (1967): The rheology of activated sludge. Water Pollution Control Federation, Vol.39(No.4):543-560

Dick, R. and Vesilind, P. (1969): The sludge volume index - what is it? Water Pollution Control Federation, Vol.41(No.7):1285-1291

DIN 38409 (1987): Summarische Wirkungs- und Stoffkenngrößen (Gruppe H) - Bestimmung des Gesamttrockenrückstandes, des Filtratrückstandes und des Glührückstandes (H1), Deutsches Institut für Normung e.V.

DIN 38414 (1981): Schlamm und Sedimente (Gruppe S) - Bestimmung des Schlammvolumenanteils und des Schlammindex (S10), Deutsches Institut für Normung e.V.

DIN 53019 (2008): Viskosimetrie - Messung von Viskositäten und Fließkurven mit Rotationsviskosimetern, Deutsches Institut für Normung e.V.

DVGW W-217 (2009): Flockung in der Wasseraufbereitung, Deutscher Verein des Gas- und Wasserfachs e.V.

DVGW W-235 (2009): Zentrale Enthärtung von Wasser in der Trinkwasserversorgung, Deutscher Verein des Gas- und Wasserfachs e.V.

DWA-A 131 (2015): Bemessung von einstufigen Belebungsanlagen (Entwurf), Deutsche Vereinigung für Wasserwirtschaft, Abwasser und Abfall e.V.

DWA-M 544 (2015): Ausbreitungsprobleme von Einleitungen - Prozesse, Methoden und Modelle, Deutsche Vereinigung für Wasserwirtschaft, Abwasser und Abfall e.V.

Ekama, G., Barnard, J., Günthert, F., Krebs, P., McCorquodale, J., Parker, D. and Wahlberg E. (1997): Secondary Settling Tanks: Theory, Modelling, Design and Operation. London

Eriksson, L. and Alm, B. (1991): Study of flocculation mechanisms by observing effects of a complexing agent on activated sludge properties. Water Science Technology, Vol.24(No.7):21-28

Fehlau, M. and Specht, E. (2001) Rheologisches Verhalten von Klärschlämmen und Charakterisierung der Leimphase. KA - Wasserwirtschaft, Abwasser, Abfall, Vol.48(No.7):950-960

Friedlander, S. (1977): Smoke, Dust and Haze, John Wiley and Sons, New York, London, Sydney, Toronto

Froulund, B., Palmgren, R., Keiding, K. and Nielsen, P. (1996): Extraction of extracellular polymers from activated sludge using a cation exchange resin. Water Research, Vol.30(No.8):1749-1758

Göthel, O. (2002): Simulation des Absetzverhaltens von Belebtschlamm mit einem mehrphasigen numerischen Flokkulationsmodell, assignment, Universität Hannover

Greenspan, H. and Ungarish, M. (1982): On hindered settling of particles of different sizes, International Journal of Multiphase Flow, Vol.8(No.6):587-604

Günder, B. (1999): Rheologische Eigenschaften von belebten Schlämmen und deren Einfluß auf die Sauerstoffzufuhr. KA Korrespondenz Abwasser, Vol.46(No.12):1896-1904

Häck, M. and Lange, B. (2003): Technologie zur Messung von Schlammvolumen und Schlammvolumenindex. wwt awt - wasserwirtschaft, wassertechnik mit Abwassertechnik, (1/2):28-29

Hanel, R. (1982): Der Sauerstoffeintrag und seine Messung beim Belebungsverfahren unter besonderer Betrachtung der Viskosität und Oberflächenspannung. PhD thesis, Technische Hochschule Darmstadt

Härtel, L. and Pöpel, H. (1992): A dynamic secondary clarifier model including process of sludge thickening. Water Science Technology, Vol.25(No.6):267-284

Holmer, F. (2014): Umstellung der Grundwasserenthärtung beim Zweckverband Landeswasserversorgung. Energie Wasser Praxis, Vol.65(No.5):27-31

Keudel, L. (2002): Bestimmung des Absetzverhaltens von belebtem Schlamm zur Bemessung von Kläranlagen nach dem Sequencing Batch Reactor (SBR) - Verfahren. PhD thesis, Technische Universität Braunschweig

Kinzelbach, W. (1987): Numerische Methoden zur Modellierung des Transports von Schadstoffen im Grundwasser. Oldenburg

Klinksieg, K. (2010): Charakterisierung des Absetzverhaltens von kommunalen Klärschlämmen mit Hilfe rheologischer Messungen. PhD thesis, Technische Universität Braunschweig

Knecht, C. (2013): Numerische Modellierung eines Absetzversuchs mit Faulschlamm, assignment, Technische Universität Darmstadt (unpublished)

Knoch, A. (1997): Einfluß des nicht-newtonschen Fließverhaltens auf die charakteristischen Größen eines Rührprozesses. Chemie Ingenieur Technik, Vol.69(No.10):1426-1432

Knoch, D. and Malcherek, A. (2011): A numerical model for simulation of fluid mud with different rheological behaviors. Ocean Dynamics, Vol.61(No.2-3):245-256

Kobus, H. (1984): Symposium on scale effects in modeling hydraulic structures, 3-6. September 1984. Technische Akademie Esslingen

Koppers, H. (2014): Rohstoffe aus dem Wasser. Energie Wasser Praxis, Vol.65(No.10):34-40

Köster, S. and Tacke, D. (2006): Modellierung des Absetzverhaltens und der Transportprozesse von belebtem Schlamm in Nachklärbecken - Erfahrungen beim Einsatz eines Kunstschlammes aus Polysulfon. Das Gas- und Wasserfach. Ausgabe Wasser, Abwasser, Vol.147(No.7/8):516-521

Kraft, S., Wang, Y. and Oberlack, M. (2011): Large eddy simulation of sediment deformation in a turbulent flow by means of level-set method. Journal of Hydraulic Engineering, Vol.137(No.11):1394-1405

Krebs, D., Armbruster, M. and Rodi, W. (2000): Numerische Nachklärbecken-Modelle. KA - Wasserwirtschaft, Abwasser, Abfall, Vol.47(No.7):985-999

Krishnappan, B. (1990): Modeling of settling and flocculation of fine sediments in still water. Canadian Journal of Civil Engineering, Vol.17:763-770

Lakehal, D., Krebs, P., Krijgsman, J. and Rodi, W. (1999): Computing shear flow and sludge blanket in secondary clarifiers. Journal of Hydraulic Engineering, Vol.125:253-262

Lipp, P. and Dammann, E. (2013): Wasserwerksrückstände: Ergebnis einer Umfrage 2012. Energie Wasser Praxis, Vol.64(No.12):42-48

Lotito, V., Spinosa, L., Mininni, G. and Antonacci, R. (1997): The rheology of sewage sludge at different steps of treatment. Water Science Technology, Vol.36(No.11):79-85

Merkel, W. (1971): Untersuchungen über das Verhalten des belebten Schlammes im System Belebungsbecken - Nachklärbecken. PhD thesis, Rheinisch-Westfaelische Technische Hochschule Aachen

Monteiro, P. (1997): The influence of the anaerobic digestion process on the sewage sludges rheological behaviour. Water Science Technology, Vol.36(No.11):61-67

Moshage, U. (2004): Rheologie kommunaler Klärschlämme - Messmethoden und Praxisrelevanz. PhD thesis, Technische Universität Braunschweig

Nezu, I. and Nakagawa, H. (1993): Turbulence in Open-Channel Flows. IAHR, Balkema and Rotterdam and Brookfield

Oertel, H., Böhme, M. and Reviol, T. (1999): Strömungsmechanik für Ingenieure und Naturwissenschaftler. Springer Vieweg, Wiesbaden

Pflanz, P. (1966): Über das Absetzen des belebten Schlammes in horizontal durchströmten Nachklärbecken. PhD thesis, Technische Universität Braunschweig

Poitou, A., Racineux, G. and Burlion, N. (1997): Identification and measurement of pastes rheological properties - effects of water dissociation. Water Science Technology, Vol.36(No.11):19-26

Proff, E. and Lohmann, J. (1997a): Calculation of pressure drop in the tube flow of sewage sludges with the aid of flow curves. Water Science Technology, Vol.36(No.11):27-32

Proff, E. and Lohmann, J. (1997b): Rheologische Charakterisierung flüssiger Klärschlämme. KA Korrespondenz Abwasser, Vol.44(No.9):1615-1621

Ratkovich, N., Chan, C., Bentzen, T. and Rasmussen, M. (2012): Experimental and CFD simulation studies of wall shear stress for different

impeller configurations and MBR activated sludge. Water Science Technology, Vol.65(No.11):2061-2070

Rodi, W. (1993): Turbulence Models and their Application in Hydraulics: A state-of-the art review. IAHR, Balkema and Rotterdam and Brookfield, 3 edition

Rosenberger, S., Kubin, K. and Kraume, M. (2002): Rheologie von Belebtschlamm in Membranbelebungsreaktoren. Chemie Ingenieur Technik, Vol.74(No.4):487-494

Roth, J.-E. (1991): Grenzflächeneffekte bei der Fest/Flüssig-Trennung. Chemie Ingenieur Technik, Vol.63(No.2):104-115

Schneider, S. (1995): Rückstände aus der Trinkwasseraufbereitung in Deutschland: Mengen, Zusammensetzung und Entsorgungswege. Technical report, ESWE-Institut, Wiesbaden (unpublished)

Schumacher, S. (2006): Leistungsbestimmende Prozesse in Nachklärbecken - Einflussgrößen, Modellbildung und Optimierung. PhD thesis, Universität Hannover

Siew, P., Reizes, J., Horsley, R. and Lye, S. (1992): A method for the determination of the plug interface and the flow of a bingham fluid between rotating cylinders. In 11th Australasian Fluid Mechanics Conference

Slatter, P. (1997): The rheological characterisation of sludges. Water Science Technology, Vol.36(No.11):9-18

Sobeck, D. and Higgins, M. (2002): Examination of three theories for mechanisms of cation-induce bioflocculation. Water Research, Vol.36(No.3):527-538

Sozanski, M., Kempa, E., Grocholsky, K. and Bien, J. (1997): The rheological experiment in sludge properties research. Water Science Technology, Vol.36(No.11):69-78

Stobbe, G. (1964): Über das Verhalten von belebtem Schlamm in aufsteigender Wasserbewegung. PhD thesis, Technische Hochschule Hannover

Takács, I., Patry, G. and Nolasco, D. (1991): A dynamic model of the clarification - thickening process. Water Research, Vol.25(No.10):1263-1271

Tanner, R. and Milthorpe, J. (1983): Numerical simulation of the flow of fluids with yield stresses. In 3rd International Conference Numerical Methods in Laminar and Turbulent Flow

Toorman, E. (1997): Modeling the thixotropic behaviour of dense cohesive sediment suspensions. Rheologica Acta, Vol.36:56-65

Urban, F. (2014): Berücksichtigung von Fragen der Reststoffverwertung in der Planung von Trinkwasseraufbereitungsanlagen. Energie Wasser Praxis, Vol.65(No.10):42-48

van Rijn, L. (1993): Principles of Sediment Transport in Rivers, Estuaries and Coastal Seas. Aqua Publications, Amsterdam

van Wazer, J., Lyons, J., Kim, K. and Colwell, R. (1963): Viscosity and Flow Measurement: A Laboratory Handbook of Rheology. Interscience Publishers, St. Louis

Vesilind, P. (1968): Design of prototype thickeners from batch settling tests. Water and Sewage Works, Vol.115(No.7):302-307

Wahlberg, E. and Keinath, T. (1980): Development of settling flux curves using SVI. Water Pollution Control Federation, Vol.60(No.12):2095-2100

Weilbeer, J. (2004): Modellierung des Partikeltransports in Nachklärbecken als Mehrphasenströmung. PhD thesis, Universität Hannover

Weyand, S. (2012): Numerische Modellierung eines Prozessviskosimeters, assignment, Technische Universität Darmstadt (unpublished)

Wichmann, K. and Akkiparambath, A. (2001): Wasserwerksrückstände - Auswertung der aktuellen Umfrage aus 1999. Energie Wasser Praxis, Vol.52(No.7/8):23-25

Wichmann, K. and Riehl, A. (1997): Mechanical properties of waterwork sludges - shear strength. Water Science Technology, Vol.36(No.11):43-55

Winterwerp, H. (1999): On the dynamics of high-concentrated mud suspensions. PhD thesis, Delft University of Technology

Worrall, W. and Tuliani, S. (1964): Viscosity changes during the ageing of clay-water suspensions, University of Leeds

Wurpts, A. (2006): Numerische Simulation von Dichteeffekten am Beispiel der Umlagerung von Baggergut im Ästuarbereich. PhD thesis, Technische Universität Darmstadt

Zanke, U. (1982): Grundlagen der Sedimentbewegung, Springer Verlag, Berlin, Heidelberg, New York

Zhang, D., Li, Z., Lu, P., Zhang, T. and Xu, D. (2006): A method for characterizing the complete settling process of activated sludge. Water Research, Vol.40(No.14):2637-2644

Appendix

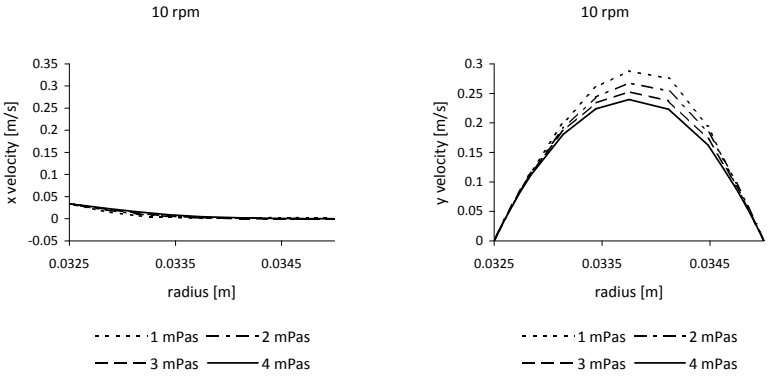

(a) (b)

Figure 98: Flow in the measuring gap at a rotational speed of 10.0 rpm for different Newtonian viscosities: horizontal velocity profile (left), vertical velocity profile (right)

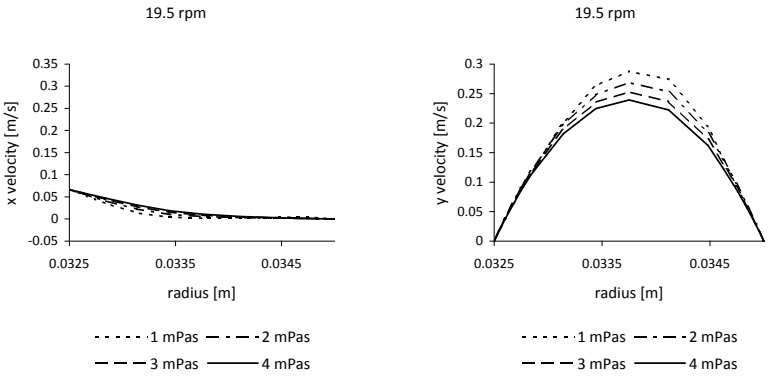

(a) (b)

Figure 99: Flow in the measuring gap at a rotational speed of 19,5 rpm for different Newtonian viscosities: horizontal velocity profile (left), vertical velocity profile (right)

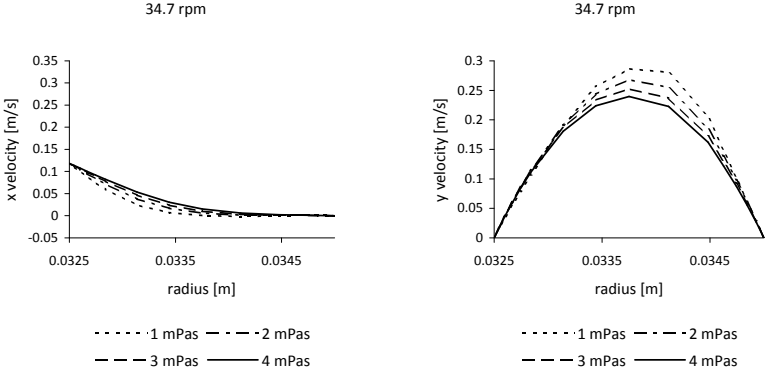

(a) (b)

Figure 100: Flow in the measuring gap at a rotational speed of 34,7 rpm for different Newtonian viscosities: horizontal velocity profile (left), vertical velocity profile (right)

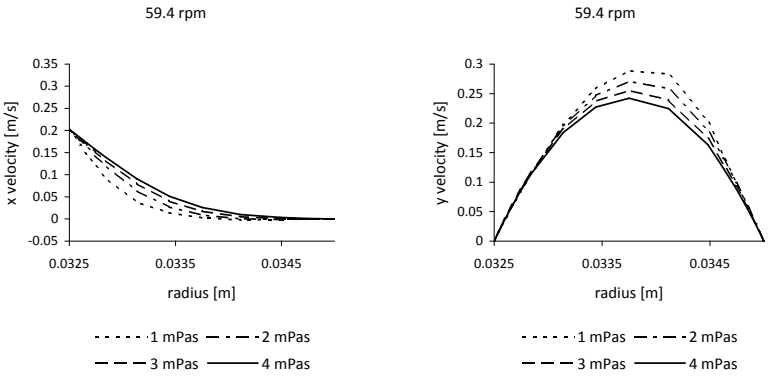

(a) (b)

Figure 101: Flow in the measuring gap at a rotational speed of 59.4 rpm for different Newtonian viscosities: horizontal velocity profile (left), vertical velocity profile (right)

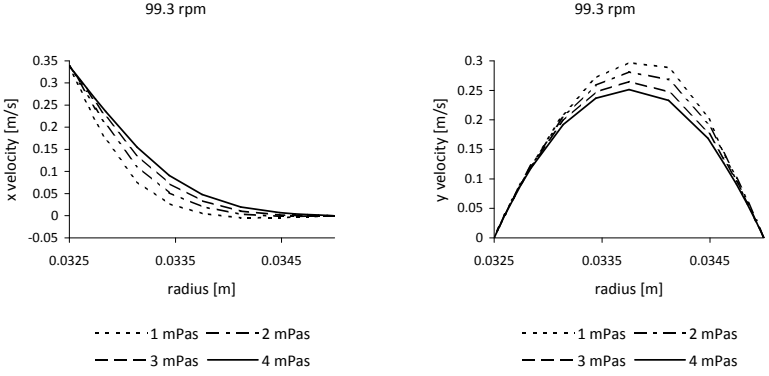

(a) (b)

Figure 102: Flow in the measuring gap at a rotational speed of 99.3 rpm for different Newtonian viscosities: horizontal velocity profile (left), vertical velocity profile (right)

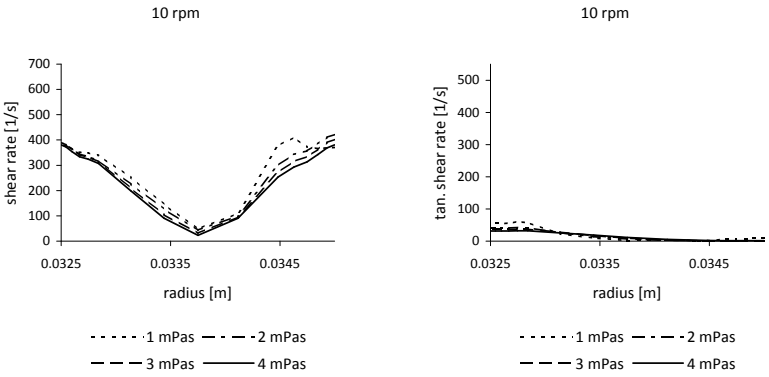

(a) (b)

Figure 103: Shear rates in the measuring gap at a rotational speed of 10 rpm for different Newtonian viscosities: total shear rate (left), horizontal shear rate (right)

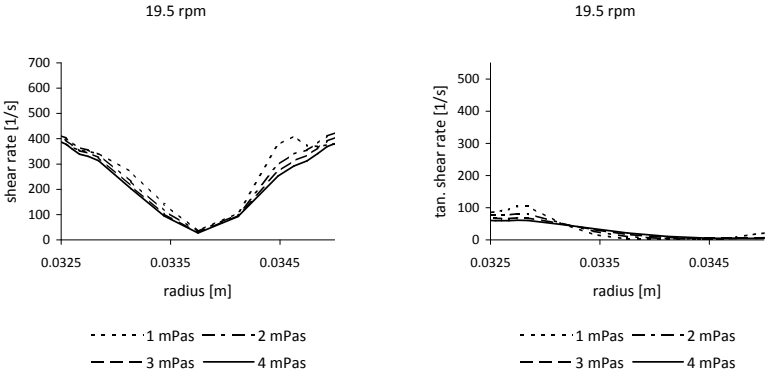

(a) (b)

Figure 104: Shear rates in the measuring gap at a rotational speed of 19.5 rpm for different Newtonian viscosities: total shear rate (left), horizontal shear rate (right)

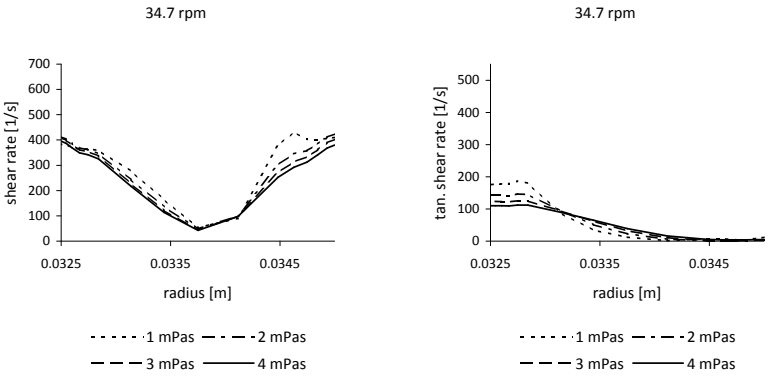

(a) (b)

Figure 105: Shear rates in the measuring gap at a rotational speed of 34.7 rpm for different Newtonian viscosities: total shear rate (left), horizontal shear rate (right)

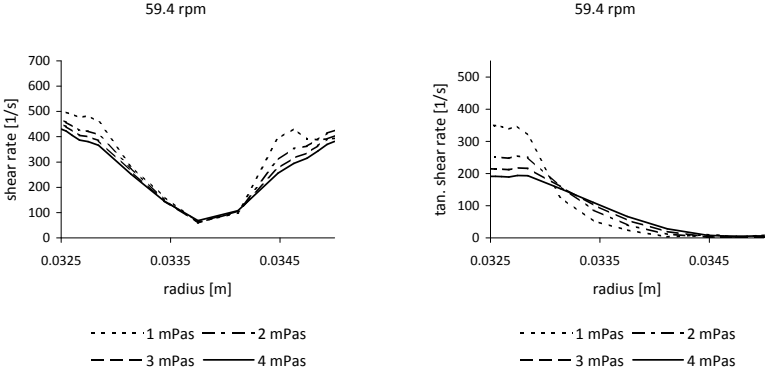

(a) (b)

Figure 106: Shear rates in the measuring gap at a rotational speed of 59.4 rpm for different Newtonian viscosities: total shear rate (left), horizontal shear rate (right)

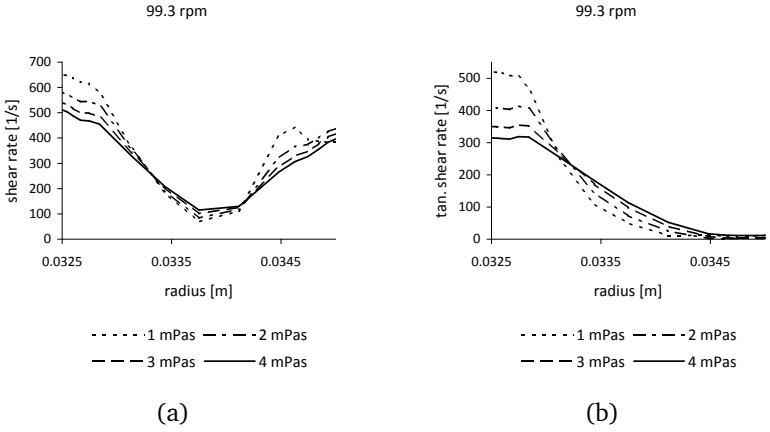

Figure 107: Shear rates in the measuring gap at a rotational speed of 99.3 rpm for different Newtonian viscosities: total shear rate (left), horizontal shear rate (right)

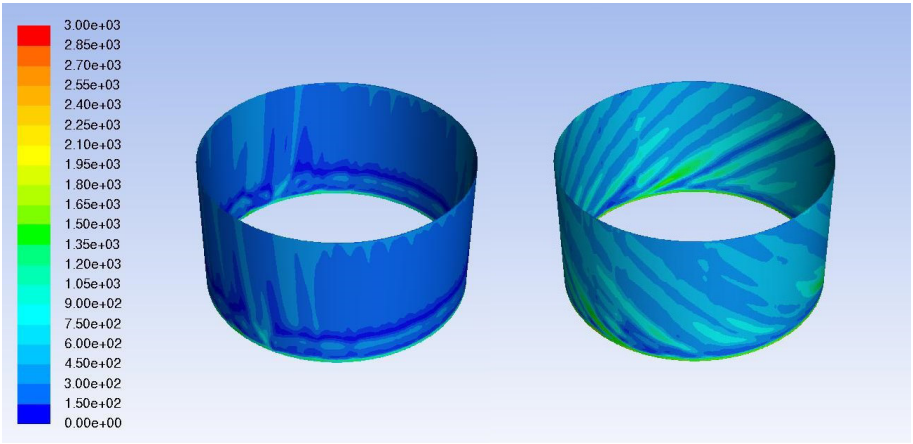

Figure 108: Shear rate contours [s^{-1}] for the outer wall of the bob of the process-viscometer with 10 rpm (left) and 99.3 rpm (right)

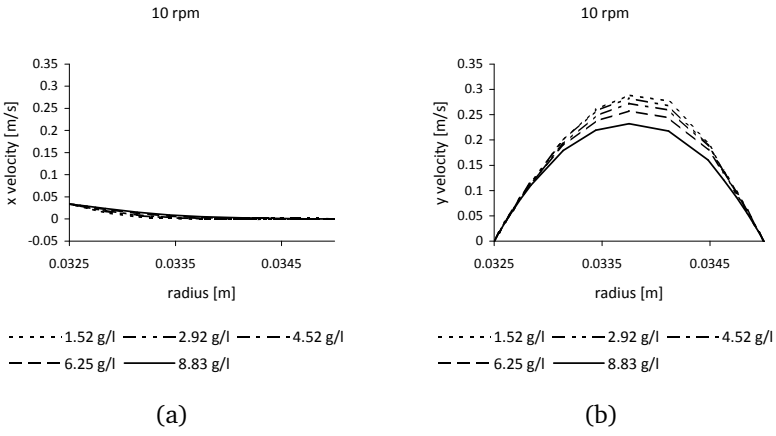

Figure 109: Flow in the measuring gap at a rotational speed of 10.0 rpm for different sludge concentrations: horizontal velocity profile (left), vertical velocity profile (right)

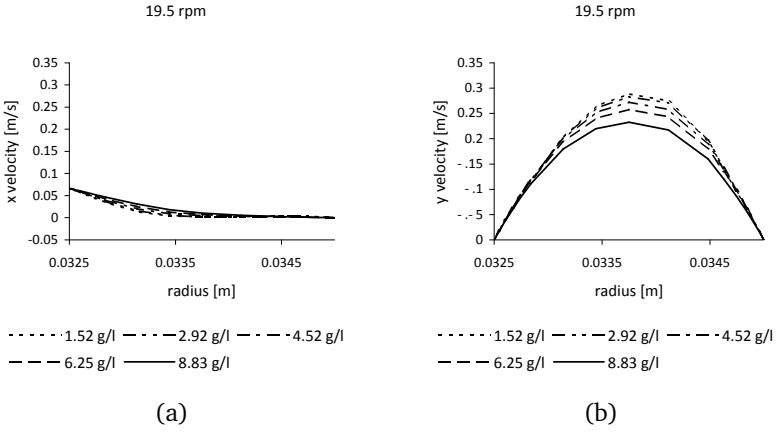

Figure 110: Flow in the measuring gap at a rotational speed of 19.5 rpm for different sludge concentrations: horizontal velocity profile (left), vertical velocity profile (right)

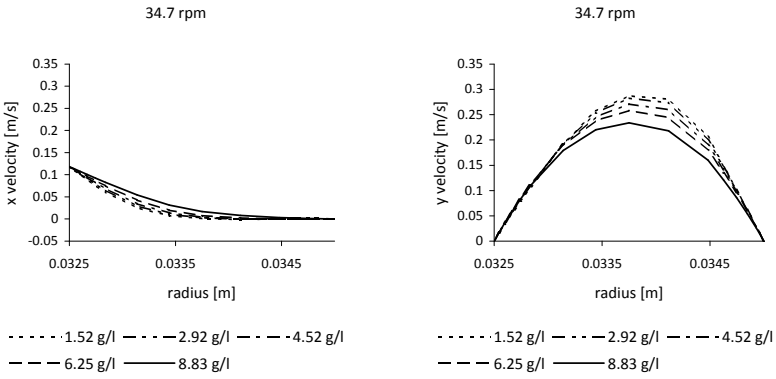

Figure 111: Flow in the measuring gap at a rotational speed of 34.7 rpm for different sludge concentrations: horizontal velocity profile (left), vertical velocity profile (right)

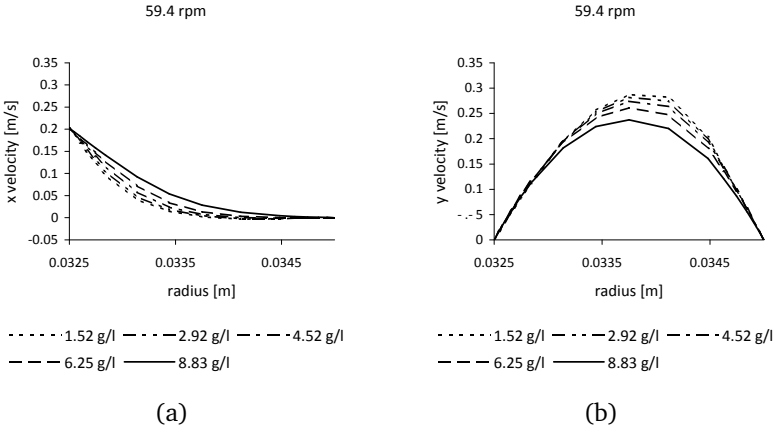

Figure 112: Flow in the measuring gap at a rotational speed of 59.4 rpm for different sludge concentrations: horizontal velocity profile (left), vertical velocity profile (right)

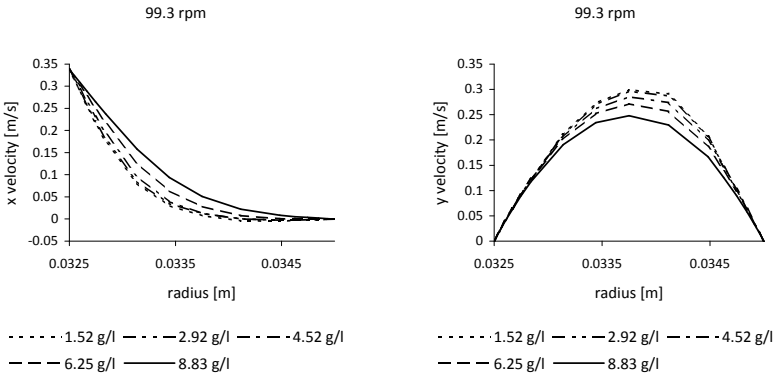

Figure 113: Flow in the measuring gap at a rotational speed of 99.3 rpm for different sludge concentrations: horizontal velocity profile (left), vertical velocity profile (right)

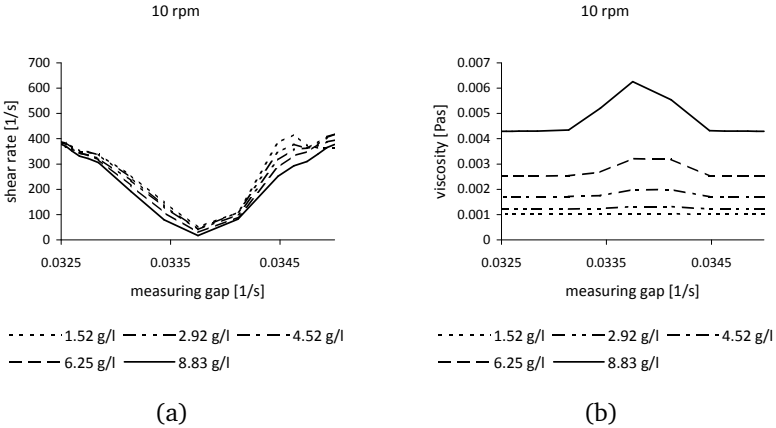

Figure 114: Shear rate and corresponding viscosity in the measuring gap at a rotational speed of 10.0 rpm for different sludge concentrations: total shear rate (left), viscosity profile (right)

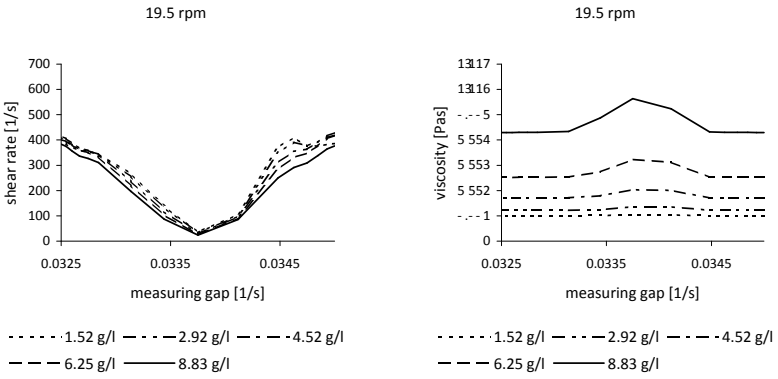

Figure 115: Shear rate and corresponding viscosity in the measuring gap at a rotational speed of 19.5 rpm for different sludge concentrations: total shear rate (left), viscosity profile (right)

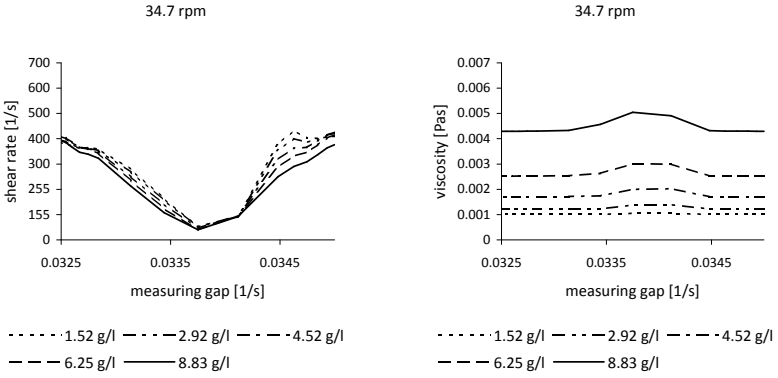

Figure 116: Shear rate and corresponding viscosity in the measuring gap at a rotational speed of 34.7 rpm for different sludge concentrations: total shear rate (left), viscosity profile (right)

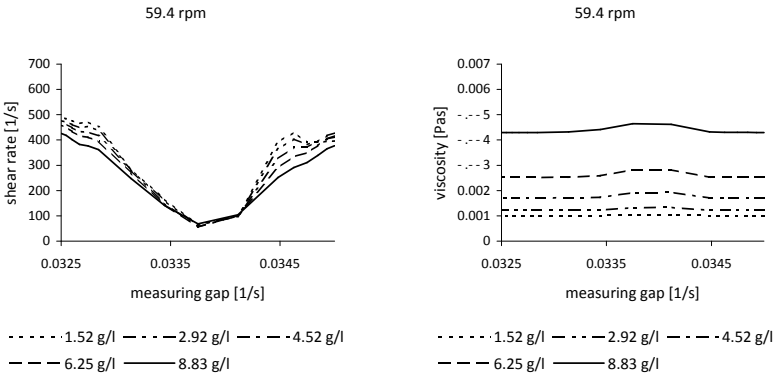

(a) (b)

Figure 117: Shear rate and corresponding viscosity in the measuring gap at a rotational speed of 59.4 rpm for different sludge concentrations: total shear rate (left), viscosity profile (right)

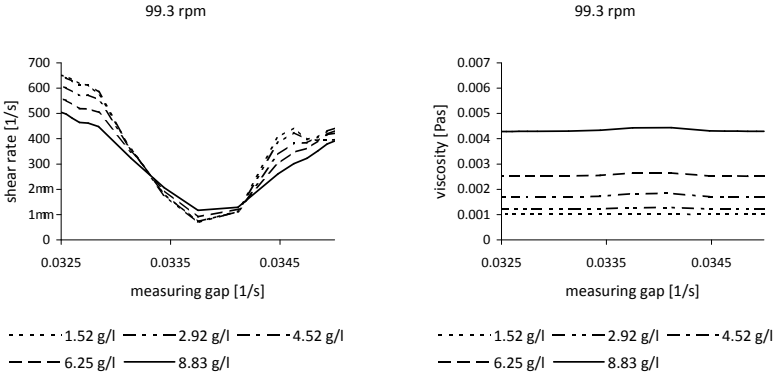

(a) (b)

Figure 118: Shear rate and corresponding viscosity in the measuring gap at a rotational speed of 99.3 rpm for different sludge concentrations: total shear rate (left), viscosity profile (right)

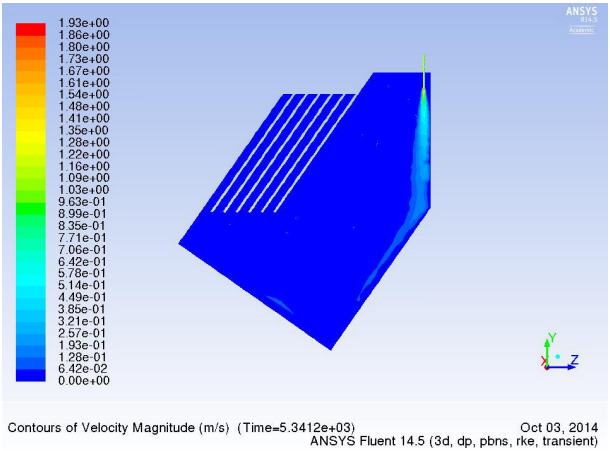

Figure 119: Flow inside the testing plant (2. simulation)

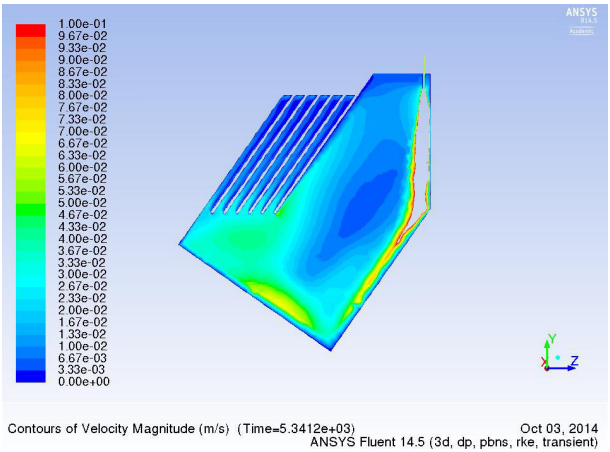

Figure 120: Flow inside the testing plant (high velocities at the inlet are not displayed, 2. simulation)

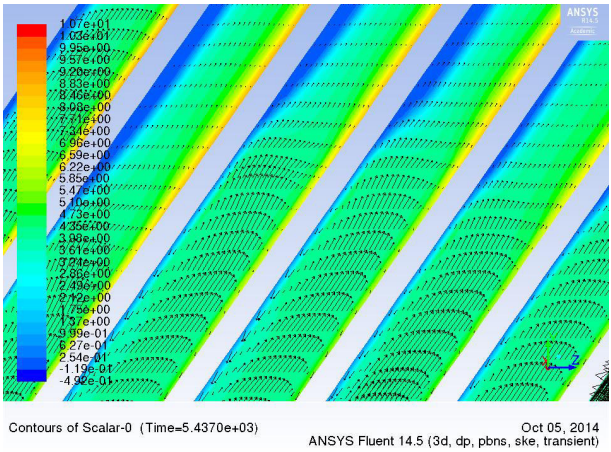

Figure 121: The vectors show the flow velocity, the color shows the sludge concentration in the interspaces between the lamellas of the 1. simulation

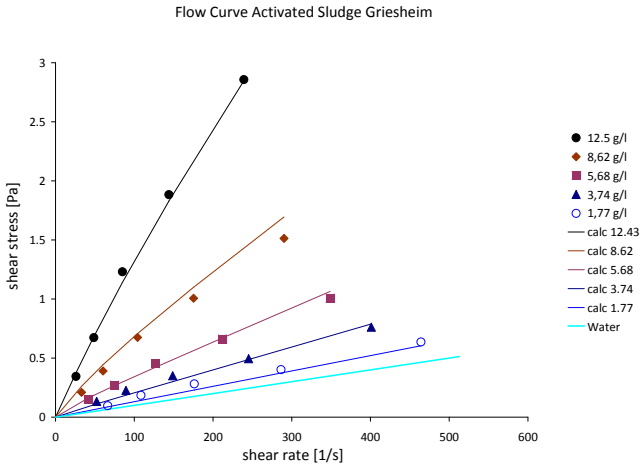

Figure 122: Flow curves of activated sludge with different concentrations in Griesheim

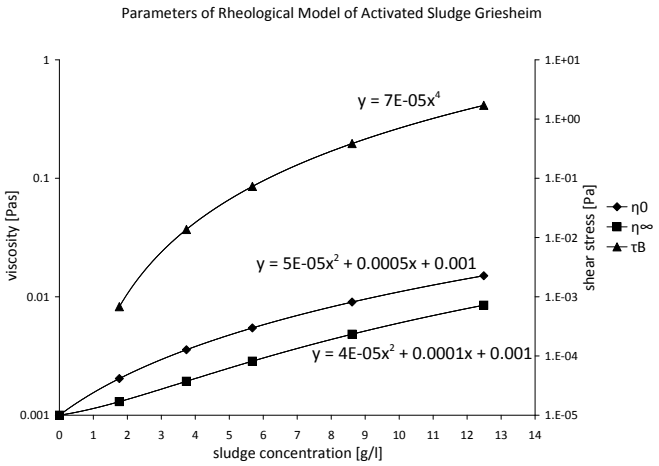

Figure 123: Parameters of the rheological model of activated sludge depending on sludge concentration in Griesheim

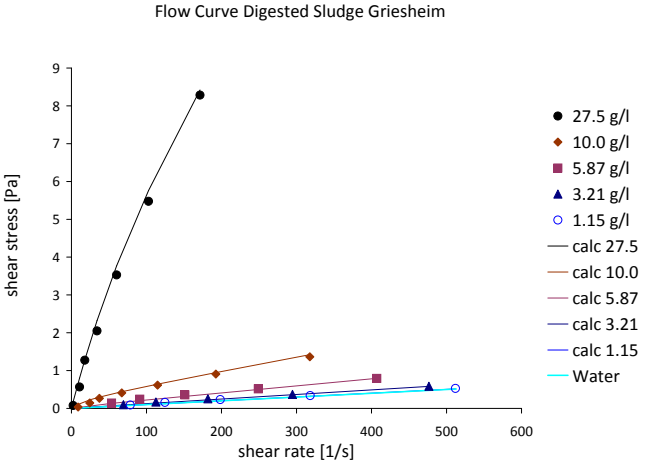

Figure 124: Flow curves of digested sludge with different concentrations in Griesheim

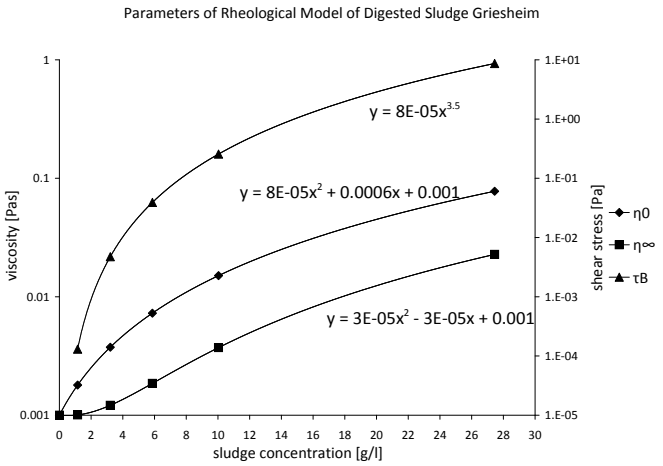

Figure 125: Parameters of the rheological model of digested sludge depending on sludge concentration in Griesheim

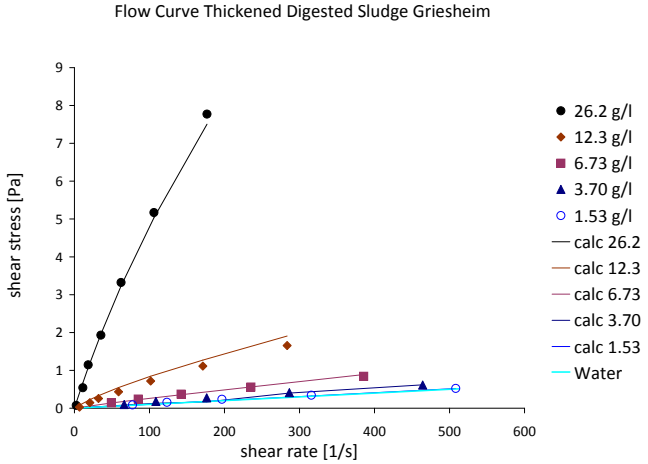

Figure 126: Flow curves of thickened digested sludge with different concentrations in Griesheim

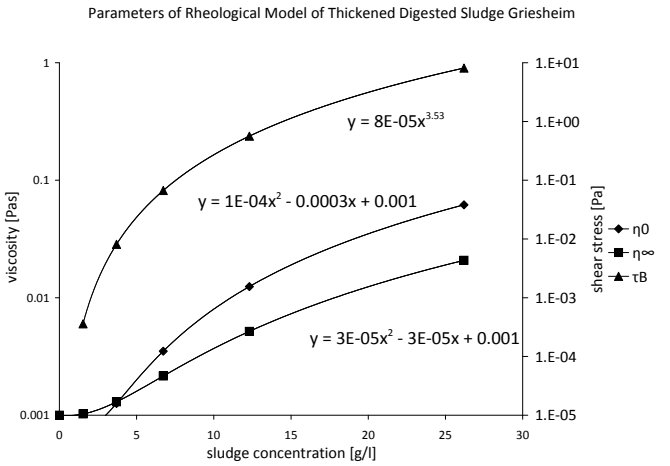

Figure 127: Parameters of the rheological model of thickened digested sludge depending on sludge concentration in Griesheim

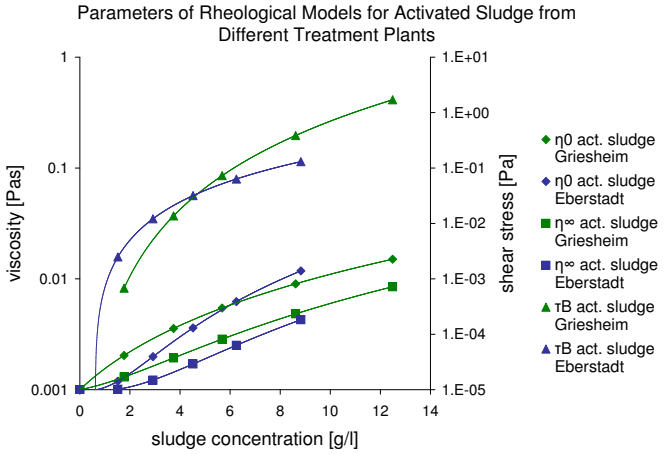

Figure 128: Comparing the parameters of the rheological model of activated sludge from two different WWTPs

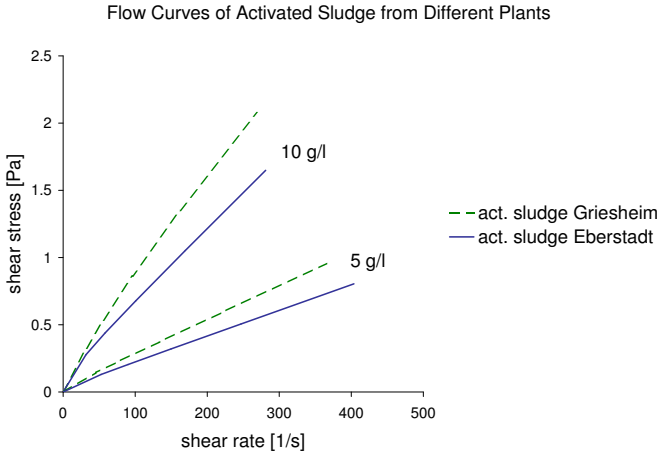

Figure 129: Comparing the flow curves of activated sludge from two different WWTPs for 10 g/l and 5 g/l

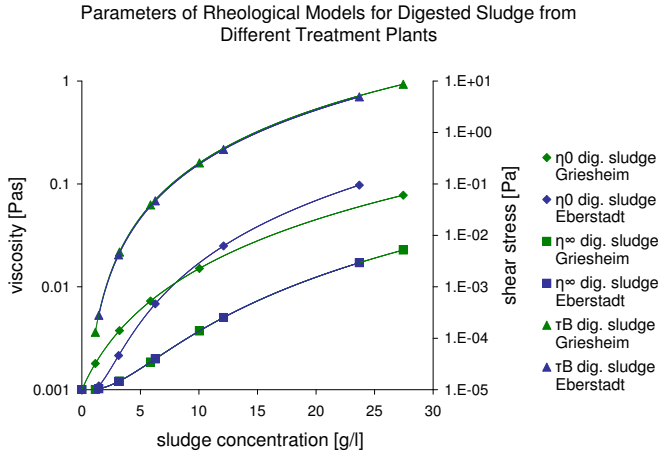

Figure 130: Comparing the parameters of the rheological model of digested sludge from two different WWTPs

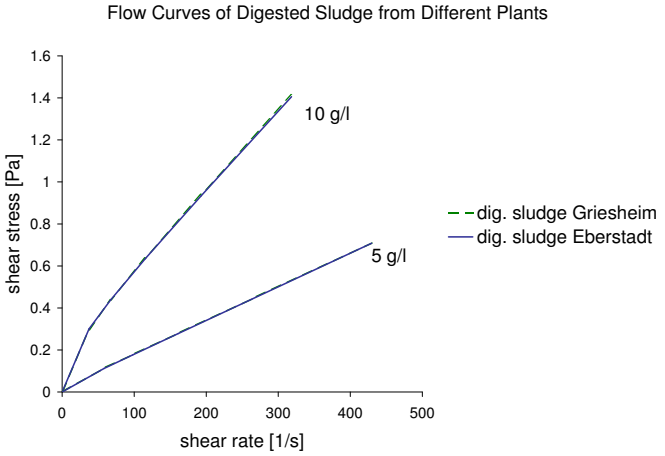

Figure 131: Comparing the flow curves of digested sludge from two different WWTPs for 10 g/l and 5 g/l

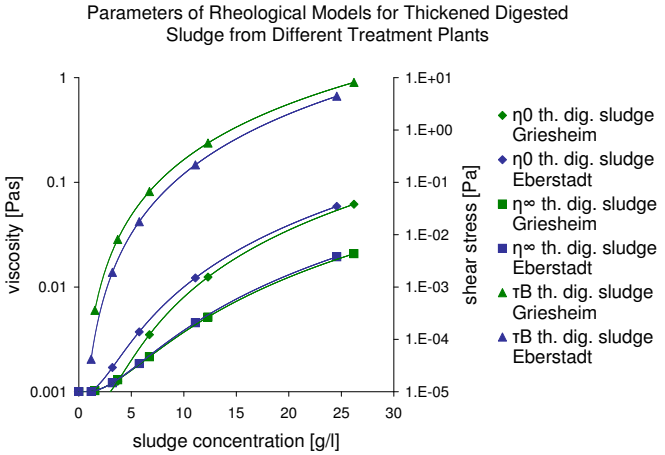

Figure 132: Comparing the parameters of the rheological model of thickened digested sludge from two different WWTPs

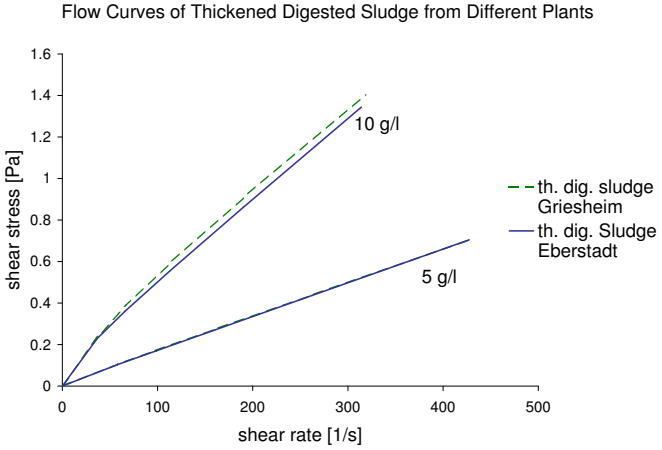

Figure 133: Comparing the flow curves of thickened digested sludge from two different WWTPs for 10 g/l and 5 g/l

In der Schriftenreihe IWAR sind erschienen:

*WA*R 1	Brunnenalterung Wassertechnisches Seminar am 13.10.1978, TH Darmstadt, 1980	10,30 €
*WA*R 2	Festschrift zum 60. Geburtstag von Prof. Dr.-Ing. Günther Rincke. TH Darmstadt, 1979	vergriffen
*WA*R 3	Gniosdorsch, Lothar Georg: Ein Beitrag über den Einfluß der in Abhängigkeit von der verfahrensmäßigen Durchführung der biologischen Abwasserreinigung bedingten Schlammeigenschaften auf die Schlammentwässerung und anschließende Verbrennung. Dissertation, FB 13, TH Darmstadt, 1979	vergriffen
*WA*R 4	Grundwassergewinnung mittels Filterbrunnen. 2. Wassertechnisches Seminar am 11.04.1980, TH Darmstadt, 1981	vergriffen
*WA*R 5	Rudolph, Karl-Ulrich: Die mehrdimensionale Bilanzrechnung als Entscheidungsmodell der Wassergütewirtschaft. Dissertation, FB 13, TH Darmstadt, 1980	vergriffen
*WA*R 6	Hantke, Hartmut: Vergleichende Bewertung von Anlagen zur Grundwasseranreicherung. Dissertation, FB 13, TH Darmstadt, 1981	vergriffen
*WA*R 7	Riegler, Günther: Eine Verfahrensgegenüberstellung von Varianten zur Klärschlammstabilisierung. Dissertation, FB 13, TH Darmstadt, 1981	vergriffen
*WA*R 8	Technisch-wissenschaftliche Grundlagen für Wasserrechtsverfahren in der öffentlichen Wasserversorgung. 3. Wassertechnisches Seminar am 05.und 06.03.1981, TH Darmstadt, 1982	25,60 €
*WA*R 9	Geruchsemissionen aus Abwasseranlagen. 4. Wassertechnisches Seminar am 15.10.1981, TH Darmstadt, 1982	vergriffen
*WA*R 10	Stadtplanung und Siedlungswasserwirtschaft in Entwicklungsländern.-Aspekte der Projektdurchführung. Vorträge in den Jahren 1980 - 1981. TH Darmstadt, 1982	vergriffen
*WA*R 11	Hierse, Wilfried: Untersuchungen über das Verhalten phosphathaltiger Schlämme unter anaeroben Bedingungen. Dissertation, FB 13, TH Darmstadt, 1982	vergriffen

*WA*R 12	Gossel, Hans: Untersuchungen zum Verhalten von Belebungsanlagen bei Stoßbelastungen. Dissertation, FB 13, TH Darmstadt, 1982	vergriffen
*WA*R 13	Hanel, Robert: Der Sauerstoffeintrag und seine Messung beim Belebungsverfahren unter besonderer Beachtung der Viskosität und Oberflächenspannung. Dissertation, FB 13, TH Darmstadt, 1982	vergriffen
*WA*R 14	Cichorowski, Georg: Regionale Differenzierung in der Gewässergütewirtschaft. Dissertation, FB 13, TH Darmstadt, 1982	23,-- €
*WA*R 15	Schreiner Horst: Stofftausch zwischen Sediment und Wasserkörper in gestauten Fließgewässern. Dissertation, FB 13, TH Darmstadt, 1982	25,60 €
*WA*R 16	Grundwasserbewirtschaftung - Grundwassermodelle, Grundwasser-anreicherung. 5. Wassertechnisches Seminar am 08.10.1982, TH Darmstadt, 1982	vergriffen
*WA*R 17	Rüthrich, Wulf: Abhängigkeit des Verhaltens der Wohnbevölkerung von Verkehrsimmissionen. Dissertation, FB 13, TH Darmstadt, 1982	vergriffen
*WA*R 18	Hill, Stefan: Untersuchungen über die Wechselwirkungen zwischen Porenverstopfung und Filterwiderstand mittels Tracermessungen. Dissertation, FB 13, TH Darmstadt, 1983	25,60 €
*WA*R 19	Kaltenbrunner, Helmut: Wasserwirtschaftliche Auswirkungen der Kühlverfahren von Kraftwerken und von Abwärmeeinleitungen in Fließgewässern. Dissertation, FB 13, TH Darmstadt, 1983	25,60 €
*WA*R 20	Roeles, Gerd: Auswirkungen von Müllverbrennungsanlagen auf die Standort-umgebung - Analyse der Wahrnehmungen von Störungen und Belästigungen. Dissertation, FB 13, TH Darmstadt, 1982	vergriffen
*WA*R 21	Niehoff, Hans-Hermann: Untersuchungen zur weitergehenden Abwasserreinigung mit vorwiegend biologischen Verfahrensschritten unter besonderer Berücksichtigung der Grundwasseranreicherung. Dissertation, FB 13, TH Darmstadt, 1983	vergriffen

*WA*R 22	Biologische Verfahren in der Wasseraufbereitung. 6. Wassertechnisches Seminar am 06.04.1984, TH Darmstadt, 1985	vergriffen
*WA*R 23	Optimierung der Belüftung und Energieeinsparung in der Abwassertechnik durch Einsatz neuer Belüftungssysteme. 7. Wassertechnisches Seminar am 16.11.1984, TH Darmstadt, 1985	vergriffen
*WA*R 24	Wasserverteilung und Wasserverluste. 8. Wassertechnisches Seminar am 30.05.1985, TH Darmstadt, 1985	vergriffen
*WA*R 25	Professor Dr. rer. nat. Wolters zum Gedächtnis - 1. Januar 1929 bis 26. Februar 1985. Beiträge von Kollegen, Schülern und Freunden. TH Darmstadt, 1986	vergriffen
*WA*R 26	Naturnahe Abwasserbehandlungsverfahren im Leistungsvergleich - Pflanzenkläranlagen und Abwasserteiche. 9. Wassertechnisches Seminar am 07.11.1985, TH Darmstadt, 1986	vergriffen
*WA*R 27	Heuser, Ernst-Erich: Gefährdungspotentiale und Schutzstrategien für die Grundwasser-vorkommen in der Bundesrepublik Deutschland. Dissertation, FB 13, TH Darmstadt, 1986	vergriffen
*WA*R 28	Rohrleitungen und Armaturen in der Wasserversorgung. 10. Wassertechnisches Seminar am 24.04.1986, TH Darmstadt, 1986	vergriffen
*WA*R 29	Bau, Kurt: Rationeller Einsatz der aerob-thermophilen Stabilisierung durch Rohschlamm-Vorentwässerung. Dissertation, FB 13, TH Darmstadt, 1986	vergriffen
*WA*R 30	Wehenpohl, Günther: Selbsthilfe und Partizipation bei siedlungswasserwirtschaftlichen Maßnahmen in Entwicklungsländern - Grenzen und Möglichkeiten in städtischen Gebieten unterer Einkommensschichten. Dissertation, FB 13, TH Darmstadt, 1987	vergriffen
*WA*R 31	Stickstoffentfernung bei der Abwasserreinigung - Nitrifikation und Denitrifikation. 11. Wassertechnisches Seminar am 13.11.1986, TH Darmstadt, 1987	vergriffen

*WA*R 32	Neuere Erkenntnisse beim Bau und Betrieb von Vertikalfilterbrunnen. 12. Wassertechnisches Seminar am 14.05.1987, TH Darmstadt, 1987	vergriffen
*WA*R 33	Ist die landwirtschaftliche Klärschlammverwertung nutzbringende Düngung oder preiswerte Abfallbeseitigung? Standpunkte und Argumente. 13. Wassertechnisches Seminar am 12.11.1987, TH Darmstadt, 1988	vergriffen
*WA*R 34	Automatisierung in der Wasserversorgung - auch für kleinere Unternehmen 14. Wassertechnisches Seminar am 09.06.1988, TH Darmstadt, 1988	33,20 €
*WA*R 35	Erkundung und Bewertung von Altlasten-Kriterien und Untersuchungsprogrammen. 15. Wassertechnisches Seminar am 12.10.1988, TH Darmstadt, 1989	vergriffen
*WA*R 36	Bestimmung des Sauerstoffzufuhrvermögens von Belüftungssystemen in Reinwasser und unter Betriebsbedingungen. Workshop am 15. u. 16.03.1988, TH Darmstadt, 1989	vergriffen
*WA*R 37	Belüftungssysteme in der Abwassertechnik - Fortschritte und Perspektiven. 16. Wassertechnisches Seminar am 10.11.1988, TH Darmstadt, 1989	vergriffen
*WA*R 38	Farinha, Joao António Muralha Ribeiro: Die stufenweise Versorgung mit Anlagen der Technischen Infrastruktur in Abhängigkeit von der Entwicklung der sozioökonomischen Verhältnisse der Bevölkerung - dargestellt am Beispiel der Bairros Clandestinos der Region Lissabon. Dissertation, FB 13, TH Darmstadt, 1989	vergriffen
*WA*R 39	Sicherstellung der Trinkwasserversorgung Maßnahmen und Strategien für einen wirksamen Grundwasserschutz zur langfristigen Erhaltung der Grundwassergewinnung. 17. Wassertechnisches Seminar am 01.06.1989, TH Darmstadt, 1989	33,20 €
*WA*R 40	Regenwassernutzung in privaten und öffentlichen Gebäuden -Qualitative und quantitative Aspekte, technische Anlagen. Studie für den Hessischen Minister für Umwelt und Reaktorsicherheit. TH Darmstadt, 1981	vergriffen

*WA*R 41	Folgenutzen kontaminierter Betriebsflächen unter besonderer Berücksichtigung der Sanierungsgrenzen. 18. Wassertechnisches Seminar am 11.10.1989, TH Darmstadt, 1989	vergriffen
*WA*R 42	Privatisierung öffentlicher Abwasseranlagen - Ein Gebot der Stunde? 19. Wassertechnisches Seminar am 09.11.1989, TH Darmstadt, 1989	30,70 €
*WA*R 43	Pöpel, H. Johannes; Joachim Glasenapp; Holger Scheer: Planung und Betrieb von Abwasserreinigungsanlagen zur Stickstoff-elimination. Gutachten für das Hess. Ministerium für Umwelt und Reaktorsicherheit. TH Darmstadt, 1990	35,80 €
*WA*R 44	Abfallentsorgung Hessen. Standpunkte - Gegensätze – Perspektiven. Abfallwirtschaftliches Symposium am 31.10.1989, TH Darmstadt, 1990	30,70 €
*WA*R 45	Brettschneider, Uwe: Die Bedeutung von Sulfaten in der Siedlungswasserwirtschaft und ihre Entfernung durch Desulfurikation. Dissertation, FB 13, TH Darmstadt, 1990	vergriffen
*WA*R 46	Grabenlose Verlegung und Erneuerung von nicht begehbaren Leitungen - Verfahren, Anwendungsgrenzen, Erfahrungen und Perspektiven. 20. Wassertechnisches Seminar am 29.03.1990, TH Darmstadt, 1990	35,80 €
*WA*R 47	Härtel, Lutz: Modellansätze zur dynamischen Simulation des Belebtschlamm-verfahrens. Dissertation, FB 13, TH Darmstadt, 1990	vergriffen
*WA*R 48	Pflanzenkläranlagen - besser als ihr Ruf? 21. Wassertechnisches Seminar am 18.09.1990, TH Darmstadt, 1990	vergriffen
*WA*R 49	Umweltverträglichkeitsprüfung (UVP) in der Wasserwirtschaft - administrativer Wildwuchs oder ökologische Keule? Dokumentation der Beiträge zum Interdisziplinären Kolloquium am 23.02.1990 und zum Sachverständigengespräch am 23.02.1990, TH Darmstadt, 1991	vergriffen
*WA*R 50	UVP in der abfallwirtschaftlichen Planung. 22. Wassertechnisches Seminar am 18.10.1990, TH Darmstadt, 1991	vergriffen

*WA*R 51	Biologische und chemische Phosphatelimination - Technische Möglichkeiten und Grenzen. 23. Wassertechnisches Seminar am 15.11.1990, TH Darmstadt, 1991	35,80 €
*WA*R 52	Pöpel, H. Johannes; Tankred Börner: Wurzelraum-Modellanlage Hofgeismar-Beberbeck - Pilotprojekt des Landes Hessen. Gutachten für das Hess. Ministerium für Umwelt und Reaktorsicherheit. TH Darmstadt, 1991	30,70 €
*WA*R 53	Wagner, Martin: Einfluß oberflächenaktiver Substanzen auf Stoffaustauschmechanismen und Sauerstoffeintrag. Dissertation, FB 13, TH Darmstadt, 1991	35,80 €
*WA*R 54	Belüftungssysteme in der Abwassertechnik 1991 - Fortschritte und Perspektiven. 1. gemeinsames Abwassertechnisches Seminar mit der Hochschule für Architektur und Bauwesen Weimar am 11. und 12.04. 1991 in Weimar, TH Darmstadt, 1991	30,70 €
*WA*R 55	Neuere gesetzliche Anforderungen und moderne technische Lösungen zur Sicherung der Wasserversorgung - Erkennen, Vermeiden und Beseitigen von Schadstoffen. 24. Wassertechnisches Seminar am 16.05.1991 TH Darmstadt, 1991	vergriffen
*WA*R 56	Zhang, Jiansan: Energiebilanzierung anaerob-mesophiler Stabilisierungsanlagen mit vorgeschalteter aerob-thermophiler Stufe. Dissertation, FB 13, TH Darmstadt, 1991	vergriffen
*WA*R 57	Glasenapp, Joachim: Leistungsfähigkeit und Wirtschaftlichkeit von Verfahrensvarianten zur Sickstoffelimination beim Belebtschlammverfahren. Dissertation, FB 13, TH Darmstadt, 1992	vergriffen
*WA*R 58	Börner, Tankred: Einflußfaktoren für die Leistungsfähigkeit von Pflanzenkläranlagen. Dissertation, FB 13, TH Darmstadt, 1992	vergriffen
*WA*R 59	Erzmann, Michael: Untersuchungen zur biologischen Elimination von chlorierten Lösemitteln aus Abwasser. Dissertation, FB 13, TH Darmstadt, 1992	35,80 €
*WA*R 60	Erfassung und Sanierung schadhafter Abwasserkanäle. 26. Wassertechnisches Seminar am 28.11.1991, TH Darmstadt, 1992	35,80 €

*WA*R 61	Realisierung von Entsorgungsanlagen Umsetzungsprobleme und Lösungsansätze aus planerischer, verwaltungsrechtlicher und politischer Sicht. 25. Wassertechnisches Seminar am 07.11.1991, TH Darmstadt, 1992	vergriffen
*WA*R 62	Koziol, Matthias: Umwelteffekte durch Förderung von Energieeinsparmaßnahmen in innerstädtischen Althausgebieten. Dissertation, FB 13, TH Darmstadt, 1992	25,60 €
*WA*R 63	Lautner, Gerd: Einführung in das Bauordnungsrecht. 7. erw. Auflage TH Darmstadt, 1992	vergriffen
*WA*R 64	Abwasserkanäle - Bemessung, Ausführung, Sanierung. 2. gemeinsames Seminar -Abwassertechnik- mit der Hochschule für Architektur und Bauwesen Weimar am 18. und 19.03.1992 in Weimar, TH Darmstadt, 1992	vergriffen
*WA*R 65	Optimierung der Grundwassergewinnung über Filterbrunnen Neue Bau- und Betriebserkenntnisse. 27. Wassertechnisches Seminar am 21.05.1992, TH Darmstadt, 1992	40,90 €
*WA*R 66	Kläschlammbehandlung und Klärschlammentsorgung -Stand und Entwicklungstendenzen. 31. Darmstädter Seminar -Abwassertechnik- am 12.11.1992, TH Darmstadt, 1992	35,80 €
*WA*R 67	Kreislaufwirtschaft Bau - Stand und Perspektiven beim Recycling von Baurestmassen. 32. Darmstädter Seminar -Abfalltechnik- am 09.03.1993, TH Darmstadt, 1993	30,70 €
*WA*R 68	Bewertung von Geruchsemissionen und –immissionen. 29. Darmstädter Seminar -Immissionsschutz- am 08.10.1992, TH Darmstadt, 1993	25,60 €
*WA*R 69	Möglichkeiten und Grenzen der Klärschlammentsorgung. 3. gemeinsames Seminar -Abwassertechnik- mit der Hochschule für Architektur und Bauwesen Weimar am 31.03. und 01.04.1993, TH Darmstadt, 1993	46,-- €
*WA*R 70	Sichere Wasserversorgung durch moderne Rohrleitungstechnik. 33. Darmstädter Seminar -Wasserversorgungstechnik- am 11.03.1993, TH Darmstadt, 1993	30,70 €

*WA*R 71	Aktuelle Aufgaben der Abwasserreinigung und Schlammbehandlung. 35. Darmstädter Seminar -Abwassertechnik- am 05. + 06.05.1993, TH Darmstadt, 1993	46,-- €
*WA*R 72	Raumordnungsverfahren mit Umweltverträglichkeitsprüfung und Umweltleitbilder für die Landes- und Regionalplanung. 28. und 30. Darmstädter Seminar -Raumplanung- am 17.09. und 05.11.1992, TH Darmstadt, 1993	40,90 €
*WA*R 73	Grohmann, Walter: Vergleichende Untersuchungen von Belüftungs- und Durchmischungssystemen zur bioverfahrenstechnischen Optimierung der aerob-thermophilen Stabilisation (ATS). Dissertation, FB 13, TH Darmstadt, 1993	35,80 €
*WA*R 74	Dioxinimmissionen und Quellen . 34. Darmstädter Seminar -Immissionsschutz- am 15.04.1993, TH Darmstadt, 1994	30,70 €
*WA*R 75	Betrieb von Abwasserbehandlungsanlagen Optimierung, Prozeßstabilität, Kosteneinsparung. 36. Darmstädter Seminar -Abwassertechnik- am 04.11.1993 in Darmstadt und 5. gemeinsames Seminar -Abwassertechnik- mit der Fakultät Bauingenieurwesen der Hochschule für Architektur und Bauwesen Weimar am 23. und 24.03.1994 in Weimar, TH Darmstadt, 1994	46,-- €
*WA*R 76	Umweltgerechte Ausweisung und Erschließung von Gewerbegebieten. 4. gemeinsames Seminar -Umwelt- und Raumplanung- mit der Fakultät Architektur, Stadt- und Regionalplanung der Hochschule für Architektur und Bauwesen Weimar am 08. und 09.09.1993 in Weimar, TH Darmstadt, 1994	vergriffen
*WA*R 77	Von der Umweltverträglichkeitsprüfung zum kooperativen Planungsmanagement. Das Scoping-Verfahren als erste Stufe!? 37. Darmstädter Seminar -Umwelt- und Raumplanung- am 11.11.1993, TH Darmstadt, 1994	vergriffen
*WA*R 78	Modellbildung und intelligente Steuerungssysteme in der Umwelttechnik. 38. Darmstädter Seminar -Abfalltechnik- am 24.02.1994, TH Darmstadt, 1994	25,60 €
*WA*R 79	Brauchwassernutzung in Haushalten und Gewerbebetrieben - Ein Gebot der Stunde? 39. Darmstädter Seminar -Wasserversorgungstechnik- am 17.03.1994, TH Darmstadt, 1994	25,60 €

*WA*R 80	Restabfallbehandlung in Hessen. 41. Darmstädter Seminar -Abfalltechnik- mit dem Hessischen Ministerium für Umwelt, Energie und Bundesangelegenheiten -HMUEB- am 16.06.1994, TH Darmstadt, 1994	vergriffen
*WA*R 81	Umweltbeeinflussung durch biologische Abfallbehandlungsverfahren. 42. Darmstädter Seminar -Abfalltechnik- mit dem Institut für Hygiene der FU Berlin und dem Institut für Meteorologie der TH Darmstadt am 08. und 09.09.1994 in Berlin, TH Darmstadt, 1994	46,-- €
*WA*R 82	Zeitgemäße Planung von Anlagen der Ortsentwässerung - Kanäle, Bauwerke, Sonderbauwerke. 6. gemeinsames Seminar -Abwassertechnik- mit der Fakultät Bauingenieurwesen der Hochschule für Architektur und Bauwesen Weimar am 15. und 16.03.1995 in Weimar, TH Darmstadt, 1995	vergriffen
*WA*R 83	Grundwasseranreicherung - Stand der Technik und neuere Entwicklungen. 44. Darmstädter Seminar -Wasserversorgungstechnik- mit dem Verein des Gas- und Wasserfaches e.V. -DVGW- am 26.04.1994, TH Darmstadt, 1995	30,70 €
*WA*R 84	Auswirkungen der Phosphorelimination auf die Schlammbehandlung. Theoretische Erkenntnisse und praktische Erfahrungen. Workshop vom 24. bis 25. November 1994, TH Darmstadt, 1995	30,70 €
*WA*R 85	Stickstoffelimination mit oder ohne externe Substrate ? - Erfahrungen und Überlegungen. 43. Darmstädter Seminar -Abwassertechnik- in Abstimmung mit der Abwassertechnischen Vereinigung e.V. (ATV) am 09.11.1994, TH Darmstadt, 1995	35,80 €
*WA*R 85	Stickstoffelimination mit oder ohne externe Substrate ? - Erfahrungen und Überlegungen. 2. Auflage. Wiederholung des 43. Darmstädter Seminars -Abwassertechnik- in Abstimmung mit der Abwassertechnischen Vereinigung e.V. (ATV) am 01.02.1996 in Düsseldorf, TH Darmstadt, 1996	35,80 €
*WA*R 86	Möglichkeiten und Grenzen der Einsparung von Investitions- und Betriebskosten bei der Abwasserbehandlung. 47. Darmstädter Seminar -Abwassertechnik- am 15.11.1995, TH Darmstadt, 1995	40,90 €

*WA*R 87	Jardin, Norbert: Untersuchungen zum Einfluß der erhöhten biologischen Phosphor-elimination auf die Phosphordynamik bei der Schlammbehandlung. Dissertation, FB 13, TH Darmstadt, 1996	35,80 €
*WA*R 88	Thermische Restabfallbehandlung für kleine Planungsräume. 45. Darmstädter Seminar -Abfalltechnik- am 22.06.1995 in Hanau, TH Darmstadt, 1996	35,80 €
*WA*R 89	Ferber, Uwe: Aufbereitung und Revitalisierung industrieller Brachflächen in den traditionellen Industrieregionen Europas. Sonderprogramme im Vergleich. Dissertation, FB 13, TH Darmstadt 1996	25,60 €
*WA*R 90	Mechanisch-biologische Restabfallbehandlung unter Einbindung thermischer Verfahren für Teilfraktionen. 48. Darmstädter Seminar -Abfalltechnik- am 29.02.1996, TH Darmstadt, 1996	vergriffen
*WA*R 91	Neuere Erkenntnisse bei Planung, Bau, Ausrüstung und Betrieb von Abwasserbehandlungsanlagen. 7. gemeinsames Seminar -Abwassertechnik- mit der Fakultät Bauingenieurwesen der Bauhaus-Universität Weimar am 11. und 12.09.1996 in Weimar, TH Darmstadt, 1996	40,90 €
*WA*R 92	Hygiene in der Abfallwirtschaft. 50. Darmstädter Seminar -Abfalltechnik- am 17.10.1996, TH Darmstadt, 1996	30,70 €
*WA*R 93	Europäische Richtlinien und Normen zur Abwassertechnik - Konsequenzen und Folgerungen für die Praxis in Deutschland. 51. Darmstädter Seminar -Abwassertechnik- am 14.11.1996, TH Darmstadt, 1996	25,60 €
*WA*R 94	Dickhaut, Wolfgang: Möglichkeiten und Grenzen der Erarbeitung von Umwelt-qualitätszielkonzepten in kooperativen Planungsprozessen. Durchführung und Evaluierung von Projekten. Dissertation, FB 13, TH Darmstadt 1996	30,70 €
*WA*R 95	Lautner, Gerd: Einführung in das Bauordnungsrecht. 8. erw. und aktual. Auflage, TH Darmstadt, 1997	15,40 €
*WA*R 96	Reichert, Joachim: Bilanzierung des Sauerstoffeintrags und des Sauerstoffverbrauchs mit Hilfe der Abluftmethode. Dissertation, FB 13, TH Darmstadt 1997	46,-- €

*WA*R 97	Kuchta, Kerstin: Produktion von Qalitätsgütern in der Abfallbehandlung. Dargestellt am Beispiel der Produktion in der thermischen Abfallbehandlung. Dissertation, FB 13, TH Darmstadt 1997	30,70 €
*WA*R 98	Görg, Horst: Entwicklung eines Prognosemodells für Bauabfälle als Baustein von Stoffstrombetrachtungen zur Kreislaufwirtschaft im Bauwesen. Dissertation, FB 13, TH Darmstadt, 1997	46,-- €
*WA*R 99	Tiebel-Pahlke, Christoph: Abfallentsorgungsplanung – Beeinflussung der Umweltauswirkungen von Deponien. Dissertation, FB 13, TH Darmstadt, 1997	30,70 €
*WA*R 100	Wagner, Martin: Sauerstoffeintrag und Sauerstoffertrag von Belüftungssystemen und deren Bestimmung mit modernen Meßmethoden. Habilitation, FB 13, TH Darmstadt, 1997	vergriffen
*WA*R 101	Neue Trends bei der Behandlung und Entsorgung kommunaler und industrieller Klärschlämme. 8. gemeinsames Seminar -Abwassertechnik- mit der Fakultät Bauingenieurwesen der Bauhaus-Universität Weimar am 10. und 11.09.1997 in Weimar, TH Darmstadt, 1997	35,80 €
*WA*R 102	Senkung der Betriebskosten von Abwasserbehandlungsanlagen. 52. Darmstädter Seminar -Abwassertechnik- am 06.11.1997 in Darmstadt, TU Darmstadt, 1997	35,80 €
*WA*R 103	Sanierung und Rückbau von Bohrungen, Brunnen und Grundwasser-messstellen. 53. Darmstädter Seminar -Wasserversorgung- am 13.11.1997 in Darmstadt mit dem Deutschen Verein des Gas- und Wasserfaches e.V. (DVGW), TU Darmstadt, 1997	vergriffen
*WA*R 104	Wünschmann, Gabriele: Untersuchungen zur Kompostierbarkeit von Reststoffen der Papier-industrie und Altpapier unter besonderer Berücksichtigung von Schad-stoffbilanzierungen. Dissertation, FB 13, TU Darmstadt, 1997	25,60 €

*WA*R 105	Mechanisch-biologische Restabfallbehandlung unter Einbindung thermischer Verfahren für Teilfraktionen. 54. Darmstädter Seminar -Abfalltechnik- am 06.02.1998 in Darmstadt mit dem Hessischen Ministerium für Umwelt, Energie, Jugend, Familie und Gesundheit und der Südhessischen Arbeitsgemeinschaft Abfall-wirtschaft (SAGA), TU Darmstadt, 1998	40,90 €
*WA*R 106	Zentrale oder dezentrale Enthärtung von Trinkwasser – Konkurrenz oder sinnvolle Ergänzung ? 55. Darmstädter Seminar -Wasserversorgung- am 14.05.1998 in Darmstadt mit dem Deutschen Verein des Gas- und Wasserfaches e.V. (DVGW), TU Darmstadt, 1998	35,80 €
*WA*R 107	Dach, Joachim: Zur Deponiegas- und Temperaturentwicklung in Deponien mit Siedlungsabfällen nach mechanisch-biologischer Abfallbehandlung. Dissertation, FB 13, TU Darmstadt, 1998	35,80 €
*WA*R 108	Einsparung von Kosten für Betriebsmittel, Energie und Personal auf Abwasserbehandlungsanlagen. 9. gemeinsames Seminar -Abwassertechnik- am 16. und 17.09.1998 in Weimar mit der Fakultät Bauingenieurwesen der Bauhaus-Universität Weimar, TU Darmstadt, 1998	40,90 €
*WA*R 109	Fortschritte in der Abwassertechnik – 15 Jahre Forschungs- und Entwicklungstätigkeit von Prof. Dr.-Ing. H. Johannes Pöpel. 56. Darmstädter Seminar -Abwassertechnik- am 05.11.1998 in Darmstadt, TU Darmstadt, 1998	40,90 €
*WA*R 110	Qualitativer und Quantitativer Grundwasserschutz - Stand und Perspektiven. 57. Darmstädter Seminar -Wasserversorgung- am 10.06.1999 in Darmstadt mit dem Deutschen Verein des Gas- und Wasserfaches e.V. (DVGW), TU Darmstadt, 1999	35,80 €
*WA*R 111	Schwing, Elke: Bewertung der Emissionen der Kombination mechanisch-biologischer und thermischer Abfallbehandlungsverfahren in Südhessen. Dissertation, FB 13, TU Darmstadt, 1999	30,70 €
*WA*R 112	Schade, Bernd: Kostenplanung zur Analyse der Wirtschaftlichkeit von biologischen Restabfallbehandlungsanlagen. Dissertation, FB 13, TU Darmstadt, 1999	30,70 €

*WA*R 113	Lohf, Astrid: Modellierung der chemisch-physikalischen Vorgänge im Müllbett von Rostfeuerungsanlagen. Dissertation, FB 13, TU Darmstadt, 1999	25,60 €
*WA*R 114	Stackelberg, Daniel von: Biologische Festbettdenitrifikation von Grundwasser mit abbaubarem Trägermaterial. Dissertation, FB 13, TU Darmstadt, 1999	30,70 €
*WA*R 115	Folgerungen aus 10 Jahren Abwasserbeseitigung in den neuen Bundesländern - Erfahrungen und Perspektiven. 10. gemeinsames Seminar –Abwassertechnik- am 01. und 02.09.1999 in Weimar mit der Fakultät Bauingenieurwesen der Bauhaus-Universität Weimar, TU Darmstadt, 1999	40,90 €
*WA*R 116	Abwasserwiederverwendung in wasserarmen Regionen - Einsatzgebiete, Anforderungen, Lösungsmöglichkeiten. 58. Darmstädter Seminar –Abwassertechnik- am 11.11.1999 in Darmstadt, TU Darmstadt, 1999	vergriffen
*WA*R 117	Reinhardt, Tim: Untersuchungen zur Dynamik biologischer Prozesse in drei-Phasen-Systemen am Beispiel der Restabfallrotte unter besonderer Berücksichtigung anaerober Teilprozesse. Dissertation, FB 13, TU Darmstadt, 1999	30,70 €
*WA*R 118	Umweltfachpläne und Umweltgesetzbuch - Ein Beitrag zur Fortentwicklung des Umweltfachplanungssystems und „Von der Landschaftsplanung zur Umweltleitplanung?“ 46. Darmstädter Seminar -Umwelt- und Raumplanung- am 28.09.1995 in Darmstadt, TU Darmstadt, 1999	30,70 €
*WA*R 119	Herr, Christian: Innovative Analyse und primärseitige Prozeßführungsoptimierung thermischer Abfallbehandlungsprozesse - am Beispiel der Mülleingangsklassifizierung bei der Rostfeuerung. Dissertation, FB 13, TU Darmstadt, 2000	33,20 €
*WA*R 120	Neumüller, Jürgen: Wirksamkeit von Grundwasserabgaben für den Grundwasserschutz - am Beispiel des Bundeslandes Hessen. Dissertation, FB 13, TU Darmstadt, 2000	35,80 €
*WA*R 121	Hunklinger, Ralph: Abfalltechnische Kennzahlen zur umweltgerechten Produktentwicklung. Dissertation, FB 13, TU Darmstadt, 2000	30,70 €

*WA*R 122	Wie zukunftsfähig sind kleinere Wasserversorgungsunternehmen? 60. Darmstädter Seminar -Wasserversorgung- am 29. Juni 2000 in Darmstadt, TU Darmstadt, 2000	35,80 €
*WA*R 123	Maßnahmen zur Betriebsoptimierung von Pumpwerken, Kanalisationssystemen und Abwasserbehandlungsanlagen. 11. gemeinsames Seminar -Abwassertechnik- in Weimar am 20. und 21. September 2000 mit der Fakultät Bauingenieurwesen der Bauhaus-Universität Weimar, TU Darmstadt, FB 13, 2000	40,90 €
*WA*R 124	Mohr, Karin: Entwicklung einer on-line Emissionsmeßtechnik zur quasi-kontinuierlichen Bestimmung von Organohalogen-Verbindungen in Abgasen thermischer Prozesse. Dissertation, FB 13, TU Darmstadt, 2000	30,70 €
*WA*R 125	El-Labani, Mamoun: Optimierte Nutzung bestehender Abfallverbrennungsanlagen durch Errichtung vorgeschalteter Reaktoren zur Behandlung heizwertreicher Abfälle. Dissertation, FB 13, TU Darmstadt, 2000	25,60 €
*WA*R 126	Durth, Anke: Einfluß von Temperatur, Anlagenkonfiguration und Auslastung auf die Ablaufkonzentration bei der biologischen Abwasserreinigung. Dissertation, FB 13, TU Darmstadt, 2000	vergriffen
*WA*R 127	Meyer, Ulrich: Untersuchungen zum Einsatz von Fuzzy-Control zur Optimierung der Stickstoffelimination in Abwasserbehandlungsanlagen mit vorgeschalteter Denitrifikation. Dissertation, FB 13, TU Darmstadt, 2000	33,20 €
*WA*R 128	Kommunale Klärschlammbehandlung vor dem Hintergrund der neuen europäischen Klärschlammrichtlinie. 61. Darmstädter Seminar -Abwassertechnik- am 09.11.2000 in Darmstadt, TU Darmstadt, FB 13, 2000	35,80 €
*WA*R 129	Mengel, Andreas: Stringenz und Nachvollziehbarkeit in der fachbezogenen Umweltplanung. Dissertation, FB 13, TU Darmstadt, 2001	46,-- €

*WA*R 130	Kosteneinsparungen durch neuartige Automatisierungstechniken in der Wasserversorgung. 62. Darmstädter Seminar -Wasserversorgung- am 07.06.2001 in Darmstadt, TU Darmstadt, FB 13, 2001	30,70 €
*WA*R 131	Aktive Zukunftsgestaltung durch Umwelt- und Raumplanung. Festschrift zum 60. Geburtstag von Prof. Dr.-Ing. Hans Reiner Böhm. TU Darmstadt, FB 13, 2001	25,60 €
*WA*R 132	Aktuelle Ansätze bei der Klärschlammbehandlung und -entsorgung. 12. gemeinsames Seminar -Abwassertechnik- in Weimar am 05. und 06. September 2001 mit der Fakultät Bauingenieurwesen der Bauhaus-Universität Weimar, TU Darmstadt, FB 13, 2001	40,90 €
*WA*R 133	Zum Bodenwasser- und Stoffhaushalt auf unterschiedlich bewirtschafteten Flächen unter Einbeziehung ökonomischer Aspekte Interdisziplinäre Projektstudie der Technischen Universität Darmstadt (TUD) mit Partner. TU Darmstadt, FB 13, 2001	30,70 €
*WA*R 134	Neues zur Belüftungstechnik - Probleme, Lösungsmöglichkeiten, Entwicklungen. 64. Darmstädter Seminar -Abwassertechnik- am 15.11.2001 in Darmstadt, TU Darmstadt, FB 13, 2001	35,-- €
*WA*R 135	Auswirkungen der Verordnung über die umweltverträgliche Ablagerung von Siedlungsabfällen und über biologische Abfallbehandlungsanlagen. 63. Darmstädter Seminar -Abfalltechnik- am 12. und 13.11.2001 in Darmstadt, TU Darmstadt, FB 13, 2001	35,-- €
*WA*R 136	Bockreis, Anke: Infrarot-Thermographie zur Überwachung von Flächenbiofiltern. Dissertation, FB 13, TU Darmstadt, 2001	35,-- €
*WA*R 137	Luft, Cornelia: Luftgetragene mikrobielle Emissionen und Immissionen an aeroben mechanisch-biologischen Abfallbehandlungsanlagen. Dissertation, FB 13, TU Darmstadt, 2002	30,-- €
*WA*R 138	Danhamer, Harald: Emissionsprognosemodell für Deponien mit mechanisch-biologisch vorbehandelten Abfällen - Schwerpunkt: Modellierung des Gashaushaltes. Dissertation, FB 13, TU Darmstadt, 2002	25,-- €

*WA*R 139	Lieth, Sabine: Stickstoffelimination aus kommunalem Abwasser mit getauchten Festbetten nach Vorbehandlung mit HCR-Reaktoren. Dissertation, FB 13, TU Darmstadt, 2002	35,-- €
*WA*R 140	Streit, Hans-Ulrich: Optimierung des Kombinationsbetriebs eines Advanced Oxidation Process mit einer Stripp-Anlage zur Grundwassersanierung. Dissertation, FB 13, TU Darmstadt, 2002	vergriffen
*WA*R 141	Spura, Patrik: Ein Vergleich des anlagebezogenen tschechischen Luftreinehalterechts mit jenem der Europäischen Union vor dem Hintergrund des anstehenden Beitritts. Dissertation, Univ. Frankfurt a.M., 2002	40,-- €
*WA*R 142	Hilligardt, Jan: Nachhaltige Regionalentwicklung durch freiwillige regionale Kooperation - Faktoren einer erfolgreichen Initiierung untersucht an der Region Starkenburg. Dissertation, FB 13, TU Darmstadt, 2002	30,-- €
*WA*R 143	Heiland, Peter: Vorsorgender Hochwasserschutz durch Raumordnung, interregionale Kooperation und ökonomischen Lastenausgleich. Dissertation, FB 13, TU Darmstadt, 2002	vergriffen
*WA*R 144	Dapp, Klaus: Informationsmanagement in der Planung am Beispiel des vorsorgenden Hochwasserschutzes. Dissertation, FB 13, TU Darmstadt, 2002	vergriffen
*WA*R 145	Schüler, Doris: Untersuchungen an der Technikumsanlage VERONA zur Bildung und zum Abbau von polyhalogenierten Dioxinen und Furanen und anderen Organohalogenverbindungen in Verbrennungsprozessen. Dissertation, FB 13, TU Darmstadt, 2002	25,-- €
*WA*R 146	Grundwasserproblematik im Hessischen Ried : Eine unlösbare Aufgabe? 65. Darmstädter Seminar -Wasserversorgung- am 23.10.2002 in Darmstadt, TU Darmstadt, FB 13, 2002	30,-- €
*WA*R 147	Rückgewinnung von Phosphor aus Klärschlamm und Klärschlammasche. 66. Darmstädter Seminar -Abwassertechnik- am 07.11.2002 in Darmstadt, TU Darmstadt, FB 13, 2002	35,-- €

*WA*R 148	Schneider, Andreas: Role of LCA concepts at the Research and Development phase of a new process for waste treatment - The Trefoil Kiln process subject to IPPC and BAT requirements. Dissertation, FB 13, TU Darmstadt, 2002	25,-- €
*WA*R 149	Sonnenburg, Alexander: Untersuchungen zur Denitrifikation von Grundwasser in Schüttungen mit abbaubarem Trägermaterial. Dissertation, FB 13, TU Darmstadt, 2002	vergriffen
*WA*R 150	Emissionen aus der Abfallbehandlung. Energie - Emissionen – Messtechnik. 67. Darmstädter Seminar -Abfalltechnik- am 13. Februar 2003 in Darmstadt, TU Darmstadt, FB 13, 2003	35,-- €
*WA*R 151	Rationalisierungsmaßnahmen in der Wasserversorgung. Umsetzungsstatus und künftige Entwicklungen. 68. Darmstädter Seminar -Wasserversorgung- am 15. Oktober 2003 in Darmstadt, TU Darmstadt, FB 13, 2003	vergriffen
*WA*R 152	Verantwortungspartnerschaft beim vorsorgenden Hochwasserschutz. 69. Darmstädter Seminar - Umwelt- und Raumplanung - am 16. Oktober 2003 in Darmstadt, TU Darmstadt, FB 13, 2003	vergriffen
*WA*R 153	Biofiltration. Renaissance eines Verfahrens durch erhöhte Anforderungen im In- und Ausland ? 70. Darmstädter Seminar -Abwassertechnik- am 06. November 2003 in Darmstadt, TU Darmstadt, FB 13, 2003	35,-- €
*WA*R 154	Seiler, Kainan: Planung der Abwasserentsorgung im ländlichen Raum anhand von räumlichen Einflussfaktoren. Dissertation, FB 13, TU Darmstadt, 2004	30,-- €
*WA*R 155	Ludwig, Thomas: Entwicklung der Emissionsmessanlage DioxinCop. Dissertation, FB 13, TU Darmstadt, 2004	25,-- €
*WA*R 156	Haffner, Yvonne: Sozialwissenschaftliche Modellierung zur Privatisierung der Wasserversorgung. Dissertation, FB 2, TU Darmstadt, 2004	vergriffen

*WA*R 157	Geruch : Messung – Wirkung – Minderung. 71. Darmstädter Seminar -Abfalltechnik- am 24. Juni 2004 in Darmstadt, TU Darmstadt, FB 13, 2004	35,-- €
*WA*R 158	Qualitätssicherung bei Wassergewinnungsanlagen - Umsetzung und aktuelle Entwicklung im Regelwerk. 72. Darmstädter Seminar –Wasserversorgung– am 06.10.2004 in Darmstadt, TU Darmstadt, 2004	vergriffen
*WA*R 159	Wasserwiederverwendung - eine ökologische und ökonomische Notwendigkeit wasserwirtschaftlicher Planung weltweit ? 73. Darmstädter Seminar –Abwassertechnik– am 04.11.2004 in Darmstadt, TU Darmstadt, 2004	vergriffen
*WA*R 160	Weil, Marcel: Ressourcenschonung und Umweltentlastung bei der Betonherstellung durch Nutzung von Bau- und Abbruchabfällen. Dissertation, FB 13, TU Darmstadt, 2004	35,-- €
*WA*R 161	Unendlicher Wachstum auf unendlicher Fläche ? 74. Darmstädter Seminar –Umwelt- und Raumplanung– am 27.01.2005 in Darmstadt, TU Darmstadt, 2005	vergriffen
*WA*R 162	Gernuks, Marko: Entwicklung einer Methode zur Bewertung von Umweltaspekten mit der Ableitung von Umweltzielen im Rahmen von EMAS. Dissertation, FB 13, TU Darmstadt, 2004	vergriffen
*WA*R 163	Rother, Elmar: Optimising Design and Operation of the Biofiltration Process for Municipal Wastewater Treatment. Dissertation, FB 13, TU Darmstadt, 2005	35,-- €
*WA*R 164	Hilligardt, Jan: Regionale Kooperation der Landkreise, Städte und Gemeinden. Stand - Potenziale - Perspektiven. Habilitation, FB 13, TU Darmstadt, 2005	vergriffen
*WA*R 165	Gramel, Stefan: Privatisierung von Wasserversorgungsunternehmen - Auswirkungen auf den Umwelt- und Ressourcenschutz? Dissertation, FB 13, TU Darmstadt, 2004	35,-- €
*WA*R 166	Krause, Stefan: Untersuchungen zum Energiebedarf von Membranbelebungsanlagen. Dissertation, FB 13, TU Darmstadt, 2005	35,-- €

*WA*R 167	Rückgewinnung von Phosphor aus Abwasser und Klärschlamm. Konzepte - Verfahren - Entwicklungen. 75. Darmstädter Seminar –Abwassertechnik- am 12./13.12.2005 in Darmstadt, TU Darmstadt, 2005	vergriffen
*WA*R 168	Hora, Maike: Abfallverursacher Elektrogeräte. Ansätze zur prospektiven Bilanzierung von Abfallströmen in der umweltgerechten Produktentwicklung. Dissertation, FB 13, TU Darmstadt, 2005	30,-- €
*WA*R 169	Zhang, Wensheng: Ökologische siedlungswasserwirtschaftliche Konzepte für urbane Räume Chinas unter Berücksichtigung deutscher Techniken und Erfahrungen. Dissertation, FB 13, TU Darmstadt, 2005	30,-- €
*WA*R 170	Steinberg, Iris: Untersuchungen zur Effizienzsteigerung von biologischen und nicht-thermischen Abluftreinigungsverfahren bei der biologischen Abfall-behandlung. Dissertation, FB 13, TU Darmstadt, 2005	30,-- €
*WA*R 171	Haupter, Birgit: Transnationale Förderprogramme zur Raumentwicklung. Untersuchungen zur Wirkung für die räumliche Planung zum Hochwasserschutz. Dissertation, FB 13, TU Darmstadt, 2006	35,-- €
*WA*R 172	Ott, Carsten: Straßenkehrichtentsorgung: Anlagenkonzept und Nachhaltig-keitsanalyse. Dissertation, FB 13, TU Darmstadt, 2006	30,-- €
*WA*R 173	1 Jahr Abfallablagerungsverordnung - Wo bleibt der Müll? 76. Darmstädter Seminar –Abfalltechnik– am 1.06.2006 in Darmstadt, TU Darmstadt, 2006	35,-- €
*WA*R 174	Wachstumsregion - Handlungsansätze für mehr Nachhaltigkeit. 77. Darmstädter Seminar –Umwelt- und Raumplanung– am 11.09.2006 in Darmstadt, TU Darmstadt, 2006	30,-- €
*WA*R 175	Interdisziplinarität in der Umwelt- und Raumplanung - Theorie und Praxis. *Festschrift für Professor Böhm* TU Darmstadt, 2006	40,-- €

*WA*R 176	Neue maschinen- und verfahrenstechnische Möglichkeiten zur Einsparung von Betriebskosten bei der Abwasserbehandlung. 78. Darmstädter Seminar -Abwassertechnik- am 02.11.2006 in Darmstadt, TU Darmstadt, 2006	35,-- €
*WA*R 177	Einsparpotenziale in der Trinkwasserversorgung durch Optimierung von Wasserverteilungsnetzen. 79. Darmstädter Seminar –Wasserversorgung- am 05.10.2006 in Darmstadt, TU Darmstadt, 2006	30,-- €
*WA*R 178	Meyer, Lutz: Exergiebasierte Untersuchung der Entstehung von Umweltbelastungen in Energieumwandlungsprozessen auf Komponentenebene: Exergoökologische Analyse. Dissertation, FB 13, TU Darmstadt, 2006	35,--
*WA*R 179	Gasafi, Edgar: Entwicklung einer lebenswegbasierten Screening-Methode zur Entscheidungsunterstützung in frühen Phasen der Verfahrens-entwicklung. Dissertation, FB 13, TU Darmstadt, 2006	35,-- €
*WA*R 180	Treskatis, Christoph: Bewirtschaftung von Grundwasserressourcen - Planung, Bau und Betrieb von Grundwasserfassungen. Habilitation, FB 13, TU Darmstadt, 2006	45,-- €
*WA*R 181	Uihlein, Andreas: Modellierung der Kohlenstoffströme zur Untersuchung der Nutzung von Kohlenstoffträgern in Deutschland. Dissertation, FB 13, TU Darmstadt, 2006	vergriffen
*WA*R 182	den Boer, Emilia: A Novel Approach for Integrating Heavy Metals Emissions from Landfills into Life Cycle Assessment - Consideration of Waste Pretreatment, Landfill Processes and Long-Term Effects Dissertation, FB 13, TU Darmstadt, 2006	30,-- €
*WA*R 183	Klimawandel - Anpassungsstrategien in Deutschland und Europa. 80. Darmstädter Seminar -Umwelt- und Raumplanung- am 29.03.2007 in Darmstadt, TU Darmstadt, 2007	25,-- €
*WA*R 184	Stephan, Henrik: Bewertungsmethodik für Fertigungsverfahren im Karosseriebau aus Sicht des betrieblichen Umweltschutzes. Dissertation, FB 13, TU Darmstadt, 2007	vergriffen

*WA*R 185	Schaum, Christian A.: Verfahren für eine zukünftige Klärschlammbehandlung –Klärschlamm-konditionierung und Rückgewinnung von Phosphor aus Klärschlamm-asche. Dissertation, FB 13, TU Darmstadt, 2007	35,-- €
*WA*R 186	Rohde, Clemens: Milchsäurefermentation von biogenen Abfällen. Dissertation, FB 13, TU Darmstadt, 2007	35,-- €
*WA*R 187	Risikoanalyse von Trinkwassereinzugsgebieten und Fassungen. 81. Darmstädter Seminar -Wasserversorgung- am 11.10.2007 in Darmstadt, TU Darmstadt, 2007	30,-- €
*WA*R 188	Cangahuala Janampa, Ana: Wasserverlustmanagement in Wasserverteilungsanlagen in Entwicklungs- ländern am Beispiel von Peru. Anwendung verschiedener Methoden zur multikriteriellen Entscheidungsunterstützung. Dissertation, FB 13, TU Darmstadt, 2007	vergriffen
*WA*R 189	Pollmann, Olaf: Optimierung anthropogener Stoffströme am Beispiel des Papier-recyclings. Dissertation, FB 13, TU Darmstadt, 2007	vergriffen
*WA*R 190	Wie sieht die Abwasserbehandlung der Zukunft aus? -Vierte, fünfte, sechste Reinigungsstufe? 82. Darmstädter Seminar -Abwassertechnik- am 15.11.2007 in Darmstadt, TU Darmstadt, 2007	35,-- €
*WA*R 191	Koffler, Christoph: Automobile Produkt-Ökobilanzierung. Dissertation, FB 13, TU Darmstadt, 2007	35,-- €
*WA*R 192	Koch, Michael: Untersuchungen zum Einfluss der Energiedissipationsdichte auf Reaktionsabläufe im "Highloaded Compact Reactor" (HCR®). Dissertation, FB 13, TU Darmstadt, 2007	35,-- €
*WA*R 193	den Boer, Jan: Sustainability Assessment for Waste Management Planning - Development and Alternative Use of the LCA-IWM Waste Management System Assessment Tool. Dissertation, FB 13, TU Darmstadt, 2007	30,-- €

*WA*R 194	Biogas - Klimaretter oder Ressourcenverschwender. 83. Darmstädter Seminar -Abfalltechnik- am 11.12.2007 in Darmstadt, TU Darmstadt, 2007	vergriffen
*WA*R 195	Scheck, Natalie: Die Strategische Umweltprüfung als Instrument zur Förderung einer nachhaltigen Entwicklung - Untersuchung am Beispiel der Regional-planung Südhessen. Dissertation, FB 13, TU Darmstadt, 2007	30,-- €
*WA*R 196	Klimawandel – Markt für Strategien und Technologien?! 84. Darmstädter Seminar -Abfalltechnik und Umwelt- und Raumplanung- am 26.06.2008 in Darmstadt, TU Darmstadt, 2008	vergriffen
*WA*R 197	Hähnlein, Christian: Numerische Modellierung zur Betriebsoptimierung von Wasserverteilnetzen. Dissertation, FB 13, TU Darmstadt, 2008	30,-- €
*WA*R 198	Berger, Jan: Biologische Methanoxidation in Deponieabdeckschichten. Dissertation, FB 13, TU Darmstadt, 2008	35,-- €
*WA*R 199	Wellge, Steffen: Evaluation von betrieblichen Umweltmanagementsystemen. Dissertation, FB 13, TU Darmstadt, 2009	35,-- €
*WA*R 200	Bieker, Susanne: Semizentrale Ver- und Entsorgungssysteme: neue Lösungen für schnell wachsende urbane Räume. Untersuchung empfehlenswerter Größen-ordnungen. Dissertation, FB 13, TU Darmstadt, 2009	35,-- €
*WA*R 201	Hoffmann, Karl Peter: Reduzierung von CO_2-Emissionen durch den Einsatz von Erdgas aus Biogas in dezentralen Stirling-KWK-Anlagen. Dissertation, FB 13, TU Darmstadt, 2009	35,-- €
*WA*R 202	Loock, Peter: Veränderung der Leistungsfähigkeit feinblasiger Membranbelüftungs-elemente unter abwassertechnischen Betriebsbedingungen. Dissertation, FB 13, TU Darmstadt, 2009	35,-- €
*WA*R 203	Warsen, Jens: Validierung von Stoffflussdaten in der Ökobilanz durch Daten aus dem öffentlichen Berichtswesen. Dissertation, FB 13, TU Darmstadt, 2009	35,-- €

*WA*R 204	Klärschlammfaulung und –verbrennung: das Behandlungskonzept der Zukunft? 85. Darmstädter Seminar -Abwassertechnik- am 13.04.2010 in Darmstadt, TU Darmstadt, 2010	35,-- €
*WA*R 205	Neue Herausforderungen und Chancen in der Wasserversorgung. Darmstädter Seminar -Wasserversorgung und Grundwasserschutz- im Rahmen des 1. Darmstädter Ingenieurkongresses Bau und Umwelt am 14. und 15.09.2009 in Darmstadt, TU Darmstadt, 2010	35,-- €
*WA*R 206	Pennekamp, Sandra: Raumentwicklung im Spannungsfeld zwischen Wachstum und Schrumpfung - was können überregionale Partnerschaften leisten? Dissertation, FB 13, TU Darmstadt, 2010	35,-- €
*WA*R 207	Frommer, Birte: Regionale Anpassungsstrategien an den Klimawandel – Akteure und Prozess. Dissertation, FB 13, TU Darmstadt, 2010	35,-- €
IWAR 208	Chang, Yue: Greywater treatment within semi-centralised supply and treatment systems by the example of the People's Republic of China. Dissertation, FB 13, TU Darmstadt, 2010	35,-- €
IWAR 209	Sakaguchi-Söder, Kaori: A new method for compound-specific stable chlorine isotope analysis. Dissertation, FB 13, TU Darmstadt, 2010	35,-- €
IWAR 210	Henkel, Jochen: Oxygen transfer phenomena in activated sludge. Dissertation, FB 13, TU Darmstadt, 2010	35,-- €
IWAR 211	Doktorandenschule Abfall 2010 Manigod / Frankreich, 5. - 8. September 2010, TU Darmstadt, 2011	40,-- €
IWAR 212	Preis und Leistung - Wasserversorgung bewerten und vergleichen. 86. Darmstädter Seminar -Wasserversorgung- am 22.02.2011 in Darmstadt, TU Darmstadt, 2011	30,-- €
IWAR 213	Siembida-Lösch, Barbara: Reduction of Membrane Fouling in Membrane Bioreactors - Development of Innovative and Sustainable Techniques. Dissertation, FB 13, TU Darmstadt, 2011	35,-- €

IWAR 214	Müller, Bodo: Weiterentwicklung und Validierung der Methode der Input-Output basierten Sachbilanz für deutsche Gebäudeökobilanzen. Dissertation, FB 13, TU Darmstadt, 2011	35,-- €
IWAR 215	Eren, Onat: Automatisierung von numerischen Kurzzeit-Wasserbedarfsprognose-verfahren und ihre Anwendung in der Wasserversorgung. Dissertation, FB 13, TU Darmstadt, 2011	35,-- €
IWAR 216	Biobasierte Produkte und Energie aus Biomasse. 87. Darmstädter Seminar Abfalltechnik- am 08.12.2011 in Darmstadt, TU Darmstadt, 2011	vergriffen
IWAR 217	Meda, Alessandro: Einsatz von Biofiltern für die Wasser- und Nährstoffwiederverwendung und für die weitergehende Abwasserreinigung zur Spurenstoff-entfernung. Dissertation, FB 13, TU Darmstadt, 2012	35,-- €
IWAR 218	Hoffmann, Marc: Abfalltechnische Erweiterung von Bioabfallbehandlungsanlagen für die Herstellung biobasierter Produkte. Dissertation, FB 13, TU Darmstadt, 2012	35,-- €
IWAR 219	Maerz, Peter: Die Metalle der Schlacken aus Abfallverbrennungsanlagen. Dissertation, FB 13, TU Darmstadt, 2012	35,-- €
IWAR 220	Petzet, Sebastian: Phosphorrückgewinnung in der Abwassertechnik - Neue Verfahren für Klärschlamm und Klärschlammaschen. Dissertation, FB 13, TU Darmstadt, 2012	35,-- €
IWAR 221	Günkel-Lange, Tobias: Sauerstoffzufuhr und α-Werte feinblasiger Belüftungssysteme beim Belebungsverfahren - Abhängigkeiten und Bemessungsempfehlungen. Dissertation, FB 13, TU Darmstadt, 2013	35,-- €
IWAR 222	Zhang, Guomin: Abwasserreinigung und Wasserkreislaufführung in der Papierindustrie – Weiterentwicklung deutscher Techniken für den chinesischen Markt -. Dissertation, FB 13, TU Darmstadt, 2013	35,-- €
IWAR 223	Back, Sonja: Anwendungspotential der mikrobiellen Methanoxidation im Deponie-Schwachgasbereich – Feldstudie auf einer MBA-Deponie. Dissertation, FB 13, TU Darmstadt, 2013	35,-- €

IWAR 224	Zimmermann, Martin: Sustainable Transformations of Water Supply Regimes. The Cuvelai-Etosha Basin in Central Northern Namibia. Dissertation, FB 13, TU Darmstadt, 2013	35,-- €
IWAR 225	Bischoff, Astrid: Desinfektion von behandeltem Abwasser – Vergleich verschiedener Desinfektionsverfahren Dissertation, FB 13, TU Darmstadt, 2013	35,-- €
IWAR 226	Zeig, Carola: Stoffströme der Co-Vergärung in der Abwasserwirtschaft Dissertation, FB 13, TU Darmstadt, 2014	35,-- €
IWAR 227	Knapp, Steffen: Analyse und Bewertung des Co-Firings als Instrument einer kosteneffizienten Reduktion von CO_2-Emissionen Dissertation, FB 13, TU Darmstadt, 2014	35,-- €
IWAR 228	Alraee, Wael: Modeling the failure of drinking water distribution networks through the usage of artificial networks Dissertation, FB 13, TU Darmstadt, 2014	35,-- €
IWAR 229	Benz, Philipp: Konzept zum Nachhaltigkeitscontrolling in der Siedlungswasser-wirtschaft Dissertation, FB 13, TU Darmstadt, 2014	35,-- €
IWAR 230	Kannengießer, Jan: Nutzung biologischer Siedlungsabfälle zur Generierung biobasierter Produkte und Kraftstoffe auf Basis von mittel- und langkettigen Fettsäuren – Feldstudie am Beispiel eines Kompostwerks Dissertation, FB 13, TU Darmstadt, 2015	35,-- €
IWAR 231	Brenda, Marian: Hybrid Sludge Modeling in Water Treatment Processes Dissertation, FB 13, TU Darmstadt, 2015	35,-- €

Bestellungen über: Technische Universität Darmstadt
Institut I*WA*R
Franziska-Braun-Straße 7
D-64287 Darmstadt
E-Mail: raumplanung@iwar.tu-darmstadt.de

Telefon: +49 (0)6151 / 16 36 48
FAX: +49 (0)6151 / 16 37 39